DISSERTATION

INVESTIGATING NEW PROTEIN COMPONENTS OF THE ENDOCYTIC MACHINERY IN *SACCHAROMYCES CEREVISIAE*

Submitted by

Kristen Farrell

Graduate Degree Program in Cell and Molecular Biology

In partial fulfillment of the requirements

For the Degree of Doctor of Philosophy

Colorado State University

Fort Collins, Colorado

Spring 2016

Doctoral Committee:

Advisor: Santiago Di Pietro

James Bamburg
Diego Krapf
Michael Tamkun

ABSTRACT

INVESTIGATING NEW PROTEIN COMPONENTS OF THE ENDOCYTIC MACHINERY IN *SACCHAROMYCES CEREVISIAE*

Clathrin-mediated endocytosis is an essential eukaryotic process which allows cells to control membrane lipid and protein content, signaling processes, and uptake of nutrients among other functions. About 60 proteins have been identified that compose the endocytic machinery in *Saccharyomes cerevisiae*, or budding yeast. Clathrin-mediated endocytosis is highly conserved between yeast and mammals in terms of both protein content and timing of protein arrival. First, there is an immobile phase in which clathrin and other coat components concentrate at endocytic sites. Second, another wave of proteins assembles about 20 seconds before localized actin polymerization. Third, a fast mobile stage of endocytosis occurs coinciding with local actin polymerization and culminates with vesicle scission. Fourth, most coat proteins disassemble from the internalized vesicle. Despite the knowledge of so many endocytic proteins, gaps still remain in the complete understanding of the endocytic process. We attempt to fill some of these gaps with a screen of the yeast GFP library for novel endocytic-related proteins using confocal fluorescence microscopy.

We identified proteins colocalizing with RFP-tagged Sla1, a clathrin adaptor that serves as a well-known marker of endocytic sites. Ubx3 and Tda2, two unstudied proteins, were selected for further investigation based on high degree of colocalization with Sla1. Ubx3 shows fluorescent patch dynamics similar to an endocytic coat protein. Ubx3 is dependent on clathrin for patch lifetime and binds clathrin via a W-box, the first identification of this clathrin binding

motif in a non-mammalian species. Uptake assays performed in a knockout strain of Ubx3 display a reduction in both bulk endocytosis by fluorescent dye Lucifer Yellow and cargo-specific endocytosis by methionine transporter Mup1. The Ubx3 knockout cells also show a significant increase in lifetime of early endocytic protein Ede1, and removing its UBX domain alone results in similar defects to the Ubx3 knockout. The endocytic defect may be due to lack of recruitment of ubiquitin regulator AAA ATPase Cdc48 to the endocytic site. Inactivation of Cdc48 reduces Lucifer yellow uptake to minimal levels and causes aggregates of early endocytic protein Ede1-GFP. This is the first identification of a UBX domain-containing protein in clathrin-mediated endocytosis.

Tda2 appears at the tail end of each endocytic site, suggesting a function in late stage endocytosis. A Tda2 knockout strain shows similar reductions in bulk and cargo dependent endocytosis through Lucifer yellow and Mup1 uptake assays. Tda2 appears unaffected by clathrin disruption, but is no longer recruited to the endocytic site when cells are treated with the actin depolymerizing agent LatA, suggesting it is associated with the actin cytoskeleton. A crystal structure of Tda2 reveals it is a homolog of mammalian dynein light chain TcTex-1. Tda2 is associated with a larger protein complex in the cytosol but does not co-purify with dynein and is unaffected by addition of the microtubule depolymerizing drug Nocodazole. Tda2 has similar localization to actin capping proteins Cap1/2 which localize to the plus end of actin filaments near the plasma membrane. Tda2 deletion increases Cap1 patch lifetime but reduces its fluorescent intensity. Aim21 fluorescent intensity at endocytic sites is reduced to half without Tda2. When Aim21 is deleted, Tda2 is no longer recruited to endocytic sites and the large Tda2-containing complex is no longer present in the cytosol. Tda2 is a newly identified component of the actin cytoskeleton in stable complex with Aim21. This is the first identification of a TcTex

type dynein light chain in yeast and the first dynein light chain associated with clathrin-mediated endocytosis.

Thus, we have identified two novel components of endocytic machinery by screening the yeast GFP library. The successful identification of previously uncharacterized endocytic proteins indicates the unique advantages of the GFP library screening. Many previous screens for endocytic proteins rely on the yeast knockout library or cargo accumulation, which have many disadvantages. The GFP library screening method has potential for use with other cellular processes that have distinct cellular localizations and established fluorescent markers. The GFP library also has potential for use in a screen for cargo proteins dependent on clathrin-mediated endocytosis. Additionally, more proteins of the endocytic machinery may be further characterized from the list of Sla1-colocalizing proteins identified in our screen.

ACKNOWLEDGMENTS

I would like to thank all of the Di Pietro lab members, who have always provided helpful discussions and suggestions for experiments especially when working through confusing data. My yeast counterparts have been especially helpful, including Thomas Tolsma and Lauren Barry. The undergraduates who have worked with me, Caitlin Grossman and Colette Worchester, have also been extremely helpful in contributing to this project. I would also like to thank my advisor Santiago Di Pietro for accepting me into his lab and teaching me to become a successful scientist. The entire Biochemistry and Molecular Biology department earns my thanks as well, for welcoming a Cell and Molecular Biology program student into their ranks.

I would also like to thank everyone outside of the academic community who has contributed to my graduate career. My family has always been a constant support, despite being far in distance they have provided me with life advice and aid whenever I needed it. My friends, also both near and far, for keeping me sane during my studies and always providing weekend entertainment and mountain exploration companions. Finally I would like to thank Andrew Burkhart for always supporting me and pushing me to better myself in many aspects.

TABLE OF CONTENTS

LIST OF TABLES

LIST OF FIGURES

CHAPTER 1

INTRODUCTION

1.1 Overview

Protein trafficking is a crucial process for the maintenance of eukaryotic membrane-bound organelles. Uptake of material from the plasma membrane through clathrin-mediated endocytosis (CME) is essential and regulates many aspects of cell homeostasis including signaling, nutrient uptake, lipid composition, cell wall synthesis, and viral entry. CME is marked by the formation and dissociation of a protein coat at the plasma membrane resulting in an internalized vesicle. The process includes recognition of a protein internalization signal and the numerous proteins involved in this process typically have weak interaction strengths that allow transient association.

Coat and adaptor proteins recognize cargo, recruit clathrin, bind the plasma membrane, and shape the vesicle. Actin polymerization, which is tightly regulated, provides the force necessary to tubulate the membrane. Scission frees the vesicle, which is then uncoated, allowing proteins to be used again at a new endocytic site. Ubiquitin is used in CME both as an internalization signal on cargo proteins and in regulation of endocytic machinery. There are about sixty proteins in yeast that have been established to participate in this process but not all are necessary for successful internalization. Proteins arrive at each endocytic site in a predictable and reproducible order. Early arriving proteins have a more variable patch lifetime, while later arriving proteins have shorter and less variable lifetimes. Even with the identification of so many protein components, many questions about CME are still unanswered.

CME is highly conserved between yeast and mammals in protein content, dynamics, and function. However, yeast and mammals differ in the essentiality of specific proteins such as clathrin, AP-2, and dynamin as well as actin filaments. As CME is a pervasive cell process, it has many and diverse implications for human health. Errors in the process or mutations in cargo proteins cause misregulation of trafficking, while normal CME can be hijacked by pathogens for cell entry.

In this study, the budding yeast *Saccharomyces cerevisiae* is used as a model organism to study CME. Yeast have been used by humans for thousands of years and demonstrate many benefits in their use as a model organism, including homologous recombination, simple genomics, and homology to mammals. More recently, complete sequencing of the yeast genome has allowed quick genetic manipulation and fluorescent microscopy has allowed easy identification of protein-specific sub-cellular localizations. Creation of the yeast GFP library yielded an important resource for cell biology research and allows genome wide screening and application of cellular localization data.

1.2 Clathrin-mediated endocytosis

1.2.1 Protein trafficking and functions of endocytosis

Eukaryotic cells are defined by the presence of membrane-bound organelles. Organelles provide separation of distinct processes and allow creation of environments necessary for specific functions such as proteolytic degradation. Each membrane-bound organelle is characterized by a specific subset or enrichment of lipids and proteins that give it unique properties, function, and label it for recognition. A system providing discrete and accurate

delivery and transfer of proteins, lipids, and luminal cargo must exist for the maintenance of separate and specialized organelles.

Small membrane-bound vesicles were first imaged by Dalton & Felix in 1954 [1] and Roth & Porter in 1964 [2]. Clathrin was recognized as the major coat component of what are now known as clathrin-coated vesicles in 1975 by Pearse [3], who coined the name clathrin after the clathrate structures that were observed. Observation of both flat clathrin lattices and tightly curved structures suggested a transition may occur between the two configurations [4]. Clathrin-coated vesicles are formed from the plasma membrane by CME, from the trans-Golgi network, and from endosomes [5]. Distinguishing various cellular transport mechanisms are the adaptor and coat proteins. Accessory and adaptor proteins vary for distinct clathrin-dependent trafficking events, with five different heterotetrameric adaptor protein complexes (AP1-5) identified in mammalian cells [6], as well as SNARE proteins providing target-specific recognition. Vesicles budding from the ER use a COPII coat, while retrograde transport from the Golgi uses COPI coated vesicles.

Clathrin-mediated endocytosis provides protein trafficking from the plasma membrane. The plasma membrane functions to contain the cell environment and control entry and exit of molecules to and from the cell, yet the cell must be able to sense and communicate with the outside environment. Transmembrane proteins provide the cell with such abilities. Secretory trafficking processes bring these proteins to the membrane, however these secretory processes must be balanced by subsequent removal of membrane and protein. This balance is demonstrated by mutants of many secretory proteins. These mutants result in accumulation of secretory vesicles and also portray endocytic defects [7].

Proteins internalized by CME, referred to as cargo, include receptors, channels, signaling proteins, and other cell surface proteins. A portion of extracellular fluid is internalized in the vesicle as well, referred to as bulk endocytosis, which includes molecules from the environment not able to diffuse across the membrane or internalize via channels or transporters. Internalization of receptors upon signal binding is important for downregulation of the signaling cascade. Regulation of transporters in response to nutrient availability is another important function of CME. In yeast, lactate transporter Jen1 is ubiquitinated and internalized in response to glucose availability [8]. Methionine transporter Mup1 is similarly ubiquitinated and internalized via CME in response to adequate methionine levels [9]. Besides nutrient regulation, maintenance of the plasma membrane and cell wall also rely on CME. Wsc1, a cell wall stress sensor important for cell wall synthesis, is regulated by CME and defects in trafficking result in sensitivity to cell wall perturbation [10]. Cells with endocytic defects portray overly-thick cell walls, likely due to lack of internalization of cell wall stress sensors and synthesis enzymes [11]. Heat-induced damage of transmembrane proteins is recognized by the ART-Rsp5 ubiquitin-ligase adaptor network, without which accumulation of damaged proteins results in loss of plasma membrane integrity [12].

The endocytic protein coat selects cargo and provides mechanical forces for formation of the vesicle from the membrane. Most protein interactions in this system, especially cargo binding, have K_d values in the μM range. These relatively low binding affinities suggest transient interactions, allowing a dynamic system of binding and release where more stable binding would cause trafficking proteins to interfere with the function of the cargo or non-release of the vesicle. However, the presence of multiple weak binding sites increases the relative affinity for proteins over that of a single motif. By scattering multiple binding motifs throughout

large unfolded regions, the protein can "search" a larger area for binding partners [13]. The multiple interaction capacity of the majority of endocytic proteins exemplifies these concepts. In many cases, perturbation of a single domain or even knockout of multiple proteins in CME has little effect on its function. It is the cooperation of multiple weak interactions that amplifies and stabilizes coat formation for this essential process.

Other pathways for endocytosis that do not rely on clathrin also exist, referred to as clathrin-independent endocytosis (CIE). In mammalian cells, invaginations occur in cholesterol-rich lipid rafts called caveolae, aided by caveolins which oligomerize upon association with the membrane [14]. A clathrin-independent endocytic pathway in yeast has also been uncovered, and is dependent on formin and GTPase Rho1, analogous to a RhoA-dependent pathway in mammalian cells [15]. Clathrin-independent endocytic pathways are less well-studied and less pervasive throughout cell types and species than CME, yet CIE pathways often depend on actin polymerization and scission by dynamin, as is the case with CME. In this study, investigations focus on established as well as novel proteins and functions for clathrin-mediated endocytosis.

1.2.2 Protein machinery in clathrin-mediated endocytosis

Clathrin-mediated endocytosis consists of a large number and diversity of proteins contributing to a single vesicle-generating event generally lasting less than two minutes. Multiple events in various stages occurring simultaneously throughout the cell indicate the quantity of proteins and the regulation required at each site. The ribosomal exclusion zone present in EM images of endocytic sites also displays the large volume of proteins present at the site of CME [16]. A list of established proteins of the yeast endocytic machinery and their mammalian homolog is provided in Table 1.1. Table 1.2 lists the common binding partner of

Table 1.1: Proteins involved in clathrin-mediated endocytosis. Adapted from [16, 17]. Proteins with no mammalian homolog listed either have no mammalian homolog or it is undetermined.

Stage (Lifetime)	Yeast Protein	Mammalian homolog	Domains	Brief description of known roles in yeast
Early (60-120 sec)	Ede1	Eps15	EHs, CC, UBA	Ubiquitinated, oligomerizes via coiled coil region, important for endocytic site initiation, deletion reduces number of endocytic sites, binds Syp1, Yap1801/2, Pal1/2, and Ent1/2
	Syp1	FCho1/2	F-BAR, AP-2 mu homology, PR	Important for endocytic site initiation, inhibits Las17 NPF activity, binds Ede1
	Chc1	Clathrin heavy chain	β-propeller	Component of clathrin triskelion, deletion reduces number of endocytic sites, binds Clc1 and clathrin box motifs (CBM)
	Clc1	Clathrin light chain		Component of clathrin triskelion, binds Chc1 and Sla2
	Pal1/2		NPF motif	Localizes to cell periphery and endocytic sites, interacts with Ede1
	Apl1	AP-2 beta subunit		Component of AP-2 complex not essential for endocytosis, may be cargo specific adaptor
	Apl3	AP-2 alpha subunit		Component of AP-2 complex not essential for endocytosis, may be cargo specific adaptor
	Apm4	AP-2 mu subunit		Component of AP-2 complex not essential for endocytosis, may be cargo specific adaptor, essential for trafficking of Mid2
	Aps2	AP-2 sigma subunit		Component of AP-2 complex not essential for endocytosis, may be cargo specific adaptor
Intermed-iate coat (~40 sec)	Yap1801/2	AP180/ CALM	ANTH, NPF motifs, CBM	Adaptor for Snc1, double deletion has no phenotype, binds Pan1, Ede1, and Chc1
	Sla2	Hip1R, Hip1	ANTH, CC, THATCH	Dimerizes, links actin cytoskeleton to membrane, deletion results in actin comet tails from non-productive sites, binds Clc1, Sla1, End3, Pan1, and actin filaments
	Ent1/2	Epsin	ENTH, NPF motifs, UIMs, CBM	Ubiquitinated by Rsp5, double deletion requires ENTH domain for viability, binds Pan1, Ede1, Chc1, and ubiquitin
Late Coat (~35 sec)	Pan1	Intersectin	EH, CC, WH2, PR, acidic motif	An Arp2/3 NPF, essential scaffold protein, binds Sla1, End3, Sla2, Yap1801/2, Ent1/2, Myo3/5, Scd5, and actin

	Sla1	Intersectin/ CIN85	SH3s, SHD1, SHD2, PR, CBM, SR	Multi-domain protein, inhibits Las17 via SH3 domains, binds Ub through third SH3 domain, binds NPFXD-cargo via a SHD1 domain, binds Pan1 and End3 via SR domain, binds clathrin heavy chain via LLDLQ motif, oligomerizes via SHD2 domain, binds Sla2 and Scd5
	End3	Eps15	EH, CC	Binds Sla1, Pan1, Scd5
	Lsb3	SH3YL1a	SH3	Promotes actin polymerization and bundling, binds Las17 and Ldb17
	Ysc84	SH3YL1a	SH3	Bundles actin, stimulates Las17, binds Ldb17
	Lsb5	GGA		Activates Arf3, binds ubiquitin, Sla1, and Las17
	Gts1	SMAP2	UBA	Arf3 regulator, contains UBA domain
WASP/ MYO (15-35 sec)	Las17	WASP/ N-WASP	WH1, PR, WH2, LGM, acidic motif	Most potent NPF for Arp2/3 complex through WH2 domain, acidic motif, and LGM. Inhibited by Sla1, binds Vrp1, Bbc1, Syp1, Lsb3/5, Ysc84, Bzz1, Myo3/5, Rvs167
	Vrp1	WIP/WIRE	PR, WH2	Proline-rich actin associated protein related to Las17, promotes actin nucleation via Myo activation, binds Las17 and actin
	Bzz1	Syndapin	F-BAR, SH3s, PR	Relieves Sla1 inhibition of Las17, arrives just before actin at endocytic site, binds Las17 and Ldb17
	Scd5			Targets Glc7 phosphatase to Ark1/Prk1-phosphorylated endocytic factors, binds Sla1, End3, and Pan1
	Myo3/5	Myosin-1E	SH3, TH1, TH2, motor, acidic motif	Type 1 myosins, monomeric, single deletion has no phenotype, membrane-binding TH1 domain, is an Arp2/3 NPF, binds Pan1, Vrp1, Las17, actin filaments
	Bbc1		SH3, PR	Localizes to cortical actin patches, inhibits Las17, binds SH3 domains of Myo3/5
	Ldb17	DIP/WISH/ SPIN90	PR	Dependent on Sla1 for recruitment to actin patches, binds Sla1, Bzz1, Lsb3, and Ysc84
Actin (~15 sec)	Aim21			Localizes to actin cytoskeleton
	Act1	Actin		Monomer for production of actin filaments with a barbed and pointed end
	Arc15/18/19/ 35/40 Arp2/3	Arp2/3 complex subunits	ARP, β-propeller	Nucleates branched actin filaments at 70˚ angle from mother filament, required for motility of endocytic patches, binds Las17, Myo3/5, Pan1, Abp1, Crn1

	Abp1	ABP1	ADFH, PR, SH3, acidic motif	Actin filament binding through ADFH domain, is an Arp2/3 NPF, inhibits barbed end elongation, binds Rvs167, Aim3, Srv2, Scp1, Ark1, Prk1, and Sjl2
	Cap1	Capping protein alpha		Forms heterodimer with Cap2, binds barbed end of actin to prevent elongation, binds Twf1
	Cap2	Capping protein beta		Forms heterodimer with Cap1, binds barbed end of actin to prevent elongation, binds Twf1
	Sac6	Fimbrin	CH	Actin bundling protein, deletion with Scp1 results in non-productive sites despite actin polymerization
	Scp1	Transgelin	CH, PR	Binds and cross-links actin filaments, deletion with Sac6 results in non-productive sites despite actin polymerization, binds Abp1
	Twf1	Twinfilin	ADFH	Actin monomer sequestering, contains two cofilin-like regions, binds Cap1/2 and Srv2
	Crn1	Coronin	CC, β-propeller	Regulates Arp2/3 complex, trimerizes through CC domain, binds Cof1, and actin
	Cof1	Cofilin	ADFH	Binds ADP-actin filaments to promotes fragmentation and depolymerization, binds Srv2, Crn1, Aip1
	Aip1	Aip1	β-propeller	Binds barbed end of actin after Cof1 severing, binds Cof1 and Srv2
	Srv2	Cyclase-associated protein (CAP)	PR, WH2	Catalylzes cofilin-mediated severing of actin filaments, binds and recycles ADP-actin monomers, binds adenylate cyclase, Cof1, Pfy1, Abp1, Twf1, and Aip1
	Gmf1	GMF	ADFH	Debranches actin filaments, binds Arp2/3
	Bsp1			Links synaptojanins to cortical actin cytoskeleton
	Pfy1	Profilin	SH3	Binds actin, PIP2, polyproline regions, and Srv2
	Aim3		PR, NPF motif	Inhibits barbed-end actin elongation, interacts with Rvs167 and Abp1
Scission (~10 sec)	Rvs161	Amphiphysin	N-BAR	Interacts with Rvs167 and membrane
	Rvs167	Amphiphysin /endophilin	N-BAR, SH3	Ubiquitinated by Rsp5, binds Rvs161, Abp1, Las17, and membrane
	App1			Phosphatidate phosphatase
	Sjl1/2	Synaptojanin -1	PR	PIP2 phosphatase, recruited by SH3 domain of Abp1
	Vps1	Dynamin	GTPase	Dynamin-like GTPase in endocytosis and vacuolar sorting, bundles actin filaments, binds Sla1

Ub processes	Rsp5	Nedd4		E3 Ligase, responsible for ubiquitination of endocytic machinery Ede1, Ent2, and Rvs167, binds Sla1
	Ubp2			Deubiquitinase, de-ubiquitinates Rsp5, Art2, and Ede1
	Ubp7/11	Usp2		Deubiquitinase, de-ubiquitinates Ede1
	Art1/5	Alpha-arrestin		Alpha-arrestin for Ub-dependent endocytosis, recruits Rsp5
	Art2/Csr2	Alpha-arrestin		Alpha-arrestin for Ub-dependent endocytosis, ubiquitinated by Rsp5, de-ubiquitinated by Ubp2
	Rog3/Rod1	Alpha-arrestin		Alpha-arrestin for Ub-dependent endocytosis
	Aly1/2	Alpha-arrestin		Alpha-arrestin for Ub-dependent endocytosis, recruits Rsp5
Other	Arf3	Arf6		GTPase of Ras superfamily, localizes to plasma membrane and modulates PtdIns(4,5)P2 levels to facilitate endocytosis
	Ark1/Prk1/Akl1	GAK/AAK1	PR, Ser/Thr Kinase	Kinases, phosphorylate Pan1, Ent1/2, Sla1, Yap1801/2, and Scd5 during uncoating, deletion has cytosolic aggregates of coat proteins, membrane, and actin, binds Abp1
	Swa2	Auxilin		Involved in clathrin uncoating, is heavily phosphorylated, ubiquitin binding
	Mss4			Phosphatidylinositol-4-phosphate 5-kinase
	Glc7			PP1 protein phosphatase, binds Sla1 and Scd5

Table 1.2: Common binding partners of some domains and motifs found in the endocytic machinery

Domain	Binding partner
Acidic motif	Arp2/3 complex
ADFH	F-actin
ANTH	PIP2
Clathrin box motif (CBM)	Clathrin heavy chain
Coiled coil (CC)	Oligomerization or other
EH	NPF motif
ENTH	PIP2
F-BAR/N-BAR	Membrane
NPF motif	EH domain
Proline-rich (PR)/Polyproline motif	SH3 domain
SH3	Polyproline motif (Ub in Sla1)
SHD1	NPFXD sequence
SHD2	SHD2 oligermization, CBM
TH1	Membrane
TH2	F-actin
THATCH	F-actin
UBA	Ubiquitin
UIM	Ubiquitin
WH1	Proline-rich (PR) domain
WH2	G-actin (F-actin in Pan1)

domains of the endocytic machinery indicated in Table 1.1. Abbreviations are listed in Appendix 2. Though many proteins have been identified and functions defined for many of them, unresolved aspects of CME demonstrate there may be proteins, functions, or regulators of the process that are still unknown.

Proteins involved in the clathrin-mediated endocytic machinery have a finely choreographed order of arrival and dispersal from the endocytic site that is predictable and reproducible at each individual site (Figure 1.1) [18]. The process can be divided into distinct modules in which proteins of specific functions or sub-processes are recruited (Table 1.1) [19]. First, coat proteins assemble on the membrane forming scaffolding interactions and binding cargo, clathrin, membrane, and other coat proteins, forming the base network of protein interactions for endocytic coat structure. The earliest arriving coat proteins have a variable patch lifetime, while intermediate and late arriving coat proteins have more precise lifetimes (patch lifetime refers to time the fluorescent labeled protein is visible at the endocytic site). After coat proteins, proteins of the WASP/MYO module arrive, which consists of actin regulatory proteins that are recruited and controlled by coat proteins. These proteins then initialize actin polymerization. The actin module is characterized by robust branched actin polymerization nucleated by the Arp2/3 complex and presence of numerous actin-binding, stabilizing, and depolymerizing proteins. Finally, the scission module, with a short 10 second patch lifetime, indicates completion of the vesicle and movement to the cell interior. Additionally listed in Table 1.1 are proteins involved in ubiquitin regulatory processes in CME, which are important for cargo internalization and machinery interactions, and proteins involved in protein and lipid phosphoregulation, which play important roles in scission and uncoating.

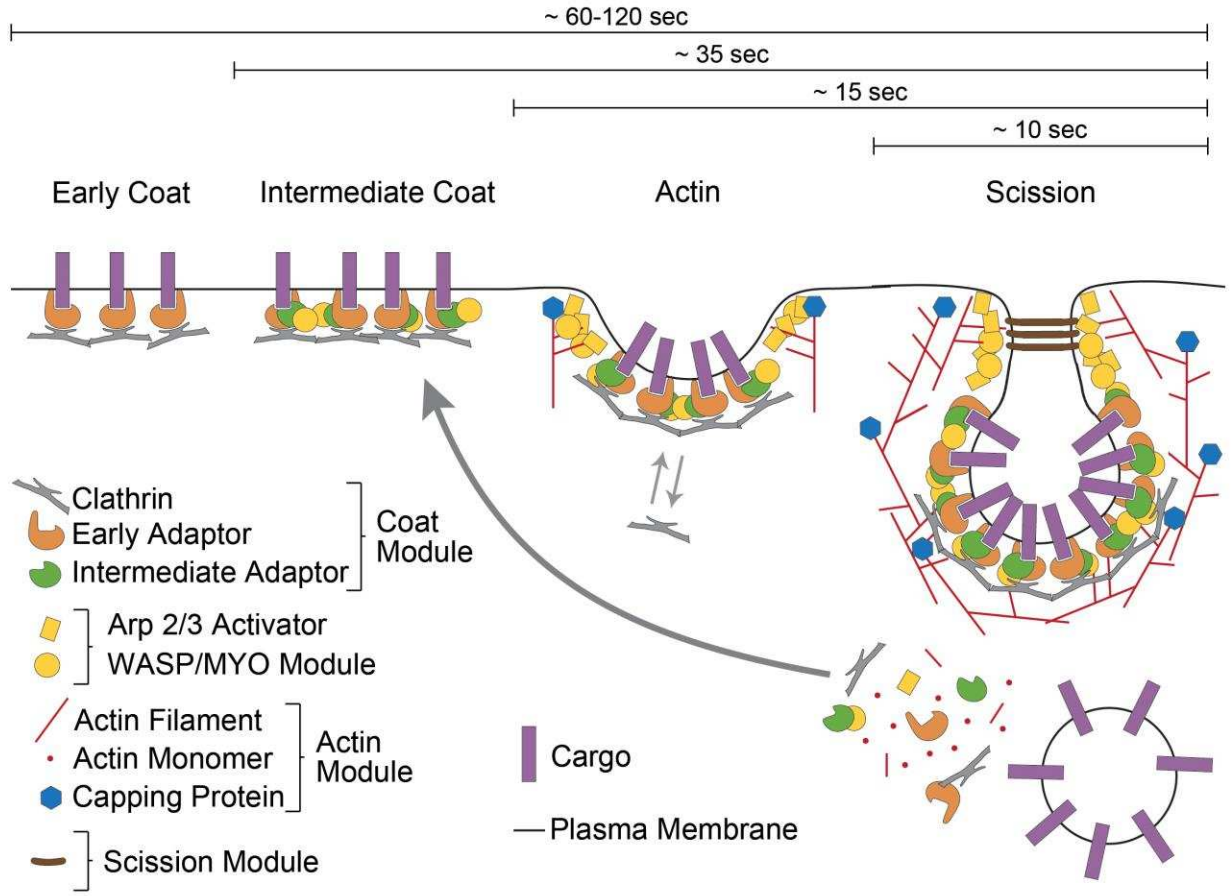

Figure 1.1: Modules of clathrin-mediated endocytosis. Coat proteins arrive first at the endocytic site, linking cargo with clathrin, and have a variable lifetime. Some Arp2/3 activators and regulators arrive with the intermediate coat and promote actin polymerization during the last ~15 seconds. Actin and actin-associated proteins arrive and produce membrane invagination and scission proteins complete invagination and pinch off the vesicle. Proteins are then recycled to a new endocytic site.

Clathrin, the namesake coat protein of CME, consists of two proteins: clathrin heavy chain (Chc1) and clathrin light chain (Clc1). A clathrin triskelion is formed from three heavy chains and three light chains and assembles into a polyhedral lattice. The C-terminus of the heavy chains form a hub at the center of the triskelion where the light chains regulate clathrin actin assembly [20]. In yeast, clathrin-coated endocytic sites are tubular shaped after polymerization, with clathrin located at the tip of the tubule, while other machinery can be distributed along the tubule or close to the membrane (Figure 1.2.B) [21]. Clathrin does not bind directly to the plasma membrane or cargo proteins, and thus requires adaptor proteins for recruitment to the endocytic site. Clathrin adaptors are modular proteins with discrete folded domains linked by unstructured regions which allow numerous simultaneous interactions without steric hindrance (Figure 1.2.A). Often contained in these unstructured regions is a clathrin-binding motif. Clathrin-binding motifs bind to the N-terminal β-propeller of the heavy chain (except for Sla2/Hip1R which bind the light chain) [13]. This terminal domain protrudes inward from the clathrin lattice, allowing interaction with adaptors [6]. The first identified clathrin-binding motif, or clathrin box, was LΦxΦ[DE], where Φ is a bulky hydrophobic residue (leucine, isoleucine, methionine, phenylalanine, or valine) [22]. Later, another clathrin box was identified with the sequence PWDLW. This WXXW motif, termed the W-box, binds at a distinct location on the β-propeller from the classical clathrin box, allowing both motifs to bind simultaneously and non-competitively [23].

Clathrin is present at nearly all endocytic sites in yeast [19], yet knockout of the clathrin heavy or light chain is not lethal in most yeast backgrounds. However, clathrin knockout cells are unhealthy and display a significant reduction in the number of endocytic sites and cargo internalization [19, 24]. Interestingly, mutation of the clathrin box binding region in the clathrin

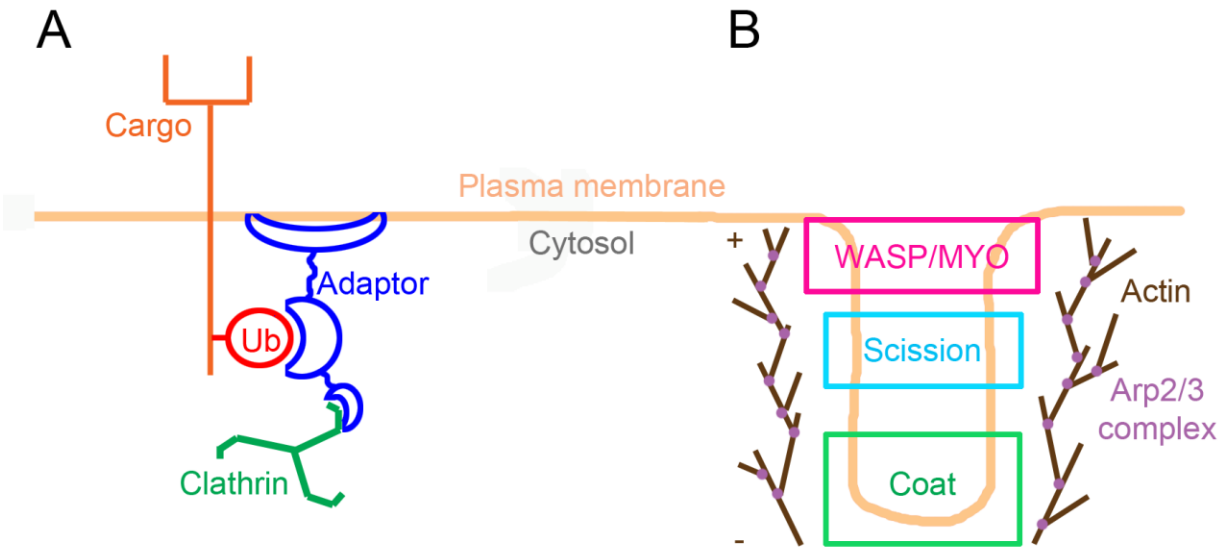

Figure 1.2: Schematics of the organization of proteins at the clathrin-mediated endocytic site. A) Adaptor proteins have folded domains connected by unstructured regions allowing connection between clathrin, cargo, the membrane, actin, and other endocytic proteins. B) The organization of endocytic proteins on the elongated endocytic tubule. WASP/MYO proteins remain close to the membrane while clathrin and other coat proteins internalize at the tip of the tubule. Scission proteins localize to the middle of the tubule, while actin is polymerized around the tubule with monomer addition most likely towards the plasma membrane.

heavy chain does not prevent its recruitment to the endocytic site and endocytosis appears to occur normally [25], though ablation of further predicted binding regions on Chc1 does have significant affects [26]. The adaptor protein AP-2, an important component of mammalian endocytic sites, does not play a vital role in yeast CME. No general endocytic defects are observed in the absence of AP-2, and the heterotetrameric protein has significant structural differences from its mammalian counterpart. Appendage domains, which are responsible for interactions with other coat components in mammalian AP-2, are missing from all except the alpha subunit in yeast [27]. The beta subunit in mammalian cells contains a clathrin box motif and can organize clathrin molecules [20]. The sequence for the yeast beta subunit contains a clathrin box motif, but binding to clathrin has not been demonstrated. The beta subunit does bind the alpha-arrestin Aly2, which is implicated in ubiquitin-dependent endocytosis [28]. Cargo specific roles for AP-2 have also been identified in yeast; AP-2 is necessary for K28 toxicity and localized to endocytic sites [27], and is necessary for efficient trafficking of cell wall stress sensor Mid2 [11] and cargo specific internalization of Snc1 [29]. Many proteins of the early arriving and coat modules are adaptor proteins as they bind (or are predicted to bind) clathrin, cargo, and other components such as phospholipids, actin, or other coat proteins (Figure 1.2). These proteins typically consist of modular domains connected by unstructured regions, as described in the previous section.

Early coat protein Ede1 is important for recruitment of other coat proteins and initiation of endocytic sites. Ede1 contains three epsin homology (EH) domains and a C-terminal ubiquitin-binding motif. Deletion of Ede1 has similar, but much milder phenotype, than clathrin disruption; reduction in number of endocytic sites. Phosphorylation of Ede1 by Hrr25 is important for initiation of endocytic sites [30]. Ede1 has also recently been demonstrated to

oligomerize via its coiled coil region and this ability is necessary for its endocytic localization and concentration of endocytic adaptors [31]. Syp1 arrives with Ede1 to early endocytic sites and contains an AP-2 mu homology domain and N-terminal BAR domain [32]. Syp1 is also not crucial for endocytosis in yeast, though it does appear to be important for polarization of endocytic sites [33]. The Syp1 mammalian homologs FCHo1/2, along with Eps15 (Ede1) and intersectin, are required for CME [34]. Syp1 contains a curved membrane-binding F-BAR domain and unstructured central region which binds membrane with high affinity, yet the membrane remains flat during the early stages of endocytosis [34]. Ede1 and Syp1 are important for endocytic site selection, but more factors are required since deletion of both proteins simultaneously still does not abolish endocytic site initiation [35].

Ent1/2 each contain a lipid binding ENTH domain, a clathrin binding clathrin box motif [36], two NPF amino acid motifs ("NPF motif" is distinct from NPFXD amino acid sequences and nucleation promoting factors "NPF") through which Sla1 and Pan1 interact [37], and ubiquitin interacting motifs (UIM). The yeast AP180 adaptor proteins Yap1801 and Yap1802 have overlapping roles to the epsins; they bind lipids through an ANTH domain, have multiple NPF motifs, and bind clathrin [38]. The yeast epsin homologs Ent1 and Ent2 cannot be deleted in their entirety simultaneously, however all four adaptor proteins Ent1/2 and Yap1801/2 can be deleted as long as the ENTH domain of Ent1 is present [39]. The ANTH and ENTH domains bind to PtdIns(4,5)P_2 (PIP2) which is enriched in the inner leaflet of the plasma membrane. Upon membrane binding, a helix is inserted into the membrane, causing it to bend [13]. These domains in Sla2 and Ent1 co-assemble into an organized lattice structure that cooperatively binds to the membrane [40].

Early coat proteins can be individually deleted without abolishing clathrin-mediated endocytosis. Furthermore, seven of these proteins were deleted simultaneously (Ede1, Yap1801, Yap1802, Apl1, Syp1, Pal1, Pal2) without halting the endocytic process or greatly altering later stages, but showing a lower number of patches. The early stages are not required for initiation or recruitment of later factors, as clustering of later coat proteins was enough to initiate sites [35]. The early stages of CME in yeast have highly variable timing, ranging from 40 seconds to more than 4 minutes, while the later stages have much more regular lifetimes. This suggests a checkpoint or transition point that must be achieved by early proteins before the later stages can occur. Cargo has been observed to associate with clathrin-coated pits after gathering of initial coat component Ede1 but before Sla1 arrives [41], suggesting this checkpoint may be cargo related. Another possible protein with a checkpoint role is clathrin, as increased patch lifetimes of early stage proteins were observed in a Clc1 deletion [42]. Sla1 is also thought to mediate the transition from middle to late stages of coat formation.

Pan1 and End3 associate and arrive at the endocytic site slightly before Sla1, with the End3 C-terminus necessary for interaction with Pan1 and N-terminus recruiting Sla1. Pan1 is the only endocytic coat protein essential for cell viability and acts as a scaffold to many endocytic coat proteins [16]. The full Sla1/End3/Pan1 complex has also been shown to link actin assembly to endocytic site initiation [43].

Sla1 interacts with cargo containing an NPFXD amino acid motif via its SHD1 domain [44]. This sequence is found in endogenous CME cargoes Wsc1, mating pheromone receptors Ste2 and Ste3, and flipases Drs2 and Dnf1 [45, 46]. Sla1 also binds clathrin, which arrives at the endocytic site before Sla1, through a clathrin box motif variant which is regulated by its SHD2 domain. The SHD2 domain is a sterile α-motif domain with the ability to oligomerize [47]. Sla1

binds Pan1 and End3 by its C-terminal SR domain, and is also in a stable complex with the proline-rich domain of Las17 via its SH3 domains (Table 1.1) [48]. Sla1 exists in a ring around the extending membrane tubule, and between 50-100 molecules of Sla1 are present during its peak at the endocytic site [49].

Sla2 translates actin polymerization to membrane bending through binding of actin filaments (THATCH domain), the membrane (ANTH domain), coat proteins (coiled coil region), and clathrin light chain. With a Sla2 deletion, early endocytic components are recruited, but actin polymerization is non-productive, resulting in comet tails of actin initiating from the endocytic site without producing membrane invagination [18]. Advanced microscopy methods revealed Sla2 in an extended conformation at the endocytic site with its N-terminus near the membrane and C-terminus extended 30 nm outward [49]. This span would allow simultaneous interaction with the membrane, the clathrin lattice, and actin.

Many associations between endocytic coat proteins are mediated by multiple low affinity interactions. An example of this is the binding of SH3 domains to polyproline motifs (PXXP). Proline-rich (PR) domains, which contain polyproline motifs, as well as SH3 domains are common among endocytic machinery (Table 1.1). The first two SH3 domains of Sla1 bind the proline-rich (PR) region of Las17 to inhibit its Arp2/3 nucleation activity [48]. Bzz1 may alleviate the inhibition of Las17 by competing off Sla1 via its SH3 domain. The SH3 domains of Lsb3 and Ysc84 are suggested to recruit and assemble many endocytic proteins [50]. Bbc1 contains an SH3 domain as well as PR domain which interacts with Myo3/5, which contain SH3 domains themselves and associate with the Vrp1 PR domain. An Abp1 SH3 domain recruits Sjl1/2, while it also contains a PR domain. Many proteins in the system contain both PR domains and SH3 domains, allowing multiple sites for regulation and interaction. A variation of

these binding partners is the third SH3 domain of Sla1 which binds ubiquitin opposed to the canonical polyproline motif [51]. EH domain binding to the NPF amino acid motif is another low affinity interaction displayed by multiple proteins of the endocytic machinery, mediating interactions of numerous proteins.

BAR domains are also found in multiple proteins of the endocytic machinery and are vital for membrane binding and curvature. BAR domains are made up of three α-helices that wrap round each other to form a long curved helical bundle, which dimerizes to form an elongated banana-shape [52]. Positively charged residues on the concave surfaces of BAR domain homodimers interact with negatively charged lipid headgroups preferentially binding curved membranes and forming tubules when bound to membrane at high concentrations [6]. Combined with the force from actin polymerization, BAR domains stabilize the transition from a flat membrane to tubular structure [53]. Syp1, Bzz1, and Rvs161/7 are BAR domain-containing proteins found throughout stages of the endocytic machinery.

Actin polymerization at the endocytic site is highly regulated and drives membrane invagination. Many components of the WASP/MYO module which regulate and promote actin polymerization can be replaced with a single engineered protein which revealed the requirement for a membrane-actin linkage, with corresponding recruitment to the endocytic site and Arp2/3 activation, during this phase [54]. Despite this, numerous proteins are recruited in the WASP/MYO and actin modules of endocytosis. A variety of actin binding and depolymerizing proteins are also seen at the endocytic site. Actin-associated proteins are discussed in the following section. In the final stages of endocytosis, a transition from a stationary to a highly mobile site is observed, with this movement directed toward the cell center [18].

The scission module completes vesicle internalization and breaks the connection with the plasma membrane. Amphiphysins Rvs161 and Rvs167 are thought to enhance tubulation and scission. Rvs161/7 bind the membrane via their BAR domains and form heterodimers at the neck of the endocytic tubule between the clathrin-coated tip and the base of the invagination [21]. Movement of endocytic proteins is observed at the peak of Rvs161/Rvs167 fluorescence, and deletion of these proteins causes retraction of the membrane tubule in many cases indicating their role in scission [19]. Dynamin was first thought to play little role in yeast endocytosis based on lack of endocytic defect upon deletion. However, recent studies have now visualized Vps1, the yeast homolog of dynamin, at the endocytic site and have observed a modest retraction phenotype upon deletion [55, 56]. Vps1 has also been demonstrated to bind and bundle actin at the endocytic site and mutation of the actin binding site causes elongated pits characteristic of a scission defect [57].

A model for how scission occurs portrays the N-BAR domain-containing amphiphysins and other PIP2-binding proteins as creating a protected region from phosphatases Sjl1/2. Dephosphorylation of PIP2 outside the protected region creates a charge differential and lipid boundary, which combined with tension from actin polymerization, creates energetically favorable scission [58]. This is supported by observations that deletion of the Synaptojanin homologs Sjl1/2 cause a stalled elongated tubule [59], and deletion of the amphiphysins cause retraction or other inconsistent patch behavior [18]. Membranes at endocytic sites are enriched in PIP2 when coat factors are recruited, but this enrichment disappears upon scission. Mss4 PIP kinase and Sjl1/2 PIP2 phosphatase deletions both show endocytic defects despite the diffuse localization of Mss4 throughout the membrane under normal conditions [17]. Other lipids such

as sphingolipids and ergosterol may also be important for endocytosis but their roles are still unclear [17].

Uncoating of the internalized vesicle allows recycling of coat components and interaction of the vesicle with its correct cellular components. Synaptojanin-mediated dephosphorylation of PIP2s promotes release of PIP2 binding by Sla2, Ent1/2, and Yap1801/2 [60]. The Ark1 and Prk1 kinases phosphorylate a number of endocytic coat components, including Pan1, Ent1/2, Sla1, Yap1801/2, and Scd5, to promote dissociation. Deletion of these kinases causes cytosolic aggregates of coat proteins, membrane, and actin, indicating incomplete uncoating [34, 61]. Scd5 then targets Glc7 protein phosphatase 1 to endocytic components that were phosphorylated by Ark1/Prk1, allowing recycling of components to new endocytic sites [62]. Without Scd5, Sla2 and Sla1 lifetimes were increased and Sla1 recruitment was severely decreased [63]. Uncoating occurs after vesicle internalization, as clathrin is visualized moving 200 nm inwards before disappearing [19], as endocytic vesicles move towards early endosomes on actin cables [41]. Prk1 also inhibits Pan1 actin binding and NPF activity, causing negative regulation of actin assembly [64]. The branched actin network is also broken down following scission, though later than the coat proteins, as detailed in the following section.

1.2.3 Actin polymerization and regulation in clathrin-mediated endocytosis

Actin is a globular protein that can polymerize to form filaments with various structural and trafficking functions in the cell. Filaments have a barbed or plus end, which is enriched in ATP-bound actin monomers and undergoes high levels of monomer addition for elongation, and a pointed or minus end, which is enriched in ADP-bound actin and undergoes low levels of monomer addition. ATP bound by actin subunits is hydrolyzed to ADP•Pi and Pi is released to

leave ADP-bound actin subunits. Yeast cells contain three distinct actin structures: cortical actin patches, actin cables, and the cytokinetic ring. Cortical actin patches were first observed in fixed cells more than thirty years ago [65], though their connection with endocytosis was not appreciated until immuno-electron microscopy correlated these patches with membrane invagination [66]. A requirement for proteins of the actin cytoskeleton in CME was recognized early in the investigation into the process [67, 68], and was further confirmed with two-color fluorescent microscopy [18].

Treatment of cells with Latrunculin A (LatA) ablates cortical actin patches [69], and sequestering actin monomers with Latrunculin, or stabilizing actin with jasplakinolide prevents endocytosis. Stalling of coat components at the membrane in LatA treated cells showed that the initial stages of endocytosis occur without actin, but polymerization is necessary for vesicle internalization [18, 19]. Proteins dependent on filamentous actin for recruitment to the endocytic site such as Cap1/2, Sac6, and Rvs161 portray a diffuse cytosolic localization upon LatA treatment [19]. The requirement for actin polymerization is caused by the high turgor pressure in yeast. Reduction of turgor pressure with sorbitol reduced the requirement for actin-bundling proteins Sac6 and Scp1 in CME, while increased turgor pressure reduced the success rate of endocytic internalization to 10% and greatly increased Abp1 patch lifetime [70].

Unsurprisingly, based on the observations of actin requirement for endocytosis and appearance of cortical actin patches, the Arp2/3 complex components and actin portray some of the highest number of molecules of any protein recruited to the endocytic site. Based on these quantifications, the average actin filament length would be about 40 nm [49], indicating a densely branched actin network. Loss of unbranched actin filament nucleator formin does not result in any defect in endocytosis or cortical actin polymerization [71]. In branched actin

filament networks, a nucleation promoting factor (NPF) activates the Arp2/3 complex. The Arp2/3 complex nucleates the formation of a new actin filament, or branch, at a 70˚ angle from a mother filament [72, 73]. The Arp2/3 complex in yeast consists of five proteins (Arc15, Arc18, Arc19, Arc35, and Arc40) that provide the structural framework for two actin-related proteins (Arp2 and Arp3) which contribute the first two subunits of the new filament [74]. Both binding to a mother filament and an NPF are necessary to provide a conformational change in the Arp2/3 complex to a "closed" state, or primed for nucleation conformation, to initiate actin filament elongation [16].

There are five known NPFs in endocytosis: Pan1, Las17, Myo3, Myo5, and Abp1. Mutation of the NPF domains of Las17 and Myo3/5 result in patches that fail to internalize, similar to the phenotype of LatA treatment [18], while Pan1 and Abp1 have relatively weak NPF activity. Other endocytic proteins control the ability of these NPFs to activate Arp2/3. Pan1 and Las17 arrive well before actin polymerization, indicating the requirement for inhibition to prevent early actin initiation. Pan1 is negatively regulated by Sla2 [75], while Las17 is inhibited by Sla1 and Syp1 [48, 76]. Las17, the strongest NPF, contains two actin binding motifs: a WH2 motif which binds G-actin and an arginine-dependent Las17 G-actin binding motif (LGM). In addition, a central acidic motif binds the Arp2/3 complex. All of these Las17-actin interactions are important for normal actin dynamics at the endocytic site [77]. Bzz1 and Vrp1 arrive with the exit of Syp1 from the endocytic site, conceivably recruiting the first actin molecules to the site. Bzz1 may also lift the regulation of Las17 by competing for binding of Sla1[34]. Bzz1 binds Las17 via its SH3 domains and dimerizes via its F-BAR domains, remaining at the base of the tubulating membrane [16]. Components of the WASP/MYO module generally do not

internalize with the vesicle but stay near the plasma membrane (Figure 1.2) [19], as demonstrated with Las17, Bzz1, and Myo5 [49].

Vrp1 recruits type-1 myosins Myo3 and Myo5, which are held inactive by calmodulin in the cytosol before recruitment [78]. Myo3 and Myo5 are type 1 unconventional myosins due to their single-headed non-processive motor activity and lipid association. Myo3/5 are functionally redundant as both must be deleted to cause severe endocytic and actin defects [16]. Deletion of Vrp1 or both myosins results in endocytic patches defective in inward movement, suggesting these proteins provide force for membrane bending [79]. Actin nucleation, motor activity, and membrane anchoring are all essential to produce directional force for internalization [54]. The weak NPF activity of Abp1 is poorly understood, and seems to require the presence of other proteins such as Vrp1. NPF inhibitor Bbc1 arrives late in the process to prevent excessive actin polymerization and may play a role in termination of nucleation, yet this is not fully understood [34]. Aim21 localizes to the actin patch similar to actin regulatory proteins, but its function is not known.

This network of proteins is only part of the actin module, tightly regulating initiation of actin polymerization through activation of the Arp2/3 complex. Actin filaments are further regulated once nucleation has occurred. The concentration of actin in the yeast cytosol is well above the critical concentration for assembly, thus proteins must prevent the excessive growth of actin filaments. Profilin binds actin monomers which prevents their addition to pointed ends, thus restricting addition to only the barbed ends of actin filaments [16]. The barbed ends of actin filaments are bound by heterodimeric actin capping proteins (CPs), Cap1 and Cap2 in yeast [80], which prevent further elongation of the filament and thereby promotes a denser network of shorter actin filaments [81]. Deletion of a single CP prevents formation of the complex, leaving

a single CP unable to bind the actin filament. Knockout of either CP increases the amount of actin present at the endocytic site and patch lifetimes of actin associated proteins [19]. Aip1 and Cap1/2 work together to prevent elongation of cofilin-bound ADP-actin, and Abp1 and Aim3 also collaborate with CPs to prevent elongation of newly formed filaments and direct the polarity of fragments in the actin network [82]. Aip1 deletion changes localization of CPs from near the plasma membrane to a more uniform distribution throughout the actin patch, suggesting competition between these barbed end binding proteins [82]. Mutations of both Aip1 and CPs are synthetic lethal, indicating the importance of regulating barbed end growth [83].

Actin bundling proteins Sac6 and Scp1 are present at the endocytic site and are important for internalization despite the presence of branched actin without obvious bundled filaments. Deletion of Sac6 abolished inward movement despite presence of Abp1 which labels filamentous actin at the endocytic site [19]. Though deletion of Scp1 alone has no clear defects, in combination with Sac6 extensive abnormalities in endocytosis and actin are observed [84]. When Abp1 is deleted, Sla1 persists into the fast movement phase instead of dissociating as occurs in wild type cells. Sac6 also persists longer after vesicle movement into the cytoplasm, suggesting Abp1 may have a role in uncoating and depolymerization [19]. Additional potential actin bundling and stabilizing proteins localize to the endocytic site, such as Abp140 and Tef1/2, but their roles are still under investigation [16].

Actin filament disassembly factors arrive only 3-7 seconds after the initial stages of actin assembly [85]. Cof1, Aip1, and Crn1 are recruited to the endocytic site after the peak of actin polymerization, coinciding with disassembly [86]. ADP-bound actin filaments are bound by cofilin (Cof1) [87] which stimulates actin filament disassembly [88]. Multiple Cof1 molecules can bind to an actin filament, producing twisting in the filament leading to severing [89], while

Crn1 directs Cof1 binding to older actin filaments. Aip1 binds the newly exposed barbed ends of actin after severing [90] and converts fragments to monomers [85], while Srv2 binds Cof1 to displace it from actin [91]. The Cof1 gene is essential in yeast, and Cof1 or Crn1 mutants result in longer actin lifetime at the membrane prior to internalization, and further inward movement upon mobilization [86]. Filaments with a V159N mutation in actin depolymerize slowly, causing increased amounts of actin at endocytic patches and reduced levels of endocytic internalization, as well as synthetic lethality with Cof1 or Pfy1 mutants [92]. Gmf1, a protein with structural similarity to cofilin, catalyzes de-branching of actin filaments with preferential binding to ADP-Arp2/3 [16]. Twf1 may also have a similar role in actin turnover or actin monomer sequestering, but its role is still unclear [16]. Actin binding proteins are visualized moving into the cell with the vesicle for several seconds after endocytic proteins have dissociated, indicating depolymerization occurs parallel with and after uncoating [93].

As stated previously, the activation of the Arp2/3 complex requires both a NPF and a mother filament for conformational change. The origin of the required mother filament is an outstanding question in the field. One study indicates cofilin-induced depolymerization produces small actin filament fragments which are then incorporated into new endocytic sites as mother filaments for Arp2/3 nucleation of branches [94]. Other theories for the Arp2/3 mother filament include recruitment of sufficient actin monomers to the endocytic site to form a binding site for the complex (such as Las17 which contains multiple actin binding motifs), or sufficient conformational change in the Arp2/3 complex induced by binding to the endocytic machinery itself [16].

The direction of actin monomer addition, either towards the membrane or towards the tip of the invaginating vesicle, has also been debated. Observations detailing both directions have

been published; barbed ends toward the cytosol [95, 96], and monomer addition to barbed ends near the membrane [18, 19, 49]. In support of monomer addition near the membrane, PIP2 has been shown to weaken interactions between CP and actin filament barbed ends, suggesting that higher availability of barbed ends closer to the membrane can direct actin growth [97].

1.2.4 Roles of ubiquitin in clathrin-mediated endocytosis

Ubiquitin is a highly conserved 76 amino acid protein that is covalently linked to the lysine residue on a target protein by sequential enzymes E1 (Ub-activating), E2 (Ub-conjugating), and E3 (Ub-ligase). Ubiquitination is a reversible process reversed by de-ubiquitinases (DUBs) that hydrolyze the ubiquitin-protein isopeptide bond. Ubiquitin serves as a signal for internalization of cargo proteins into the endocytic pathway, and also acts as a regulator of the endocytic machinery. An important role for ubiquitin in CME was realized early in its investigation [98], and its recognition as a signal for cargo internalization was demonstrated with a Ub-fusion to a receptor protein [99]. Additionally, transmembrane proteins accumulated ubiquitinated forms in yeast strains defective in endocytosis [100].

Upon ligand binding to receptor, transmembrane proteins are rapidly ubiquitinated on the cytosolic tail. This mono-ubiquitination or multiple mono-ubiquitinations acts as a signal for internalization [101]. The specificity of ubiquitin addition to proteins is regulated by E3 ubiquitin ligases. Ubiquitination of cargo molecules is carried out by the Nedd4 homolog E3 ubiquitinase Rsp5, which contains WW domains that recognize PPXY motifs on target proteins. Mutagenesis of different WW domains in Rsp5 inhibits both ubiquitination and internalization/degradation of activated Ste2, the alpha factor rector [102], as well as other specific cargoes. Ubiquitination of the cargo further acts as a signal at the endosome for delivery

to the vacuole for degradation [100]. However, cargoes containing a ubiquitin fusion still require Rsp5 to be internalized, suggesting ubiquitination of machinery is also essential for endocytic function [102].

Ubiquitin-binding domains present in endocytic machinery include the ubiquitin-interacting motif (UIM), ubiquitin-associated (UBA) domain, and the third SH3 domain of Sla1 [51]. Epsin homologs Ent1 and Ent2 each contain a UIM and Ede1 and Gts1 each contain a UBA (Table 1.1). However, it is still unclear which coat proteins act as adaptors for ubiquitinated cargo. The UIMs of Ent1/2 and the UBA of Ede1 can be deleted and ubiquitinated cargoes are still internalized as efficiently as non-ubiquitin dependent cargoes [103], which could be due to the ubiquitin-binding ability of the third SH3 domain of Sla1 [51]. This also could suggest these ubiquitin-interaction motifs act as mediators of machinery protein-protein interaction, rather than in cargo recognition. Endocytic machinery Ede1, Ent2, and Rvs167 are ubiquitinated by E3 ligase Rsp5. Rsp5 itself is also ubiquitinated and its de-ubiquitination is mediated by DUB Ubp2 [104]. Many more endocytic machinery components have been shown to be ubiquitinated *in vitro*, suggesting more proteins could be involved in a ubiquitin-binding interaction network [17]. Ent1/2 and Yap1801/2, though functionally redundant, likely stabilize the huge array of protein interactions via their EH domain-NPF motif interactions and UIM-ubiquitin interactions [39]. The ubiquitination and de-ubiquitination of Ede1 has been demonstrated to be essential for its endocytic function and recruitment; a deletion of the DUBs Ubp2 and Ubp7 result in elongated endocytic patch lifetimes and recruitment of endocytic factors to internal structures while deletion of Ede1 abrogated these phenotypes and permanent ubiquitination of Ede1 replicated these phenotypes [105].

An additional class of molecules implicated in the ubiquitin dependent processes of clathrin-mediated endocytosis is the alpha-arrestins. Many Rsp5 target proteins lack PPXY motifs that bind the Rsp5 WW domains. Alpha-arrestins, which contain these PPXY motifs, target specific transmembrane proteins to the endocytic system by recruiting Rsp5 to ubiquitinate cargoes [9]. Alpha-arrestin Rod1 was demonstrated to be activated in response to glucose addition, relaying signaling to transporter endocytosis [106]. Coupling Rsp5 to specific transmembrane proteins through these arrestin-related trafficking adaptors allows cargo specific down-regulation by endocytosis [9]. Recent studies show mammalian alpha-arrestins also regulated ubiquitin-dependent endocytosis [107]. The exact mechanisms governing this newly identified ubiquitination route are still under investigation.

1.2.5 Clathrin-mediated endocytosis in mammals

Yeast and mammalian cells have highly conserved components, timing, and function of clathrin-mediated endocytosis [108, 109]. Clathrin, adaptor, and coat proteins arrive early in mammalian CME, followed by actin polymerization, scission, and uncoating. Most yeast CME proteins have homology to mammalian proteins, whether individually or as a combination of yeast proteins making up the domains of a single mammalian protein (Table 1.1), suggesting the network of interactions that hold together the machinery are conserved. Both yeast and mammals utilize ubiquitination as well as short sequences of amino acids as signals for cargo internalization, which is further described in Appendix 1.

Initiation of the mammalian endocytic site is suggested to be highly dependent on membrane bending by FCho1/2 and the presence of AP-2 and clathrin, but in yeast the deletion of homologous proteins has less effect and initiation seems to be more variable and not

dependent on a single or even multiple proteins [35]. Deletion of Eps15 and FCho1/2 in mammalian cells results in abortion of coat assembly [110] whereas these homologs and many more can be deleted in yeast [35]. Depletion of clathrin in mammalian cells completely arrests CME, suggesting it plays an essential structural role in mammalian cells while clathrin is not strictly required in yeast [16]. In yeast, clathrin appears only at the tip of the membrane tubule, while more vesicle coverage is seen in mammalian cell EM images [111]. AP-2 also has a much more central role in CME in mammalian cells than yeast, where deletion has little effect, while knockdown of AP-2 has striking effects on mammalian CME [112]. In yeast, only AP-1 has been demonstrated to bind clathrin. AP-2 and AP-3 complexes also exist in yeast, but are not known to bind clathrin [113].

Actin plays many roles in mammalian cells, such as cell cortex maintenance and cell mobility that do not occur in the yeast actin network. Actin also participates in cellular uptake through phagocytosis and clathrin-independent endocytosis, as well as cytoplasmic streaming, formation of lamellipodia and filopodia, and other functions. Disruption of the actin cytoskeleton in mammalian cells causes widespread phenotypes, rather than solely endocytic defects, making it difficult to demonstrate actin related endocytic dependence. Early studies reported varying degrees of dependence of CME on actin in mammalian cells, though now the actin requirement in mammals has been similarly linked to membrane tension as demonstrated in yeast [114]. CME is shut down during mitosis in mammalian cells, but has been demonstrated to restart when actin is available, suggesting the increased membrane tension during mitosis is the cause for the endocytic halt [115]. Actin has been visualized at mammalian endocytic sites as well as Las17 homolog WASp and its regulators by EM and fluorescent microscopy [95, 116]. The mammalian Sla2 homolog HIP1R contains an actin binding motif, functionally connecting

clathrin with actin in mammalian cells. Additionally, actin polymerization precedes and promotes dynamin recruitment and many actin regulators interact with dynamin [117].

Mammalian amphiphysin contains a canonical clathrin box as well as a clathrin-binding W-box motif [23], while the yeast amphiphysins have not been shown to bind clathrin. Scission of the endocytic vesicle in mammals is dependent on dynamin, which forms 13 dimers to create a helical structure around the neck of the vesicle [117]. Inhibition of the dynamin GTPase activity results in loss of successful scission, whereas in yeast only a minor defect upon dynamin deletion is observed [56]. Uncoating in mammalian endocytosis relies heavily on auxilin recruitment of Hsc70, and Hsc70 recognition of clathrin is necessary for efficient uncoating [6]. Auxilin and Hsc70 yeast homologs (Swa2 and Ssa1/2 respectively) have similar functions between species but have not been demonstrated in CME-specific roles in yeast.

Much of the work performed in mammalian endocytosis follows the specific cargoes Transferrin receptor and LDLR, which are not present in yeast. The reverse is also true; in yeast, many cargo proteins have been studied that are not present in mammalian cells such as cell wall synthesis enzymes and mating pheromone receptors. Molecular inhibitors of CME have been developed for mammalian cells including dynamin inhibitor Dynasore and clathrin competitive inhibitor Pitstop2, while LatA effectively halts yeast CME allowing analogous studies. Sufficient similarities between processes allow yeast studies to be applied to mammalian cells and human disease.

1.2.6 Implications for clathrin-mediated endocytosis in human disease

As clathrin-mediated endocytosis is fundamental and pervasive eukaryotic process, errors in its function can cause serious and diverse maladies. Furthermore, pathogen hijacking of the

normal CME process can result in illness. Clathrin-mediated endocytosis is the means for internalization of many viruses, including Influenza, Hepatitis C, and rabies [118]. A/B toxins such as Ricin, Shiga, and Cholera toxins also depend on endocytosis and trafficking for toxicity [27].

HIV also uses normal CME to evade the immune system via its Nef protein inducing internalization of the CD4 molecules on helper T cells, causing reduction of expression of class I MHC molecules on infected T cells [20]. Clathrin-mediated endocytosis also has numerous native immune system functions which cause illness upon disruption. Endocytosis helps regulate the cell surface expression of antigen receptors and signaling molecules, as well as in the process of sorting molecules for antigen processing and presentation by class II histocompatibility molecules [20]. Wiskott-Aldrich syndrome is an immunodeficiency caused by mutations in the Wiskott-Aldrich syndrome protein (WASp), the Las17 homolog, which cause defects in the actin cytoskeleton of hematopoietic cells [119]. *Listeria monocytogenes* hijack normal actin polymerization processes to move within the cytoplasm of an infected cell and invade adjacent cells. These bacteria express protein ActA, a mimic of WASp, which enduces actin polymerization by the Arp2/3 complex and creating an actin comet tail at the surface of the bacteria [120].

In neurons, clathrin coated vesicles are required for the reformation of synaptic vesicles following exocytosis of transmitters. However, recent studies indicate that endocytosis from the synaptic membrane may be clathrin-independent and clathrin is only involved in generation of vesicles from the endosome [121]. Clathrin-mediated endocytosis is also required for the processing of amyloid precursor protein to Aβ, which forms plaques characteristic of Alzheimer's disease. This processing occurs in endosomes after internalization by CME, and

cells and mice deficient in endocytosis produce less Aβ [122]. Mislocalization of clathrin light chain and reduction in AP-2 and AP180 expression have been observed in the brain of Alzheimer's patients [20].

Maintenance of cell polarity is also mediated by clathrin-mediated endocytosis and vesicular trafficking. Many cell types maintain apical and basolateral membrane polarization, which is essential for their function, such as the intestinal epithelium. Incorrect removal or lack of removal of proteins from specific cell surfaces can cause serious pathological conditions. The dependence of polarity on CME is demonstrated in yeast with cargo protein Wsc1. A mutation in the amino acid endocytic signal or mutation of the adaptor protein recognition results in loss of polarity of this protein to the bud, further resulting in inappropriate cell wall synthesis around the mother cell [10]. Loss of cell polarity is often observed in tumors, and trafficking disruption of growth factor receptors and integrin/cadherin adhesion complexes are also observed in cancers [123].

Additional diseases result from mutations in CME cargo or adaptor protein recognition of cargo. Liddle's syndrome is a hereditary form of arterial hypertension caused by mutation of amiloride-sensitive epithelial Na+ channel (ENaC), stabilizing it on apical membranes. The PPXY motif of this protein is mutated, preventing ubiquitination by Nedd4 and consequent endocytosis [124]. Familial hypercholesterolemia, a disease characterized by high levels of LDL, is caused by mutations in the LDL particle receptor (LDLR) which cause it to not be internalized by clathrin-mediated endocytosis upon particle binding [125]. Hereditary hemochromatosis is disruption of iron metabolism caused by mutation in the protein recognizing the transferrin receptor and misregulating internalization [126].

Numerous and diverse human diseases are caused by errors in clathrin-mediated endocytic processing, machinery, or cargo. Pathogens can also hijack this system for cellular entry and toxicity. Many more ailments not listed here are involved with clathrin-mediated endocytosis, marking this basic cellular process as an important area of continued research.

1.3 Yeast and the GFP library

1.3.1 Yeast as a model system

Human manipulation of the budding yeast *Saccharomyces cerevisiae* dates back thousands of years and has evolved with time. The fermentation process which creates carbon dioxide and ethanol has been vital to baking and alcoholic beverage production for the entirety of budding yeast history. More recently, yeast has been recognized for its nutritional value and biotechnology has expanded yeast use to biofuel and pharmaceutical production. In the past century, this organism has also played an important role in cell biology research.

Budding yeast have many technical advantages in research such as quick division rate, cost effectiveness, non-pathogenic, well-defined genetics, single cellularity, and competence for transformation and genetic manipulation. Additionally as a eukaryote, yeast portray a much higher homology rate with mammalian cells than bacteria, which have many of the same technical advantages. Yeast have 16 chromosomes existing in a stable haploid or diploid state, allowing easy blending of strains that can be separated by micromanipulator for manifestation of recessive traits. Few yeast genes contain introns and the *S. cerevisiae* genome is dense with 72% consisting of open reading frames (ORFs), thus reducing complications from splicing variants and allowing replication of genes directly from genomic DNA without creation of a cDNA library. The ability of yeast to undergo transformation, express and replicate plasmids, and

perform homologous recombination has allowed this species to become an essential model system for eukaryotic cell biology. Engineered DNA sequences can be added to or replace endogenous sequences allowing full gene knockouts without reliance on siRNA or similar mammalian techniques. It was the first eukaryotic genome sequenced in 1996, and now entire sequences of multiple strains are available. Sequences and up to date research information on every gene in the yeast genome are available in the *Saccharomyces* Genome Database (www.yeastgenome.org) [127]. The high homology rate of many yeast genes with those implicated in human disease allows study and genetic manipulation of these genes and proteins in a simpler organism [128].

Laboratory strains of *S. cerevisiae* all carry some array of genetic modifications or mutations; no strains are truly "wild type". Laboratory strains with deletions in enzymes essential for specific amino acid or nucleotide production allow the quick identification and selection of modified strains. Examples of such strains, YPH501, YPH500, and YPH499, were created with using non-reverting deletion alleles of the URA3, HIS3, TRPl and LEU2 genes via gene replacement techniques using transplacement vectors in the genetic background S288C [129]. The background strain used in this study (BY4741/2) was also derived from S288C for the creation of the deletion library, and contains minimal homology remaining for commonly used marker genes, reducing plasmid integration events [130]. The genotype for this strain can be found in the Material and Methods sections of Chapters 2 and 3.

Yeast are also able to express and replicate plasmids. pRS plasmids with selective markers HIS3, TRPl, LEU2 and URA3 were created with ampicillin resistance for bacterial production [129], and the addition of a yeast centromere sequence and an autonomously replicating sequence resulted in the pRS313-6 yeast plasmids for expression and replication in

yeast [129]. The creation of the pFA6a series of plasmids for PCR, containing selective markers along with GFP, 3HA, and 13-Myc tags, and GAL-inducible promoters, further advanced the ability of those in the yeast field to modify endogenous genes with tagging, overexpression, or deletion through a simple PCR-mediated technique [131]. An efficient method for transformation of DNA fragments and plasmids into yeast was developed using polyethylene glycol and Lithium acetate, which induce binding of DNA to the yeast surface [132]. Foreign DNA is targeted to homologous sequences in the yeast genome, allowing introduction of a tag or disruption of a gene by addition of a selective marker in its place. The ability of laboratory yeast strains to contain multiple selection genes allows changes to multiple genes in a single strain. Additionally, these techniques have allowed creation of multiple commercially available genomic libraries in yeast, including the knockout, TAP-tag, HA-tag, and GFP libraries.

Yeast can also be used to investigate protein interactions from any species using the yeast two-hybrid system. In this method, the transcription activator for a reporter gene is divided into a DNA binding domain and an activation domain. Two proteins of interest are cloned as fusion proteins with these domains. Upon interaction of the proteins of interest, the binding and activation domains are brought together, resulting in transcription of the reporter gene. The benefits and applications for yeast in cell biology research are diverse and are certain to continue expanding for years to come.

1.3.2 Fluorescent microscopy with yeast

Antonie van Leeuwenhoek first observed yeast microscopically in 1680 when he observed what he described as small globular particle. In 1835, Charles Cagniard de la Tour demonstrated by microscopy that yeast were single celled living organisms and multiplied by

budding [127]. Advances in microscopy have further revealed the inner functions of yeast and expanded their use in research; from sporulation and tetrad dissection to subcellular localizations and molecular phenotypes.

Development of the strains and plasmids described in the previous section has allowed fluorescent microscopy to be a standard method to study CME and other processes in yeast. Early experiments confirmed many of the endogenously GFP-tagged and expressed endocytic proteins do not cause growth or endocytic defects in the cell [18, 19]. Two-color fluorescent microscopy has been instrumental in determining the modular dynamics of endocytic proteins, identification of new endocytic factors, as well as description of subtle defects upon mutation or deletion. The size of the endocytic site or clathrin-coated pit, which is approximately 50 nm wide and up to 180 nm long [21], is below that of the diffraction limit for fluorescent microscopy, which is about 250 nm. Thus using fluorescent microscopy, we see diffraction limited discs, which are referred to as fluorescent patches, at the cell cortex. This imagery is useful for confirmation of protein localization to the endocytic site and timing studies, but cannot distinguish membrane shape or precise distribution of proteins at the site. Electron microscopy can distinguish membrane shape and specific localization of proteins with immuno-EM, but can only be performed on fixed cells, allowing only a snapshot of the highly dynamic endocytic process.

Correlative light and electron microscopy (CLEM) has allowed connection of membrane shape with the presence of particular proteins, and showed that membrane bending begins with actin polymerization and scission occurs halfway through the lifetime of Rvs167 [133]. In a fluorescence-based super-resolution method, the centroid positions of each endocytic protein were calculated and aligned with time resolved electron microscopy profiles to detail the

molecular architecture of the endocytic site with a resolution of close to 10 nm, as well as to estimate the number of each molecule at the site [49]. The numbers of molecules estimated using this method were similar to those calculated for clathrin-mediated endocytosis in fission yeast [134].

Fluorescent imaging of clathrin at endocytic sites is difficult due to the high levels of clathrin at interior cell locations such as the endosomes and Golgi. TIRF microscopy is challenging in yeast as the cell wall moves the membrane to the outer limits of the evanescent wave, but CME sites can be imaged using this method to prevent imaging of interior fluorescence, and there has been some success imaging clathrin at the membrane using TIRF [18].

Advances are further being made in super-resolution microscopy as well as quantification and analysis programs. The future for fluorescent microscopy with yeast is bright, and more is still being uncovered about yeast CME even with more traditional fluorescent microscopy methods.

1.3.3 Creation of the yeast GFP library

Yeast genetic techniques have allowed manipulation of the entire yeast genome through simpler and quicker means than in mammalian cells. Expression of proteins with a fluorescent tag from the endogenous locus, as described in Section 1.3.1, has been occurring for longer than recent zinc-finger nucleases or CRISPR-Cas9 technologies have allowed in mammalian cells. Thus the localization for many endogenously expressed GFP-labeled proteins have been established by individual studies without reliance on epitope tagging or overexpression of the protein. GFP signal can be visualized in live cells without disturbing cell function and integrity.

The creation of the yeast GFP library has expanded this endogenous tagging method and fluorescent microscopy technology to a fuller potential.

Creation of the yeast GFP library and subsequent determination of subcellular localization is described in Huh *et al.* 2003 [135]. The yeast GFP library was created using oligonucleotides, replicated with the GFP sequence and HIS3MX6 selective marker, with sequences identical to the C-terminal end of each annotated ORF in the yeast genome. The yeast then incorporate the DNA fragment containing the GFP and selective marker into their genome at the location of the identical sequences. Of the 6,234 ORFs attempted, 6,029 haploid yeast strains were confirmed to have insertion of the GFP and marker sequence. Upon analysis with fluorescent microscopy, 4,156 of these genes expressed GFP above background levels, representing 75% of the yeast proteome. Haploid GFP strains were then mated with cells expressing RFP-fusion proteins of established cellular localization. 1,839 GFP-labeled proteins had specific subcellular localization measured by colocalization with RFP. The localization classifications performed in this study were highly accurate when compared with the manually curated *Saccharomyces* Genome Database and known genetic and physical interactions. Complete lists of subcellular localizations as well as photos of each GFP-expressing strain are available online (yeastgfp.yeastgenome.org). Individual strains as well as the complete library of GFP-tagged ORFs are commercially available.

The screening performed in this study with the yeast GFP library for proteins colocalizing with Sla1 to the clathrin-mediated endocytic machinery is detailed in Chapter 2. Advantages and disadvantages of this method are further discussed in Chapter 4. The creation of the yeast GFP library contributed a valuable resource for yeast cell biology research.

REFERENCES

1. Dalton, A.J. and M.D. Felix, *Cytologic and cytochemical characteristics of the Golgi substance of epithelial cells of the epididymis in situ, in homogenates and after isolation.* Am J Anat, 1954. **94**(2): p. 171-207.
2. Roth, T.F. and K.R. Porter, *Yolk protein uptake in the oocyte of the mosquito Aedes aegypti. L.* J Cell Biol, 1964. **20**: p. 313-32.
3. Pearse, B.M., *Coated vesicles from pig brain: purification and biochemical characterization.* J Mol Biol, 1975. **97**(1): p. 93-8.
4. Heuser, J., *Three-dimensional visualization of coated vesicle formation in fibroblasts.* J Cell Biol, 1980. **84**(3): p. 560-83.
5. Stoorvogel, W., V. Oorschot, and H.J. Geuze, *A novel class of clathrin-coated vesicles budding from endosomes.* J Cell Biol, 1996. **132**(1-2): p. 21-33.
6. Kirchhausen, T., D. Owen, and S.C. Harrison, *Molecular structure, function, and dynamics of clathrin-mediated membrane traffic.* Cold Spring Harb Perspect Biol, 2014. **6**(5): p. a016725.
7. Riezman, H., *Endocytosis in yeast: several of the yeast secretory mutants are defective in endocytosis.* Cell, 1985. **40**(4): p. 1001-9.
8. Paiva, S., N. Vieira, I. Nondier, R. Haguenauer-Tsapis, M. Casal, and D. Urban-Grimal, *Glucose-induced ubiquitylation and endocytosis of the yeast Jen1 transporter: role of lysine 63-linked ubiquitin chains.* J Biol Chem, 2009. **284**(29): p. 19228-36.
9. Lin, C.H., J.A. MacGurn, T. Chu, C.J. Stefan, and S.D. Emr, *Arrestin-related ubiquitin-ligase adaptors regulate endocytosis and protein turnover at the cell surface.* Cell, 2008. **135**(4): p. 714-25.
10. Piao, H.L., I.M. Machado, and G.S. Payne, *NPFXD-mediated endocytosis is required for polarity and function of a yeast cell wall stress sensor.* Mol Biol Cell, 2007. **18**(1): p. 57-65.
11. Chapa-y-Lazo, B., E.G. Allwood, R. Smaczynska-de, II, M.L. Snape, and K.R. Ayscough, *Yeast endocytic adaptor AP-2 binds the stress sensor Mid2 and functions in polarized cell responses.* Traffic, 2014. **15**(5): p. 546-57.
12. Zhao, Y., J.A. Macgurn, M. Liu, and S. Emr, *The ART-Rsp5 ubiquitin ligase network comprises a plasma membrane quality control system that protects yeast cells from proteotoxic stress.* Elife, 2013. **2**: p. e00459.
13. Owen, D.J., B.M. Collins, and P.R. Evans, *Adaptors for clathrin coats: structure and function.* Annu Rev Cell Dev Biol, 2004. **20**: p. 153-91.
14. Liu, P., W.P. Li, T. Machleidt, and R.G. Anderson, *Identification of caveolin-1 in lipoprotein particles secreted by exocrine cells.* Nat Cell Biol, 1999. **1**(6): p. 369-75.
15. Prosser, D.C., T.G. Drivas, L. Maldonado-Baez, and B. Wendland, *Existence of a novel clathrin-independent endocytic pathway in yeast that depends on Rho1 and formin.* J Cell Biol, 2011. **195**(4): p. 657-71.
16. Goode, B.L., J.A. Eskin, and B. Wendland, *Actin and endocytosis in budding yeast.* Genetics, 2015. **199**(2): p. 315-58.
17. Weinberg, J. and D.G. Drubin, *Clathrin-mediated endocytosis in budding yeast.* Trends Cell Biol, 2012. **22**(1): p. 1-13.

18. Kaksonen, M., Y. Sun, and D.G. Drubin, *A pathway for association of receptors, adaptors, and actin during endocytic internalization.* Cell, 2003. **115**(4): p. 475-87.
19. Kaksonen, M., C.P. Toret, and D.G. Drubin, *A modular design for the clathrin- and actin-mediated endocytosis machinery.* Cell, 2005. **123**(2): p. 305-20.
20. Brodsky, F.M., C.Y. Chen, C. Knuehl, M.C. Towler, and D.E. Wakeham, *Biological basket weaving: formation and function of clathrin-coated vesicles.* Annu Rev Cell Dev Biol, 2001. **17**: p. 517-68.
21. Idrissi, F.Z., H. Grotsch, I.M. Fernandez-Golbano, C. Presciatto-Baschong, H. Riezman, and M.I. Geli, *Distinct acto/myosin-I structures associate with endocytic profiles at the plasma membrane.* J Cell Biol, 2008. **180**(6): p. 1219-32.
22. Dell'Angelica, E.C., J. Klumperman, W. Stoorvogel, and J.S. Bonifacino, *Association of the AP-3 adaptor complex with clathrin.* Science, 1998. **280**(5362): p. 431-4.
23. Miele, A.E., P.J. Watson, P.R. Evans, L.M. Traub, and D.J. Owen, *Two distinct interaction motifs in amphiphysin bind two independent sites on the clathrin terminal domain beta-propeller.* Nat Struct Mol Biol, 2004. **11**(3): p. 242-8.
24. Payne, G.S., T.B. Hasson, M.S. Hasson, and R. Schekman, *Genetic and biochemical characterization of clathrin-deficient Saccharomyces cerevisiae.* Mol Cell Biol, 1987. **7**(11): p. 3888-98.
25. Collette, J.R., R.J. Chi, D.R. Boettner, I.M. Fernandez-Golbano, R. Plemel, A.J. Merz, M.I. Geli, L.M. Traub, and S.K. Lemmon, *Clathrin functions in the absence of the terminal domain binding site for adaptor-associated clathrin-box motifs.* Mol Biol Cell, 2009. **20**(14): p. 3401-13.
26. Willox, A.K. and S.J. Royle, *Functional analysis of interaction sites on the N-terminal domain of clathrin heavy chain.* Traffic, 2012. **13**(1): p. 70-81.
27. Carroll, S.Y., P.C. Stirling, H.E. Stimpson, E. Giesselmann, M.J. Schmitt, and D.G. Drubin, *A yeast killer toxin screen provides insights into a/b toxin entry, trafficking, and killing mechanisms.* Dev Cell, 2009. **17**(4): p. 552-60.
28. Hatakeyama, R., M. Kamiya, T. Takahara, and T. Maeda, *Endocytosis of the aspartic acid/glutamic acid transporter Dip5 is triggered by substrate-dependent recruitment of the Rsp5 ubiquitin ligase via the arrestin-like protein Aly2.* Mol Cell Biol, 2010. **30**(24): p. 5598-607.
29. Burston, H.E., L. Maldonado-Baez, M. Davey, B. Montpetit, C. Schluter, B. Wendland, and E. Conibear, *Regulators of yeast endocytosis identified by systematic quantitative analysis.* J Cell Biol, 2009. **185**(6): p. 1097-110.
30. Peng, Y., A. Grassart, R. Lu, C.C. Wong, J. Yates, 3rd, G. Barnes, and D.G. Drubin, *Casein kinase 1 promotes initiation of clathrin-mediated endocytosis.* Dev Cell, 2015. **32**(2): p. 231-40.
31. Boeke, D., S. Trautmann, M. Meurer, M. Wachsmuth, C. Godlee, M. Knop, and M. Kaksonen, *Quantification of cytosolic interactions identifies Ede1 oligomers as key organizers of endocytosis.* Mol Syst Biol, 2014. **10**: p. 756.
32. Reider, A., S.L. Barker, S.K. Mishra, Y.J. Im, L. Maldonado-Baez, J.H. Hurley, L.M. Traub, and B. Wendland, *Syp1 is a conserved endocytic adaptor that contains domains involved in cargo selection and membrane tubulation.* EMBO J, 2009. **28**(20): p. 3103-16.

33. Stimpson, H.E., C.P. Toret, A.T. Cheng, B.S. Pauly, and D.G. Drubin, *Early-arriving Syp1p and Ede1p function in endocytic site placement and formation in budding yeast.* Mol Biol Cell, 2009. **20**(22): p. 4640-51.
34. Boettner, D.R., R.J. Chi, and S.K. Lemmon, *Lessons from yeast for clathrin-mediated endocytosis.* Nat Cell Biol, 2012. **14**(1): p. 2-10.
35. Brach, T., C. Godlee, I. Moeller-Hansen, D. Boeke, and M. Kaksonen, *The initiation of clathrin-mediated endocytosis is mechanistically highly flexible.* Curr Biol, 2014. **24**(5): p. 548-54.
36. Wendland, B., K.E. Steece, and S.D. Emr, *Yeast epsins contain an essential N-terminal ENTH domain, bind clathrin and are required for endocytosis.* EMBO J, 1999. **18**(16): p. 4383-93.
37. Aguilar, R.C., H.A. Watson, and B. Wendland, *The yeast Epsin Ent1 is recruited to membranes through multiple independent interactions.* J Biol Chem, 2003. **278**(12): p. 10737-43.
38. Wendland, B. and S.D. Emr, *Pan1p, yeast eps15, functions as a multivalent adaptor that coordinates protein-protein interactions essential for endocytosis.* J Cell Biol, 1998. **141**(1): p. 71-84.
39. Maldonado-Baez, L., M.R. Dores, E.M. Perkins, T.G. Drivas, L. Hicke, and B. Wendland, *Interaction between Epsin/Yap180 adaptors and the scaffolds Ede1/Pan1 is required for endocytosis.* Mol Biol Cell, 2008. **19**(7): p. 2936-48.
40. Skruzny, M., A. Desfosses, S. Prinz, S.O. Dodonova, A. Gieras, C. Uetrecht, A.J. Jakobi, M. Abella, W.J. Hagen, J. Schulz, et al., *An organized co-assembly of clathrin adaptors is essential for endocytosis.* Dev Cell, 2015. **33**(2): p. 150-62.
41. Toshima, J.Y., J. Toshima, M. Kaksonen, A.C. Martin, D.S. King, and D.G. Drubin, *Spatial dynamics of receptor-mediated endocytic trafficking in budding yeast revealed by using fluorescent alpha-factor derivatives.* Proc Natl Acad Sci U S A, 2006. **103**(15): p. 5793-8.
42. Carroll, S.Y., H.E. Stimpson, J. Weinberg, C.P. Toret, Y. Sun, and D.G. Drubin, *Analysis of yeast endocytic site formation and maturation through a regulatory transition point.* Mol Biol Cell, 2012. **23**(4): p. 657-68.
43. Sun, Y., N.T. Leong, T. Wong, and D.G. Drubin, *A Pan1/End3/Sla1 complex links Arp2/3-mediated actin assembly to sites of clathrin-mediated endocytosis.* Mol Biol Cell, 2015. **26**(21): p. 3841-56.
44. Howard, J.P., J.L. Hutton, J.M. Olson, and G.S. Payne, *Sla1p serves as the targeting signal recognition factor for NPFX(1,2)D-mediated endocytosis.* J Cell Biol, 2002. **157**(2): p. 315-26.
45. Tan, P.K., J.P. Howard, and G.S. Payne, *The sequence NPFXD defines a new class of endocytosis signal in Saccharomyces cerevisiae.* J Cell Biol, 1996. **135**(6 Pt 2): p. 1789-800.
46. Liu, K., Z. Hua, J.A. Nepute, and T.R. Graham, *Yeast P4-ATPases Drs2p and Dnf1p are essential cargos of the NPFXD/Sla1p endocytic pathway.* Mol Biol Cell, 2007. **18**(2): p. 487-500.
47. Di Pietro, S.M., D. Cascio, D. Feliciano, J.U. Bowie, and G.S. Payne, *Regulation of clathrin adaptor function in endocytosis: novel role for the SAM domain.* EMBO J, 2010. **29**(6): p. 1033-44.

48. Feliciano, D. and S.M. Di Pietro, *SLAC, a complex between Sla1 and Las17, regulates actin polymerization during clathrin-mediated endocytosis.* Mol Biol Cell, 2012. **23**(21): p. 4256-72.
49. Picco, A., M. Mund, J. Ries, F. Nedelec, and M. Kaksonen, *Visualizing the functional architecture of the endocytic machinery.* Elife, 2015. **4**.
50. Tonikian, R., X. Xin, C.P. Toret, D. Gfeller, C. Landgraf, S. Panni, S. Paoluzi, L. Castagnoli, B. Currell, S. Seshagiri, et al., *Bayesian modeling of the yeast SH3 domain interactome predicts spatiotemporal dynamics of endocytosis proteins.* PLoS Biol, 2009. **7**(10): p. e1000218.
51. Stamenova, S.D., M.E. French, Y. He, S.A. Francis, Z.B. Kramer, and L. Hicke, *Ubiquitin binds to and regulates a subset of SH3 domains.* Mol Cell, 2007. **25**(2): p. 273-84.
52. Peter, B.J., H.M. Kent, I.G. Mills, Y. Vallis, P.J. Butler, P.R. Evans, and H.T. McMahon, *BAR domains as sensors of membrane curvature: the amphiphysin BAR structure.* Science, 2004. **303**(5657): p. 495-9.
53. Walani, N., J. Torres, and A. Agrawal, *Endocytic proteins drive vesicle growth via instability in high membrane tension environment.* Proc Natl Acad Sci U S A, 2015. **112**(12): p. E1423-32.
54. Lewellyn, E.B., R.T. Pedersen, J. Hong, R. Lu, H.M. Morrison, and D.G. Drubin, *An engineered minimal WASP-Myosin fusion protein reveals essential functions for endocytosis.* Dev Cell, 2015. **35**(3): p. 281-94.
55. Smaczynska-de, R., II, E.G. Allwood, S. Aghamohammadzadeh, E.H. Hettema, M.W. Goldberg, and K.R. Ayscough, *A role for the dynamin-like protein Vps1 during endocytosis in yeast.* J Cell Sci, 2010. **123**(Pt 20): p. 3496-506.
56. Nannapaneni, S., D. Wang, S. Jain, B. Schroeder, C. Highfill, L. Reustle, D. Pittsley, A. Maysent, S. Moulder, R. McDowell, and K. Kim, *The yeast dynamin-like protein Vps1:vps1 mutations perturb the internalization and the motility of endocytic vesicles and endosomes via disorganization of the actin cytoskeleton.* Eur J Cell Biol, 2010. **89**(7): p. 499-508.
57. Palmer, S.E., R. Smaczynska-de, II, C.J. Marklew, E.G. Allwood, R. Mishra, S. Johnson, M.W. Goldberg, and K.R. Ayscough, *A dynamin-actin interaction is required for vesicle scission during endocytosis in yeast.* Curr Biol, 2015. **25**(7): p. 868-78.
58. Liu, J., Y. Sun, D.G. Drubin, and G.F. Oster, *The mechanochemistry of endocytosis.* PLoS Biol, 2009. **7**(9): p. e1000204.
59. Stefan, C.J., S.M. Padilla, A. Audhya, and S.D. Emr, *The phosphoinositide phosphatase Sjl2 is recruited to cortical actin patches in the control of vesicle formation and fission during endocytosis.* Mol Cell Biol, 2005. **25**(8): p. 2910-23.
60. Toret, C.P., L. Lee, M. Sekiya-Kawasaki, and D.G. Drubin, *Multiple pathways regulate endocytic coat disassembly in Saccharomyces cerevisiae for optimal downstream trafficking.* Traffic, 2008. **9**(5): p. 848-59.
61. Cope, M.J., S. Yang, C. Shang, and D.G. Drubin, *Novel protein kinases Ark1p and Prk1p associate with and regulate the cortical actin cytoskeleton in budding yeast.* J Cell Biol, 1999. **144**(6): p. 1203-18.
62. Chang, J.S., K. Henry, B.L. Wolf, M. Geli, and S.K. Lemmon, *Protein phosphatase-1 binding to scd5p is important for regulation of actin organization and endocytosis in yeast.* J Biol Chem, 2002. **277**(50): p. 48002-8.

63. Chi, R.J., O.T. Torres, V.A. Segarra, T. Lansley, J.S. Chang, T.M. Newpher, and S.K. Lemmon, *Role of Scd5, a protein phosphatase-1 targeting protein, in phosphoregulation of Sla1 during endocytosis.* J Cell Sci, 2012. **125**(Pt 20): p. 4728-39.
64. Toshima, J., J.Y. Toshima, A.C. Martin, and D.G. Drubin, *Phosphoregulation of Arp2/3-dependent actin assembly during receptor-mediated endocytosis.* Nat Cell Biol, 2005. **7**(3): p. 246-54.
65. Adams, A.E. and J.R. Pringle, *Relationship of actin and tubulin distribution to bud growth in wild-type and morphogenetic-mutant Saccharomyces cerevisiae.* J Cell Biol, 1984. **98**(3): p. 934-45.
66. Mulholland, J., D. Preuss, A. Moon, A. Wong, D. Drubin, and D. Botstein, *Ultrastructure of the yeast actin cytoskeleton and its association with the plasma membrane.* J Cell Biol, 1994. **125**(2): p. 381-91.
67. Kubler, E. and H. Riezman, *Actin and fimbrin are required for the internalization step of endocytosis in yeast.* EMBO J, 1993. **12**(7): p. 2855-62.
68. Thanabalu, T. and A.L. Munn, *Functions of Vrp1p in cytokinesis and actin patches are distinct and neither requires a WH2/V domain.* EMBO J, 2001. **20**(24): p. 6979-89.
69. Ayscough, K.R., J. Stryker, N. Pokala, M. Sanders, P. Crews, and D.G. Drubin, *High rates of actin filament turnover in budding yeast and roles for actin in establishment and maintenance of cell polarity revealed using the actin inhibitor latrunculin-A.* J Cell Biol, 1997. **137**(2): p. 399-416.
70. Aghamohammadzadeh, S. and K.R. Ayscough, *Differential requirements for actin during yeast and mammalian endocytosis.* Nat Cell Biol, 2009. **11**(8): p. 1039-42.
71. Kim, K., B.J. Galletta, K.O. Schmidt, F.S. Chang, K.J. Blumer, and J.A. Cooper, *Actin-based motility during endocytosis in budding yeast.* Mol Biol Cell, 2006. **17**(3): p. 1354-63.
72. Mullins, R.D., J.A. Heuser, and T.D. Pollard, *The interaction of Arp2/3 complex with actin: nucleation, high affinity pointed end capping, and formation of branching networks of filaments.* Proc Natl Acad Sci U S A, 1998. **95**(11): p. 6181-6.
73. Blanchoin, L., K.J. Amann, H.N. Higgs, J.B. Marchand, D.A. Kaiser, and T.D. Pollard, *Direct observation of dendritic actin filament networks nucleated by Arp2/3 complex and WASP/Scar proteins.* Nature, 2000. **404**(6781): p. 1007-11.
74. Rotty, J.D., C. Wu, and J.E. Bear, *New insights into the regulation and cellular functions of the ARP2/3 complex.* Nat Rev Mol Cell Biol, 2013. **14**(1): p. 7-12.
75. Toshima, J., J.Y. Toshima, M.C. Duncan, M.J. Cope, Y. Sun, A.C. Martin, S. Anderson, J.R. Yates, 3rd, K. Mizuno, and D.G. Drubin, *Negative regulation of yeast Eps15-like Arp2/3 complex activator, Pan1p, by the Hip1R-related protein, Sla2p, during endocytosis.* Mol Biol Cell, 2007. **18**(2): p. 658-68.
76. Boettner, D.R., J.L. D'Agostino, O.T. Torres, K. Daugherty-Clarke, A. Uygur, A. Reider, B. Wendland, S.K. Lemmon, and B.L. Goode, *The F-BAR protein Syp1 negatively regulates WASp-Arp2/3 complex activity during endocytic patch formation.* Curr Biol, 2009. **19**(23): p. 1979-87.
77. Feliciano, D., T.O. Tolsma, K.B. Farrell, A. Aradi, and S.M. Di Pietro, *A second Las17 monomeric actin-binding motif functions in Arp2/3-dependent actin polymerization during endocytosis.* Traffic, 2015. **16**(4): p. 379-97.

78. Grotsch, H., J.P. Giblin, F.Z. Idrissi, I.M. Fernandez-Golbano, J.R. Collette, T.M. Newpher, V. Robles, S.K. Lemmon, and M.I. Geli, *Calmodulin dissociation regulates Myo5 recruitment and function at endocytic sites.* EMBO J, 2010. **29**(17): p. 2899-914.
79. Sun, Y., A.C. Martin, and D.G. Drubin, *Endocytic internalization in budding yeast requires coordinated actin nucleation and myosin motor activity.* Dev Cell, 2006. **11**(1): p. 33-46.
80. Kim, K., A. Yamashita, M.A. Wear, Y. Maeda, and J.A. Cooper, *Capping protein binding to actin in yeast: biochemical mechanism and physiological relevance.* J Cell Biol, 2004. **164**(4): p. 567-80.
81. Wear, M.A. and J.A. Cooper, *Capping protein: new insights into mechanism and regulation.* Trends Biochem Sci, 2004. **29**(8): p. 418-28.
82. Michelot, A., A. Grassart, V. Okreglak, M. Costanzo, C. Boone, and D.G. Drubin, *Actin filament elongation in Arp2/3-derived networks is controlled by three distinct mechanisms.* Dev Cell, 2013. **24**(2): p. 182-95.
83. Balcer, H.I., A.L. Goodman, A.A. Rodal, E. Smith, J. Kugler, J.E. Heuser, and B.L. Goode, *Coordinated regulation of actin filament turnover by a high-molecular-weight Srv2/CAP complex, cofilin, profilin, and Aip1.* Current Biology, 2003. **13**(24): p. 2159-2169.
84. Goodman, A., B.L. Goode, P. Matsudaira, and G.R. Fink, *The Saccharomyces cerevisiae calponin/transgelin homolog Scp1 functions with fimbrin to regulate stability and organization of the actin cytoskeleton.* Mol Biol Cell, 2003. **14**(7): p. 2617-29.
85. Okreglak, V. and D.G. Drubin, *Loss of Aip1 reveals a role in maintaining the actin monomer pool and an in vivo oligomer assembly pathway.* J Cell Biol, 2010. **188**(6): p. 769-77.
86. Lin, M.C., B.J. Galletta, D. Sept, and J.A. Cooper, *Overlapping and distinct functions for cofilin, coronin and Aip1 in actin dynamics in vivo.* J Cell Sci, 2010. **123**(Pt 8): p. 1329-42.
87. Blanchoin, L. and T.D. Pollard, *Mechanism of interaction of Acanthamoeba actophorin (ADF/Cofilin) with actin filaments.* J Biol Chem, 1999. **274**(22): p. 15538-46.
88. Michelot, A., J. Berro, C. Guerin, R. Boujemaa-Paterski, C.J. Staiger, J.L. Martiel, and L. Blanchoin, *Actin-filament stochastic dynamics mediated by ADF/cofilin.* Curr Biol, 2007. **17**(10): p. 825-33.
89. McGough, A., B. Pope, W. Chiu, and A. Weeds, *Cofilin changes the twist of F-actin: implications for actin filament dynamics and cellular function.* J Cell Biol, 1997. **138**(4): p. 771-81.
90. Okada, K., H. Ravi, E.M. Smith, and B.L. Goode, *Aip1 and cofilin promote rapid turnover of yeast actin patches and cables: a coordinated mechanism for severing and capping filaments.* Mol Biol Cell, 2006. **17**(7): p. 2855-68.
91. Chaudhry, F., K. Little, L. Talarico, O. Quintero-Monzon, and B.L. Goode, *A central role for the WH2 domain of Srv2/CAP in recharging actin monomers to drive actin turnover in vitro and in vivo.* Cytoskeleton (Hoboken), 2010. **67**(2): p. 120-33.
92. Belmont, L.D. and D.G. Drubin, *The yeast V159N actin mutant reveals roles for actin dynamics in vivo.* J Cell Biol, 1998. **142**(5): p. 1289-99.
93. Galletta, B.J., O.L. Mooren, and J.A. Cooper, *Actin dynamics and endocytosis in yeast and mammals.* Curr Opin Biotechnol, 2010. **21**(5): p. 604-10.

94. Chen, Q. and T.D. Pollard, *Actin filament severing by cofilin dismantles actin patches and produces mother filaments for new patches.* Curr Biol, 2013. **23**(13): p. 1154-62.
95. Collins, A., A. Warrington, K.A. Taylor, and T. Svitkina, *Structural organization of the actin cytoskeleton at sites of clathrin-mediated endocytosis.* Curr Biol, 2011. **21**(14): p. 1167-75.
96. Rodal, A.A., O. Sokolova, D.B. Robins, K.M. Daugherty, S. Hippenmeyer, H. Riezman, N. Grigorieff, and B.L. Goode, *Conformational changes in the Arp2/3 complex leading to actin nucleation.* Nat Struct Mol Biol, 2005. **12**(1): p. 26-31.
97. Schafer, D.A., P.B. Jennings, and J.A. Cooper, *Dynamics of capping protein and actin assembly in vitro: uncapping barbed ends by polyphosphoinositides.* J Cell Biol, 1996. **135**(1): p. 169-79.
98. Volland, C., D. Urban-Grimal, G. Geraud, and R. Haguenauer-Tsapis, *Endocytosis and degradation of the yeast uracil permease under adverse conditions.* J Biol Chem, 1994. **269**(13): p. 9833-41.
99. Terrell, J., S. Shih, R. Dunn, and L. Hicke, *A function for monoubiquitination in the internalization of a G protein-coupled receptor.* Mol Cell, 1998. **1**(2): p. 193-202.
100. Hicke, L. and R. Dunn, *Regulation of membrane protein transport by ubiquitin and ubiquitin-binding proteins.* Annu Rev Cell Dev Biol, 2003. **19**: p. 141-72.
101. Hicke, L. and H. Riezman, *Ubiquitination of a yeast plasma membrane receptor signals its ligand-stimulated endocytosis.* Cell, 1996. **84**(2): p. 277-87.
102. Dunn, R. and L. Hicke, *Multiple roles for Rsp5p-dependent ubiquitination at the internalization step of endocytosis.* J Biol Chem, 2001. **276**(28): p. 25974-81.
103. Dores, M.R., J.D. Schnell, L. Maldonado-Baez, B. Wendland, and L. Hicke, *The function of yeast epsin and Ede1 ubiquitin-binding domains during receptor internalization.* Traffic, 2010. **11**(1): p. 151-60.
104. Lam, M.H. and A. Emili, *Ubp2 regulates Rsp5 ubiquitination activity in vivo and in vitro.* PLoS One, 2013. **8**(9): p. e75372.
105. Weinberg, J.S. and D.G. Drubin, *Regulation of clathrin-mediated endocytosis by dynamic ubiquitination and deubiquitination.* Curr Biol, 2014. **24**(9): p. 951-9.
106. Becuwe, M., N. Vieira, D. Lara, J. Gomes-Rezende, C. Soares-Cunha, M. Casal, R. Haguenauer-Tsapis, O. Vincent, S. Paiva, and S. Leon, *A molecular switch on an arrestin-like protein relays glucose signaling to transporter endocytosis.* J Cell Biol, 2012. **196**(2): p. 247-59.
107. Shea, F.F., J.L. Rowell, Y. Li, T.H. Chang, and C.E. Alvarez, *Mammalian alpha arrestins link activated seven transmembrane receptors to Nedd4 family e3 ubiquitin ligases and interact with beta arrestins.* PLoS One, 2012. **7**(12): p. e50557.
108. Taylor, M.J., D. Perrais, and C.J. Merrifield, *A high precision survey of the molecular dynamics of mammalian clathrin-mediated endocytosis.* PLoS Biol, 2011. **9**(3): p. e1000604.
109. Doyon, J.B., B. Zeitler, J. Cheng, A.T. Cheng, J.M. Cherone, Y. Santiago, A.H. Lee, T.D. Vo, Y. Doyon, J.C. Miller, et al., *Rapid and efficient clathrin-mediated endocytosis revealed in genome-edited mammalian cells.* Nat Cell Biol, 2011. **13**(3): p. 331-7.
110. Cocucci, E., F. Aguet, S. Boulant, and T. Kirchhausen, *The first five seconds in the life of a clathrin-coated pit.* Cell, 2012. **150**(3): p. 495-507.

111. Avinoam, O., M. Schorb, C.J. Beese, J.A. Briggs, and M. Kaksonen, *ENDOCYTOSIS. Endocytic sites mature by continuous bending and remodeling of the clathrin coat.* Science, 2015. **348**(6241): p. 1369-72.
112. Motley, A., N.A. Bright, M.N. Seaman, and M.S. Robinson, *Clathrin-mediated endocytosis in AP-2-depleted cells.* J Cell Biol, 2003. **162**(5): p. 909-18.
113. Yeung, B.G., H.L. Phan, and G.S. Payne, *Adaptor complex-independent clathrin function in yeast.* Mol Biol Cell, 1999. **10**(11): p. 3643-59.
114. Boulant, S., C. Kural, J.C. Zeeh, F. Ubelmann, and T. Kirchhausen, *Actin dynamics counteract membrane tension during clathrin-mediated endocytosis.* Nat Cell Biol, 2011. **13**(9): p. 1124-31.
115. Kaur, S., A.B. Fielding, G. Gassner, N.J. Carter, and S.J. Royle, *An unmet actin requirement explains the mitotic inhibition of clathrin-mediated endocytosis.* Elife, 2014. **3**: p. e00829.
116. Merrifield, C.J., B. Qualmann, M.M. Kessels, and W. Almers, *Neural Wiskott Aldrich Syndrome Protein (N-WASP) and the Arp2/3 complex are recruited to sites of clathrin-mediated endocytosis in cultured fibroblasts.* Eur J Cell Biol, 2004. **83**(1): p. 13-8.
117. Grassart, A., A.T. Cheng, S.H. Hong, F. Zhang, N. Zenzer, Y. Feng, D.M. Briner, G.D. Davis, D. Malkov, and D.G. Drubin, *Actin and dynamin2 dynamics and interplay during clathrin-mediated endocytosis.* J Cell Biol, 2014. **205**(5): p. 721-35.
118. Mercer, J., M. Schelhaas, and A. Helenius, *Virus entry by endocytosis.* Annu Rev Biochem, 2010. **79**: p. 803-33.
119. Massaad, M.J., N. Ramesh, and R.S. Geha, *Wiskott-Aldrich syndrome: a comprehensive review.* Ann N Y Acad Sci, 2013. **1285**: p. 26-43.
120. Lambrechts, A., K. Gevaert, P. Cossart, J. Vandekerckhove, and M. Van Troys, *Listeria comet tails: the actin-based motility machinery at work.* Trends Cell Biol, 2008. **18**(5): p. 220-7.
121. Kononenko, N.L., D. Puchkov, G.A. Classen, A.M. Walter, A. Pechstein, L. Sawade, N. Kaempf, T. Trimbuch, D. Lorenz, C. Rosenmund, et al., *Clathrin/AP-2 mediate synaptic vesicle reformation from endosome-like vacuoles but are not essential for membrane retrieval at central synapses.* Neuron, 2014. **82**(5): p. 981-8.
122. Wu, F. and P.J. Yao, *Clathrin-mediated endocytosis and Alzheimer's disease: an update.* Ageing Res Rev, 2009. **8**(3): p. 147-9.
123. Mosesson, Y., G.B. Mills, and Y. Yarden, *Derailed endocytosis: an emerging feature of cancer.* Nat Rev Cancer, 2008. **8**(11): p. 835-50.
124. Stein, M., A. Wandinger-Ness, and T. Roitbak, *Altered trafficking and epithelial cell polarity in disease.* Trends Cell Biol, 2002. **12**(8): p. 374-81.
125. Gent, J. and I. Braakman, *Low-density lipoprotein receptor structure and folding.* Cell Mol Life Sci, 2004. **61**(19-20): p. 2461-70.
126. Enns, C.A., *Pumping iron: the strange partnership of the hemochromatosis protein, a class I MHC homolog, with the transferrin receptor.* Traffic, 2001. **2**(3): p. 167-74.
127. Cherry, J.M., E.L. Hong, C. Amundsen, R. Balakrishnan, G. Binkley, E.T. Chan, K.R. Christie, M.C. Costanzo, S.S. Dwight, S.R. Engel, et al., *Saccharomyces Genome Database: the genomics resource of budding yeast.* Nucleic Acids Res, 2012. **40**(Database issue): p. D700-5.
128. Sherman, F., *Getting started with yeast.* Methods Enzymol, 2002. **350**: p. 3-41.

129. Sikorski, R.S. and P. Hieter, *A system of shuttle vectors and yeast host strains designed for efficient manipulation of DNA in Saccharomyces cerevisiae.* Genetics, 1989. **122**(1): p. 19-27.
130. Brachmann, C.B., A. Davies, G.J. Cost, E. Caputo, J. Li, P. Hieter, and J.D. Boeke, *Designer deletion strains derived from Saccharomyces cerevisiae S288C: a useful set of strains and plasmids for PCR-mediated gene disruption and other applications.* Yeast, 1998. **14**(2): p. 115-32.
131. Longtine, M.S., A. McKenzie, 3rd, D.J. Demarini, N.G. Shah, A. Wach, A. Brachat, P. Philippsen, and J.R. Pringle, *Additional modules for versatile and economical PCR-based gene deletion and modification in Saccharomyces cerevisiae.* Yeast, 1998. **14**(10): p. 953-61.
132. Chen, P., H.H. Liu, R. Cui, Z.L. Zhang, D.W. Pang, Z.X. Xie, H.Z. Zheng, Z.X. Lu, and H. Tong, *Visualized investigation of yeast transformation induced with Li+ and polyethylene glycol.* Talanta, 2008. **77**(1): p. 262-8.
133. Kukulski, W., M. Schorb, M. Kaksonen, and J.A. Briggs, *Plasma membrane reshaping during endocytosis is revealed by time-resolved electron tomography.* Cell, 2012. **150**(3): p. 508-20.
134. Sirotkin, V., J. Berro, K. Macmillan, L. Zhao, and T.D. Pollard, *Quantitative analysis of the mechanism of endocytic actin patch assembly and disassembly in fission yeast.* Mol Biol Cell, 2010. **21**(16): p. 2894-904.
135. Huh, W.K., J.V. Falvo, L.C. Gerke, A.S. Carroll, R.W. Howson, J.S. Weissman, and E.K. O'Shea, *Global analysis of protein localization in budding yeast.* Nature, 2003. **425**(6959): p. 686-91.

CHAPTER 2

A SCREENING OF THE YEAST GFP LIBRARY REVEALS UBX3 AS A NOVEL PROTEIN OF THE ENDOCYTIC MACHINERY

2.1 Summary

The following chapter is reproduced with additions from an article published in *Genetics* (Farrell *et al.* 2015) [1]. Despite the importance of clathrin-mediated endocytosis (CME) for cell biology, it is unclear if all components of the machinery have been discovered and many regulatory aspects remain poorly understood. Here, using *Saccharomyces cerevisiae* and a fluorescence microscopy screening approach we identify previously unknown regulatory factors of the endocytic machinery. We further studied the top scoring protein identified in the screen, Ubx3, a member of the conserved ubiquitin regulatory X (UBX) protein family. *In vivo* and *in vitro* approaches demonstrate that Ubx3 is a new coat component. Ubx3-GFP has typical endocytic coat protein dynamics with a patch lifetime of 45 ± 3 sec. Ubx3 contains a W-box that mediates physical interaction with clathrin and Ubx3-GFP patch lifetime depends on clathrin. Deletion of the *UBX3* gene caused defects in the uptake of Lucifer Yellow and the methionine transporter Mup1, demonstrating that Ubx3 is needed for efficient endocytosis. Further, the UBX domain is required both for localization and function of Ubx3 at endocytic sites. Mechanistically, Ubx3 regulates dynamics and patch lifetime of the early arriving protein Ede1 but not later arriving coat proteins or actin assembly. Conversely, Ede1 regulates the patch lifetime of Ubx3. Ubx3 likely regulates CME via the AAA-ATPase Cdc48, a ubiquitin-editing complex. Ede1

patch lifetime is similarly affected by inactivation of Cdc48. Our results uncovered new components of the CME machinery that regulate this fundamental process.

2.2 Introduction

Endocytosis is essential for numerous cellular activities including nutrient uptake, regulation of signal transduction, and remodeling of the cell surface [2-8]. Clathrin-mediated endocytosis (CME) is a major endocytic pathway that collects cargo into a coated pit, invaginates and pinches off a vesicle, and transports the vesicle to endosomes (Figure 1.1). This process is carried out by a complex cellular machinery involving approximately 50 proteins to date [2-8] (Table 1.1). CME is highly conserved throughout evolution and proceeds through a well-choreographed sequence of events where most proteins are recruited from the cytosol at specific times [9-12]. Although the study of these proteins' functions in the biogenesis of clathrin-coated vesicles has shed light on the mechanisms of endocytosis, many regulatory aspects of CME are still poorly understood. Furthermore, additional CME machinery components may yet to be uncovered and their functions elucidated. Previous methods for identifying endocytic machinery proteins include knockout, synthetic lethality, cargo based, and drug sensitivity screenings [13, 14]. These methods may miss proteins for various reasons, further discussed in Chapter 4. A visual GFP-fusion protein-based screen identifies proteins localized to endocytic sites without excess stress on the cell due to drug or protein knockout and also has the potential to identify proteins that may not portray a strong endocytic defect in the knockout strain or cannot be deleted in the cell. Thus, by screening the yeast GFP collection for proteins that localize to sites of CME, we reasoned that it would be possible to identify new

components and modulators of the machinery. Using this strategy we identified a group of uncharacterized endocytic proteins and further study one of them, Ubx3.

2.3 Results

2.3.1 A GFP-based screening of Saccharomyces cerevisiae for novel endocytic proteins

We took advantage of the *S. cerevisiae* GFP library, containing the coding sequence of GFP immediately preceding the stop codon of each ORF in the yeast genome [15]. Library proteins are therefore expressed from their endogenous promoter, with a GFP tag at the carboxy-terminal end. Creators of the library performed an initial classification of the subcellular localization for 4,156 GFP-tagged proteins representing ~75% of the proteome. We noted that well-established components of the endocytic machinery were found in three localization groups: the plasma membrane, actin, and punctate composite [15]. Together the three groups contain 319 GFP-tagged proteins and include numerous proteins with unknown function. We reasoned that some of these unknown proteins may specifically localize to sites of endocytosis and constitute new components of the endocytic machinery. To test that possibility, MATa strains expressing the 319 GFP-tagged proteins in these categories were mated with MATα cells expressing Sla1–RFP from the endogenous locus and resulting diploid cells were selected with appropriate markers. Sla1 is a multifunctional clathrin adaptor and actin polymerization regulator present at all sites of CME and easily visible by fluorescence microscopy (Figure 2.1.A) [9, 10, 16-19]. Each diploid strain expressing both the corresponding GFP-fusion protein and Sla1–RFP was subjected to live cell confocal fluorescence microscopy and colocalization analysis. To ensure an unbiased study, the operator did not know the identity of the strain subjected to imaging and random images were used to determine colocalization levels.

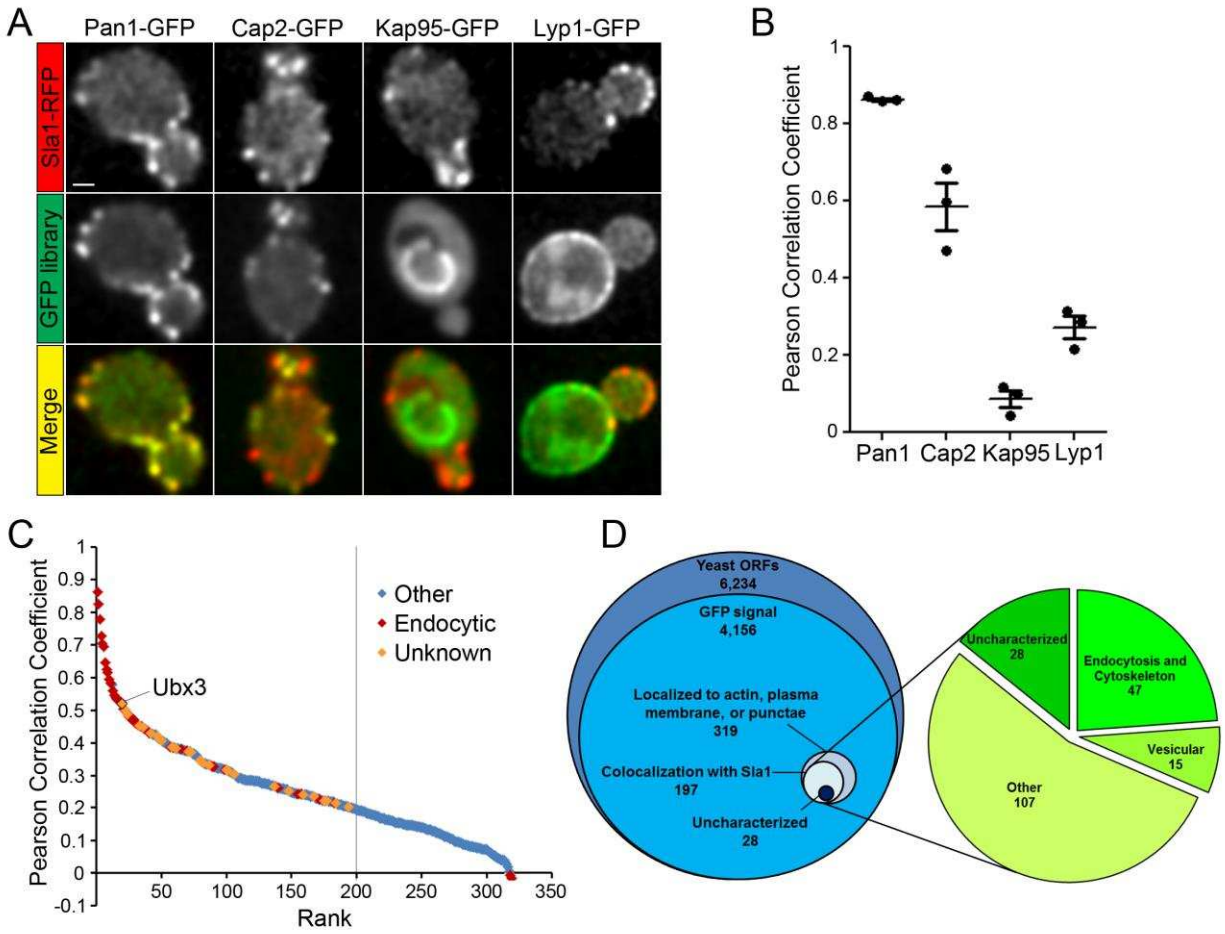

Figure 2.1: GFP-based screening for endocytic proteins. A) *S. cerevisiae* cells expressing Sla1-RFP and the indicated GFP-fusion proteins were analyzed by live cell confocal fluorescence microscopy. Bar = 1 μm. B) Pearson Correlation Coefficients between Sla1-RFP and each of the proteins demonstrated in (A). C) Distribution of PCC values for Sla1-RFP with the 319 GFP-tagged proteins tested in the screening. Endocytic proteins are indicated with red symbols and uncharacterized proteins with yellow symbols. The cutoff for colocalization (PCC = 0.2) is marked with a line. D) Left, schematic of how the yeast genome was narrowed down to the 319 proteins selected for the screen. Right, functions of the 197 proteins showing colocalization with Sla1 at a level higher than PCC = 0.2.

2.3.2 Visual and quantitative data reveal candidate endocytic proteins

The Pearson correlation coefficient (PCC) was determined for each GFP-tagged protein by averaging at least three images, each containing multiple cells with several endocytic patches. The library proteins were then ranked from highest to lowest PCC with a range of 0.86 to -0.02 (Table 2.1). Representative examples are shown in Figure 2.1. The highest scoring protein, Pan1 (0.86 ± 0.01, mean ± SD), is known to have the same dynamics as Sla1 and therefore expected to display a high colocalization level [5, 6, 9, 10]. The capping protein β-subunit, Cap2 (0.58 ± 0.11, mean ± SD), is a component of the actin network that assembles after the arrival of Sla1 [10] and shows intermediate level of colocalization. The lysine permease Lyp1 (0.27 ± 0.05, mean ± SD) localizes to the plasma membrane in a relatively uniform manner and thus represents a low colocalization level. A nuclear pore protein classified as punctate localization, Kap95 (0.09 ± 0.04, mean ± SD) serves as an example of background PCC obtained with a noncolocalizing protein (Figure 2.1). Based on these observations, proteins with PCC>0.2 were considered to show colocalization above background, totaling 197 of the 319 strains (Figure 2.1.D). The functions of the 197 colocalizing proteins were obtained from the *Saccharomyces* Genome Database [20] and the literature, showing representation from endocytic, cytoskeletal, trafficking, as well as other functions (Figure 2.1.D, Table 2.1). Of the 45 known endocytic proteins included in the screening, only two (Sac6 and Arp2) fell below the 0.2 PCC cutoff for colocalization, indicating that the group of 197 proteins includes the vast majority of machinery components analyzed in the group of 319 strains (Table 2.1 and Table 2.2). Furthermore, 31 of the top 50 PCCs corresponded to well-studied endocytic proteins, such as Sla2, Ent2, and Bbc1. Thus, a majority of the known endocytic machinery proteins were located high in this ranking (Table 2.1 and Table 2.2). Interestingly, all four subunits of the AP-2 complex scored a colocalizing PCC,

Table 2.1: Proteins visualized in the GFP screen.

Screening Rank	Systematic Name	Common Name	PCC	± SD
1	YIR006C	PAN1	0.86	±0.01
2	YNL084C	END3	0.83	±0.06
3	YFR024C	YSC85	0.78	±0.06
4	YNL243W	SLA2	0.73	±0.11
5	YLR206W	ENT2	0.70	±0.04
6	YBL007C	SLA1	0.69	±0.09
7	YHR161C	YAP1801	0.65	±0.09
8	YJR005W	APL1	0.63	±0.18
9	YLR337C	VRP1	0.62	±0.39
10	YNR035C	ARC35	0.59	±0.07
11	YIL034C	CAP2	0.58	±0.11
12	YNL138W	SRV2	0.58	±0.09
13	YJL021C	BBC1	0.56	±0.04
14	YGL181W	GTS1	0.55	±0.12
15	YIL062C	ARC15	0.54	±0.07
16	YOR181W	LAS17	0.54	±0.05
17	YLR370C	ARC18	0.53	±0.13
18	YGR080W	TWF1	0.53	±0.11
19	YKL013C	ARC19	0.53	±0.05
20	YDL091C	Ubx3	0.52	±0.26
21	YIL095W	PRK1	0.51	±0.12
22	YPL221W	BOP1	0.50	±0.12
23	YDL012C		0.50	±0.14
24	YER071C	TDA2	0.49	±0.13
25	YKL007W	CAP1	0.48	±0.12
26	YCR088W	ABP1	0.48	±0.13
27	YMR109W	MYO5	0.47	±0.05
28	YOL062C	APM4	0.47	±0.15
29	YBL042C	FUI1	0.47	±0.02
30	YOR367W	SCP1	0.46	±0.10
31	YDL161W	ENT1	0.46	±0.31
32	YCR030C	SYP1	0.46	±0.01
33	YOR104W	PIN2	0.45	±0.19
34	YBL085W	BOI1	0.45	±0.05
35	YGR241C	YAP1802	0.45	±0.07
36	YGR026W		0.45	±0.03
37	YBL047C	EDE1	0.44	±0.19
38	YNL283C	WSC2	0.44	±0.07

39	YHR136C	SPL2	0.44 ±0.18
40	YHR114W	BZZ1	0.43 ±0.20
41	YCR009C	RVS161	0.43 ±0.05
42	YBL029C-A		0.43 ±0.12
43	YLR414C	PUN1	0.43 ±0.04
44	YLL010C	PSR1	0.42 ±0.07
45	YAL053W		0.42 ±0.11
46	YGR281W	YOR1	0.42 ±0.05
47	YBR016W		0.42 ±0.05
48	YBR068C	BAP2	0.41 ±0.06
49	YDR090C		0.41 ±0.11
50	YDR034W-B		0.41 ±0.09
51	YDR508C	GNP1	0.41 ±0.15
52	YOL105C	WSC3	0.40 ±0.05
53	YDR011W	SNQ2	0.40 ±0.18
54	YGR065C	VHT1	0.40 ±0.07
55	YOR094W	ARF3	0.40 ±0.06
56	YER118C	SHO1	0.39 ±0.16
57	YLR429W	CRN1	0.39 ±0.19
58	YDR033W	MRH1	0.39 ±0.15
59	YDR388W	RVS167	0.39 ±0.12
60	YPR124W	CTR1	0.39 ±0.07
61	YMR295C		0.38 ±0.05
62	YML016C	PPZ1	0.38 ±0.11
63	YOR165W	SEY1	0.38 ±0.03
64	YMR266W	RSN1	0.38 ±0.07
65	YPR171W	BSP1	0.38 ±0.12
66	YML116W	ATR1	0.38 ±0.07
67	YNL087W	TCB2	0.38 ±0.04
68	YDR233C	RTN1	0.38 ±0.05
69	YDR093W	DNF2	0.38 ±0.02
70	YJR058C	APS2	0.38 ±0.14
71	YDR344C		0.37 ±0.05
72	YBR086C	IST2	0.37 ±0.08
73	YDR210W		0.37 ±0.05
74	YKR020W	VPS67	0.37 ±0.25
75	YGL139W		0.37 ±0.10
76	YDR039C	ENA2	0.36 ±0.12
77	YML072C		0.36 ±0.21
78	YDL240W	LRG1	0.35 ±0.06
79	YLR332W	MID2	0.35 ±0.07

80	YLR413W		0.35 ±0.01
81	YBR052C		0.34 ±0.08
82	YOR304C-A		0.34 ±0.10
83	YDL189W	RBS1	0.34 ±0.14
84	YKR100C		0.34 ±0.08
85	YCR038C	BUD5	0.33 ±0.09
86	YGL077C	HNM1	0.33 ±0.12
87	YLR407W		0.33 ±0.10
88	YLL028W	TPO1	0.33 ±0.17
89	YNL020C	ARK1	0.33 ±0.11
90	YIR003W	Aim21	0.33 ±0.08
91	YGR191W	HIP1	0.33 ±0.01
92	YOR043W	WHI2	0.32 ±0.20
93	YDR384C	ATO3	0.32 ±0.14
94	YDR038C	ENA5	0.32 ±0.15
95	YOR273C	TPO4	0.32 ±0.08
96	YER020W	GPA2	0.32 ±0.07
97	YOR086C		0.32 ±0.06
98	YMR212C	EFR3	0.32 ±0.13
99	YNL106C	INP52	0.32 ±0.09
100	YOL019W	TOS7	0.32 ±0.08
101	YOR161C		0.32 ±0.11
102	YHR107C	CDC12	0.31 ±0.30
103	YPR149W	NCE102	0.31 ±0.13
104	YER114C	BOI2	0.31 ±0.03
105	YGL233W	SEC15	0.31 ±0.12
106	YPL032C	SVL3	0.30 ±0.05
107	YPL206C		0.30 ±0.06
108	YIL147C	SLN1	0.30 ±0.08
109	YPL214C	THI6	0.29 ±0.11
110	YKL051W	SFK1	0.29 ±0.18
111	YNR055C	HOL1	0.29 ±0.09
112	YGR086C	PIL1	0.29 ±0.10
113	YML028W	TSA1	0.29 ±0.03
114	YDR040C	ENA1	0.29 ±0.19
115	YBR069C	TAT1	0.29 ±0.12
116	YLR166C	SEC10	0.29 ±0.14
117	YIL121W	QDR2	0.29 ±0.05
118	YLR319C	BUD6	0.29 ±0.05
119	YDR479C	PEX29	0.28 ±0.06
120	YPL058C	PDR12	0.28 ±0.08

121	YFL034C-B	MOB2	0.28 ±0.16
122	YIL068C	SEC6	0.28 ±0.04
123	YPL265W	DIP5	0.28 ±0.04
124	YEL060C	PRB1	0.28 ±0.25
125	YDR357C	CNL1	0.28 ±0.08
126	YMR058W	FET3	0.28 ±0.15
127	YNL173C	MDG1	0.28 ±0.17
128	YGR198W		0.28 ±0.06
129	YLR138W	NHA1	0.28 ±0.11
130	YGL008C	PMA1	0.28 ±0.12
131	YIL105C	LIT2	0.27 ±0.15
132	YDR166C	SEC5	0.27 ±0.27
133	YNL268W	LYP1	0.27 ±0.05
134	YNL233W	BNI4	0.27 ±0.16
135	YGL200C	EMP24	0.27 ±0.07
136	YGR121C	MEP1	0.27 ±0.19
137	YGL108C		0.27 ±0.19
138	YIL009W	FAA3	0.27 ±0.13
139	YDL099W		0.26 ±0.15
140	YBR234C	ARC40	0.26 ±0.07
141	YOL020W	TAT2	0.26 ±0.19
142	YBR102C	EXO84	0.26 ±0.05
143	YDR170W-A		0.26 ±0.05
144	YDR345C	HXT3	0.26 ±0.03
145	YJL186W	MNN5	0.26 ±0.13
146	YNL078W	NIS1	0.26 ±0.11
147	YOR153W	PDR5	0.26 ±0.05
148	YDR032C	PST2	0.25 ±0.08
149	YCL024W	KCC4	0.25 ±0.08
150	YFR024C-A	LSB3	0.25 ±0.18
151	YBR043C	AQR2	0.25 ±0.12
152	YOR070C	GYP1	0.25 ±0.03
153	YGR130C		0.25 ±0.06
154	YER133W	GLC7	0.24 ±0.07
155	YDR348C	PAL1	0.24 ±0.11
156	YHR146W	CRP1	0.24 ±0.11
157	YPR066W	UBA3	0.24 ±0.12
158	YKL129C	MYO3	0.24 ±0.04
159	YLR353W	BUD8	0.24 ±0.11
160	YGR138C	TPO2	0.24 ±0.06
161	YJR076C	CDC11	0.24 ±0.09

162	YOR233W	KIN4	0.24 ±0.03
163	YMR092C	AIP1	0.24 ±0.13
164	YOR042W	CUE5	0.24 ±0.09
165	YDR343C	HXT6	0.24 ±0.16
166	YEL017C-A	PMP2	0.24 ±0.05
167	YOL084W	PHM7	0.24 ±0.22
168	YOL047C		0.23 ±0.17
169	YIL140W	AXL2	0.23 ±0.05
170	YKR003W	OSH6	0.23 ±0.05
171	YBL037W	APL3	0.23 ±0.05
172	YAL055W	PEX22	0.23 ±0.09
173	YER008C	SEC3	0.23 ±0.14
174	YLL043W	FPS1	0.22 ±0.07
175	YOL070C		0.22 ±0.11
176	YBR109C	CMD1	0.22 ±0.05
177	YCR004C	YCP4	0.22 ±0.17
178	YEL063C	CAN1	0.22 ±0.15
179	YKR093W	PTR2	0.22 ±0.06
180	YGR255C	COQ6	0.22 ±0.11
181	YLR237W	THI7	0.22 ±0.01
182	YCL040W	GLK1	0.22 ±0.09
183	YBR059C	AKL1	0.22 ±0.11
184	YNL190W		0.22 ±0.06
185	YHR123W	EPT1	0.21 ±0.11
186	YLR084C	RAX2	0.21 ±0.06
187	YLR423C	APG17	0.21 ±0.08
188	YER145C	FTR1	0.21 ±0.04
189	YGL156W	AMS1	0.21 ±0.16
190	YNL085W	MKT1	0.21 ±0.04
191	YDR373W	FRQ1	0.21 ±0.11
192	YER054C	GIP2	0.21 ±0.02
193	YPR138C	MEP3	0.20 ±0.02
194	YBR255W		0.20 ±0.12
195	YDR084C	TVP23	0.20 ±0.02
196	YOR216C	RUD3	0.20 ±0.10
197	YNL142W	MEP2	0.20 ±0.05
198	YFR015C	GSY1	0.20 ±0.09
199	YOL112W	MSB4	0.20 ±0.04
200	YAL029C	MYO4	0.19 ±0.02
201	YBR200W	BEM1	0.19 ±0.21
202	YMR031C		0.19 ±0.04

203	YCR002C	CDC10	0.19 ±0.22
204	YPR049C	CVT9	0.19 ±0.08
205	YPR156C	TPO3	0.19 ±0.09
206	YHR004C	NEM1	0.19 ±0.14
207	YDR022C	CIS1	0.19 ±0.04
208	YOR326W	MYO2	0.18 ±0.10
209	YDL146W		0.18 ±0.15
210	YMR299C		0.18 ±0.15
211	YDL225W	SHS1	0.18 ±0.07
212	YPL249C	GYP5	0.18 ±0.11
213	YMR011W	HXT2	0.18 ±0.07
214	YLR258W	GSY2	0.18 ±0.05
215	YBR008C	FLR1	0.18 ±0.04
216	YHR147C	MRPL6	0.18 ±0.07
217	YOL149W	DCP1	0.17 ±0.09
218	YJL178C	ETF1	0.17 ±0.10
219	YPL010W	RET3	0.17 ±0.05
220	YNL238W	KEX2	0.17 ±0.05
221	YML052W	SUR7	0.17 ±0.16
222	YBL086C		0.17 ±0.06
223	YDL019C	OSH2	0.16 ±0.06
224	YDR497C	ITR1	0.16 ±0.07
225	YGL203C	KEX1	0.16 ±0.18
226	YKL103C	LAP4	0.16 ±0.07
227	YDL058W	USO1	0.16 ±0.01
228	YBR054W	YRO2	0.16 ±0.10
229	YPR122W	AXL1	0.16 ±0.01
230	YHL032C	GUT1	0.16 ±0.11
231	YNL130C	CPT1	0.16 ±0.04
232	YDL192W	ARF1	0.15 ±0.18
233	YHR158C	KEL1	0.15 ±0.09
234	YNL006W	LST8	0.15 ±0.14
235	YGR166W	KRE11	0.15 ±0.06
236	YNL194C		0.15 ±0.12
237	YFL036W	RPO41	0.15 ±0.03
238	YOR115C	TRS33	0.15 ±0.08
239	YPL065W	VPS28	0.15 ±0.08
240	YOL044W	PEX15	0.15 ±0.03
241	YBR288C	APM3	0.15 ±0.18
242	YKR001C	VPS1	0.15 ±0.13
243	YMR319C	FET4	0.15 ±0.16

244	YKL140W	TGL1	0.15 ±0.08
245	YLR067C	PET309	0.14 ±0.06
246	YDL222C		0.14 ±0.08
247	YJR086W	STE18	0.14 ±0.04
248	YCR024C-A	PMP1	0.14 ±0.16
249	YKL041W	VPS24	0.14 ±0.07
250	YPL004C	LSP1	0.14 ±0.04
251	YIL045W	PIG2	0.14 ±0.01
252	YMR010W		0.14 ±0.13
253	YGR229C	SMI1	0.14 ±0.08
254	YPL166W		0.14 ±0.17
255	YEL015W	EDC3	0.13 ±0.03
256	YMR163C		0.13 ±0.01
257	YDR141C	DOP1	0.13 ±0.05
258	YML085C	TUB1	0.13 ±0.03
259	YML064C	TEM1	0.13 ±0.11
260	YAR009C		0.13 ±0.06
261	YLR035C-A		0.12 ±0.04
262	YMR086W		0.12 ±0.07
263	YJL024C	APS3	0.12 ±0.15
264	YLR072W		0.12 ±0.03
265	YLR291C	GCD7	0.12 ±0.05
266	YNR056C	BIO5	0.12 ±0.07
267	YLR187W		0.11 ±0.07
268	YHR005C	GPA1	0.11 ±0.05
269	YNL126W	SPC98	0.11 ±0.08
270	YOL082W	CVT19	0.11 ±0.02
271	YCR061W		0.11 ±0.08
272	YLR250W	SSP120	0.11 ±0.06
273	YMR183C	SSO2	0.11 ±0.04
274	YHR011W	DIA4	0.10 ±0.07
275	YEL005C	VAB2	0.10 ±0.09
276	YMR253C		0.10 ±0.09
277	YPR148C		0.10 ±0.10
278	YNL065W	AQR1	0.10 ±0.05
279	YMR080C	NAM7	0.10 ±0.07
280	YOR109W	INP53	0.09 ±0.02
281	YDR150W	NUM1	0.09 ±0.00
282	YEL011W	GLC3	0.09 ±0.14
283	YLR347C	KAP95	0.09 ±0.04
284	YDR367W		0.09 ±0.07

285	YNR016C	ACC1	0.09 ±0.02
286	YLR219W	MSC3	0.08 ±0.12
287	YLL001W	DNM1	0.08 ±0.09
288	YDR484W	SAC2	0.08 ±0.03
289	YFL047W	RGD2	0.08 ±0.11
290	YBL017C	PEP1	0.08 ±0.18
291	YCL001W	RER1	0.08 ±0.06
292	YLL006W	MMM1	0.08 ±0.07
293	YGL219C	MDM34	0.08 ±0.04
294	YAR044W	OSH1	0.08 ±0.11
295	YDR517W	GRH1	0.08 ±0.09
296	YBR164C	ARL1	0.08 ±0.07
297	YJL029C	VPS53	0.07 ±0.08
298	YCL056C		0.07 ±0.02
299	YOR127W	RGA1	0.07 ±0.07
300	YHR182W		0.07 ±0.06
301	YPR029C	APL4	0.07 ±0.04
302	YNL297C	MON2	0.07 ±0.06
303	YNL118C	DCP2	0.06 ±0.03
304	YML071C	COG8	0.06 ±0.08
305	YDR027C	LUV1	0.06 ±0.09
306	YGL180W	APG1	0.05 ±0.04
307	YMR124W		0.05 ±0.04
308	YKR088C	TVP38	0.05 ±0.11
309	YGR261C	APL6	0.05 ±0.05
310	YDR270W	CCC2	0.04 ±0.06
311	YDR222W		0.04 ±0.09
312	YMR313C	TGL3	0.04 ±0.02
313	YDR525W-A	SNA2	0.04 ±0.12
314	YDR495C	VPS3	0.04 ±0.03
315	YKL092C	BUD2	0.03 ±0.01
316	YGL225W	VRG4 3	0.02 ±0.04
317	YOR284W	HUA2	0.01 ±0.05
318	YDL029W	ARP2	-0.01 ±0.09
319	YDR129C	SAC6	-0.02 ±0.03

Table 2.2: Endocytic proteins visualized in the GFP screen.

Screening Rank	Systematic Name	Common Name	PCC	±SD
1	YIR006C	PAN1	0.863	±0.01
2	YNL084C	END3	0.825	±0.06
3	YFR024C	YSC85	0.779	±0.06
4	YNL243W	SLA2	0.727	±0.11
5	YLR206W	ENT2	0.704	±0.04
6	YBL007C	SLA1	0.695	±0.09
7	YHR161C	YAP1801	0.646	±0.09
8	YJR005W	APL1	0.626	±0.18
9	YLR337C	VRP1	0.615	±0.39
10	YNR035C	ARC35	0.594	±0.07
11	YIL034C	CAP2	0.584	±0.11
13	YJL021C	BBC1	0.559	±0.04
14	YGL181W	GTS1	0.547	±0.12
15	YIL062C	ARC15	0.539	±0.07
16	YOR181W	LAS17	0.536	±0.05
17	YLR370C	ARC18	0.529	±0.13
18	YGR080W	TWF1	0.527	±0.11
19	YKL013C	ARC19	0.526	±0.05
21	YIL095W	PRK1	0.505	±0.12
25	YKL007W	CAP1	0.482	±0.12
26	YCR088W	ABP1	0.481	±0.13
27	YMR109W	MYO5	0.473	±0.05
28	YOL062C	APM4	0.473	±0.15
30	YOR367W	SCP1	0.463	±0.10
31	YDL161W	ENT1	0.460	±0.31
32	YCR030C	SYP1	0.456	±0.01
35	YGR241C	YAP1802	0.451	±0.07
37	YBL047C	EDE1	0.445	±0.19
40	YHR114W	BZZ1	0.434	±0.20
41	YCR009C	RVS161	0.430	±0.05
57	YLR429W	CRN1	0.388	±0.19
59	YDR388W	RVS167	0.386	±0.12
65	YPR171W	BSP1	0.381	±0.12
70	YJR058C	APS2	0.375	±0.14
89	YNL020C	ARK1	0.328	±0.11
90	YIR003W	AIM21	0.327	±0.08
99	YNL106C	INP52	0.318	±0.09
140	YBR234C	ARC40	0.262	±0.07

155	YDR348C	PAL1	0.244 ±0.11
158	YKL129C	MYO3	0.242 ±0.04
171	YBL037W	APL3	0.227 ±0.05
183	YBR059C	AKL1	0.216 ±0.11
318	YDL029W	ARP2	-0.005 ±0.09
319	YDR129C	SAC6	-0.016 ±0.03

consistent with recent findings that AP-2 does in fact play a role in yeast CME [14, 21]. The lower range of the 197 colocalizing proteins was enriched in proteins spanning a variety of functions and containing predicted or known transmembrane domains. Such proteins correspond to known or likely CME cargo and typically showed a relatively even distribution throughout the plasma membrane similar to Lyp1 (Figure 2.1.A-B and Table 2.1). To identify probable new machinery components, we next focused on proteins with unknown function and PCC similar to known endocytic proteins. Importantly, 28 uncharacterized proteins colocalize with Sla1 and many of them are not predicted to have a transmembrane domain and thus may not be endocytic cargo (Figure 2.1.D and Table 2.3). Most notably, nine of such uncharacterized proteins were in the top 50 PCC scores, representing highly likely new components of the endocytic machinery. The highest scoring uncharacterized protein was Ubx3 with a PCC of 0.52 ± 0.20 (Figure 2.1.C, Table 2.1, and Table 2.3). This protein was identified as having a punctate composite fluorescent pattern in the library, which also showed a higher cytosolic background compared to our images, probably due to their use of wide-field fluorescence microscopy. Ubx3 is defined by a ubiquitin-like UBX (ubiquitin regulatory X) domain in its C terminus (Figure 2.2.A) [22-24] and was subjected to further study to confirm its endocytic role.

2.3.3 Ubx3 is the first UBX domain-containing protein in the endocytic machinery

By confocal fluorescence microscopy, Ubx3–GFP displayed similar patch dynamics to Sla1–RFP and other endocytic coat proteins arriving at intermediate stages. Ubx3–GFP had a patch lifetime of 45 ± 3 sec, appearing slightly before Sla1–RFP at the endocytic site and remaining slightly after the disappearance of Sla1–RFP (Figure 2.2.B-C). Ubx3-GFP is recruited after early coat proteins such as Ede1–RFP (Figure 2.3). Ubx3–GFP patches also showed

Table 2.3: Uncharacterized proteins colocalizing with Sla1-RFP

Screening rank	Systematic name	Common name	PCC ± SD
20	YDL091C	Ubx3	0.52 ± 0.26
23	YDL012C[a]		0.50 ± 0.14
24	YER071C	TDA2	0.49 ± 0.13
33	YOR104W[b,c]	PIN2	0.45 ± 0.19
36	YGR026W[b]		0.45 ± 0.03
42	YBL029C-A		0.43 ± 0.12
47	YBR016W[a]		0.42 ± 0.05
49	YDR090C[b]		0.41 ± 0.11
50	YDR034W-B[a]		0.41 ± 0.09
58	YDR033W[b]	MRH1	0.39 ± 0.15
61	YMR295C		0.38 ± 0.05
71	YDR344C		0.37 ± 0.05
73	YDR210W[a]		0.37 ± 0.05
80	YLR413W[b]		0.35 ± 0.01
81	YBR052C	RFS1	0.34 ± 0.08
87	YLR407W		0.33 ± 0.10
100	YOL019W[b]	TOS7	0.32 ± 0.08
101	YOR161C[b]	PNS1	0.32 ± 0.11
106	YPL032C	SVL3	0.30 ± 0.05
137	YGL108C[c]		0.27 ± 0.19
148	YDR032C	PST2	0.25 ± 0.08
159	YLR353W[b]	BUD8	0.24 ± 0.11
167	YOL084W[b]	PHM7	0.24 ± 0.22
175	YOL070C	NBA1	0.22 ± 0.11
177	YCR004C[c]	YCP4	0.22 ± 0.17
184	YNL190W[a]		0.22 ± 0.06
194	YBR255W[b]	MTC4	0.20 ± 0.12

[a] Predicted tail-anchor to plasma membrane.
[b] Predicted transmembrane region(s)
[c] Predicted to be palmitoylated.

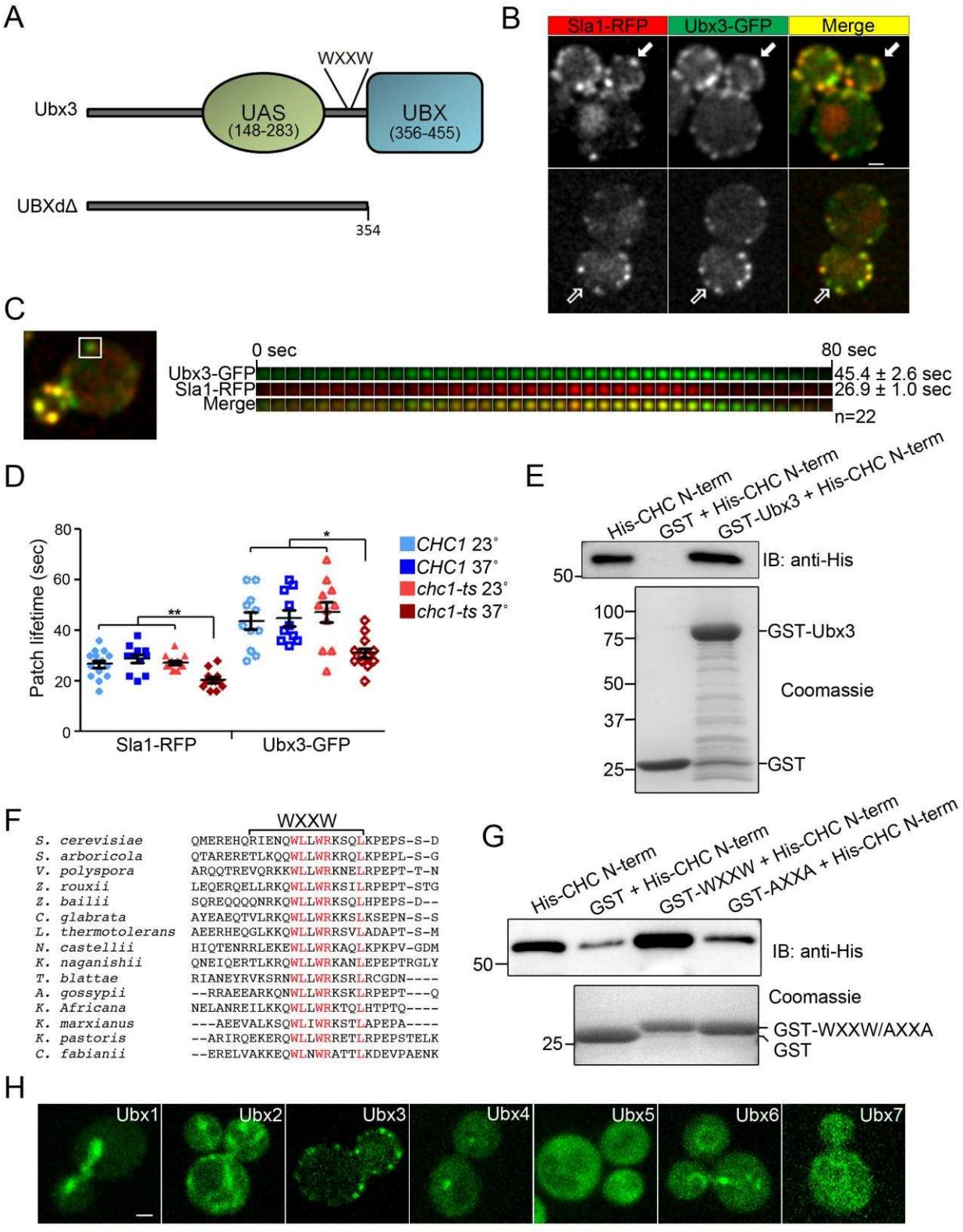

Figure 2.2: Ubx3 is a novel component of the endocytic machinery. A) Cartoon representation of Ubx3 domains predicted by the Phyre2 protein folding recognition engine [25]. UAS, domain

of unknown function. B) Ubx3-GFP shows strong colocalization with Sla1-RFP by live cell confocal fluorescence microscopy. Solid arrows show an example of an endocytic patch demonstrating strong colocalization, open arrow shows an example of Ubx3-GFP present at an endocytic patch without Sla1-RFP. Bar= 1 μm. C) Dynamics of Ubx3-GFP and Sla1-RFP at endocytic sites were compared. Left, one frame of a movie indicating with a white box the endocytic site used for constructing a kymograph. Right, kymograph demonstrating dynamics of Ubx3-GFP and Sla1-RFP, and average patch lifetimes (22 patches). Each frame = 2 sec. D) Patch lifetimes of Sla1-RFP and Ubx3-GFP were measured at room temperature and 37˚C in both wild type (*CHC1*) and temperature sensitive clathrin heavy chain (*chc1-ts*) cells (15 patches per strain and temperature, **$p<0.0001$ *$p<0.001$). E) GST-Ubx3 directly binds polyhistidine tagged clathrin heavy chain N-terminal domain as determined by GST-pulldown with purified proteins. Upper panel, eluted proteins were analyzed by immunoblotting using an antibody to the polyhistidine tag (anti-His). Lower panel, loading control coomassie stained gel of GST and GST-Ubx3 proteins bound to glutathione beads. F) Alignment of *S. cerevisiae* Ubx3 amino acid sequence with that of other fungal species demonstrates high conservation of residues matching the W-box core clathrin-binding motif. Strictly conserved residues are shown in red. The fragment fused to GST for GST-pulldown assays in Figure 2G is indicated at the top (WXXW). G) Ubx3 contains a W-box that binds the clathrin heavy chain N-terminal domain. GST alone, GST-WXXW and corresponding mutant GST-AXXA were bound to glutathione-Sepharose beads and incubated with polyhistidine tagged N-terminal domain of clathrin heavy chain. The eluted proteins were analyzed by immunoblotting using an antibody to the polyhistidine tag (anti-His). Lower panel, loading control coomassie stained gel of GST-fusion proteins bound to glutathione beads. H) Ubx3-GFP is the only UBX domain-containing protein that localizes to endocytic patches. Yeast strains expressing each of the seven Ubx proteins tagged with GFP were analyzed by confocal fluorescence microscopy. Bar= 1 μm.

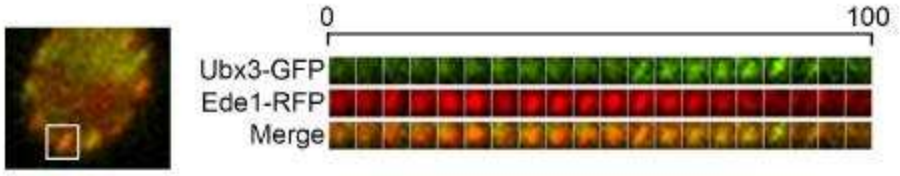

Figure 2.3: Ubx3 arrives to endocytic sites after early protein Ede1. Dynamics of Ubx3-GFP and Ede1-RFP at endocytic sites were compared. Left, one frame of a movie indicating with a white box the endocytic site used for constructing a kymograph. Right, kymograph demonstrating dynamics of Ubx3-GFP and Ede1-RFP. Each Frame = 5 sec.

movement away from the surface toward the center of the cell right before disappearing, a behavior typical of endocytic coat proteins (Figure 2.2.C). To assess whether Ubx3–GFP patch localization is affected by the endocytic coat, Ubx3–GFP dynamics were visualized in cells carrying a temperature-sensitive allele of the clathrin heavy-chain gene (*chc1-ts*) [26]. Upon incubation at 37˚, the patch lifetime of Ubx3–GFP was significantly reduced (Figure 2.2.D). In contrast, the patch lifetime of Ubx3–GFP in wild-type cells (*CHC1*) was not affected by incubation at 37˚ (Figure 2.2.D). For comparison, the clathrin-binding adaptor protein Sla1–GFP [17] was analyzed in parallel in cells carrying the *chc1-ts* allele and demonstrated a similar reduction in patch lifetime upon incubation at 37˚, whereas wild-type cells did not (Figure 2.2.D). This result indicates that Ubx3 associates with the endocytic coat in vivo. To investigate whether Ubx3 binds clathrin, we tested *in vitro* for physical interaction by GST pulldown. GST and GST–Ubx3 were immobilized on glutathione-Sepharose beads and incubated with polyhistidine-tagged clathrin heavy-chain N-terminal β-propeller domain (His–CHC N-term) [7]. Immunoblotting analysis showed binding of His–CHC N-term to GST–Ubx3 but not to GST indicating a direct physical interaction (Figure 2.2.E).

Inspection of the Ubx3 amino acid sequence for clathrin-binding motifs revealed no obvious clathrin-box (LLDLD related sequence) [27]. However, a sequence conforming to the core W-box motif (WXXW), where X represents any amino acid [28, 29], was located upstream of the UBX domain (Figure 2.2.A). Sequence alignment revealed that these residues are extremely well conserved among the Ubx3 family, suggesting functional importance (Figure 2.2.F). Consistent with a functional W-box capable of engaging the clathrin β-propeller domain, this stretch of the Ubx3 sequence is predicted to be disordered. The ability of this sequence to bind clathrin was determined by GST-pulldown. A GST-fusion protein containing the Ubx3

candidate W-box and flanking sequences (residues 337–350, GST–WXXW) bound His–CHC N-term significantly above background levels (GST) (Figure 2.2.G). Mutation of the tryptophan residues to alanine (GST–AXXA) diminished His–CHC N-term binding to background levels, showing that binding was specific (Figure 2.2.G). To our knowledge, this is the first example of a W-box type clathrin-binding motif in a non-mammalian protein. Together these results demonstrate Ubx3 binds clathrin and that it is a component of the endocytic coat. As there are seven UBX domain-containing proteins in yeast, we visualized each protein tagged with GFP to determine if any others localized to endocytic sites, but only Ubx3 displayed an endocytic punctate fluorescent pattern (Figure 2.2.H).

To further test for a role of Ubx3 in endocytosis we performed two uptake assays. First we used Lucifer yellow, a fluid-phase fluorescent dye, to track bulk intake into cells. Wild-type cells and cells carrying a deletion of the *UBX3* gene (*ubx3Δ*) were incubated with media containing Lucifer yellow and the internalized dye was quantified by fluorescence microscopy. An internalization defect was observed for *ubx3Δ* cells compared to wild-type cells (Figure 2.4.A). The extent of the defect was comparable to the one we observed for Las17- MP8-12, a mutant displaying altered Las17 recruitment to endocytic sites and misregulation of actin polymerization [18]. We also developed a strain harboring a deletion of the UBX domain in the endogenous *UBX3* gene (*ubx3*$^{\Delta UBXd}$) (Figure 2.2.A). This strain displayed a similar defect in Lucifer yellow internalization, suggesting that Ubx3 depends on its UBX domain for endocytic function (Figure 2.4.A). GFP tagging of the *ubx3*$^{\Delta UBXd}$ allele and live cell imaging showed that the mutant Ubx3 protein is not degraded but localizes to fast-moving internal structures rather than endocytic sites (Figure 2.5). Thus, the UBX domain is required for normal Ubx3 localization and function at endocytic sites. We then used Mup1–GFP to track cargo endocytosis.

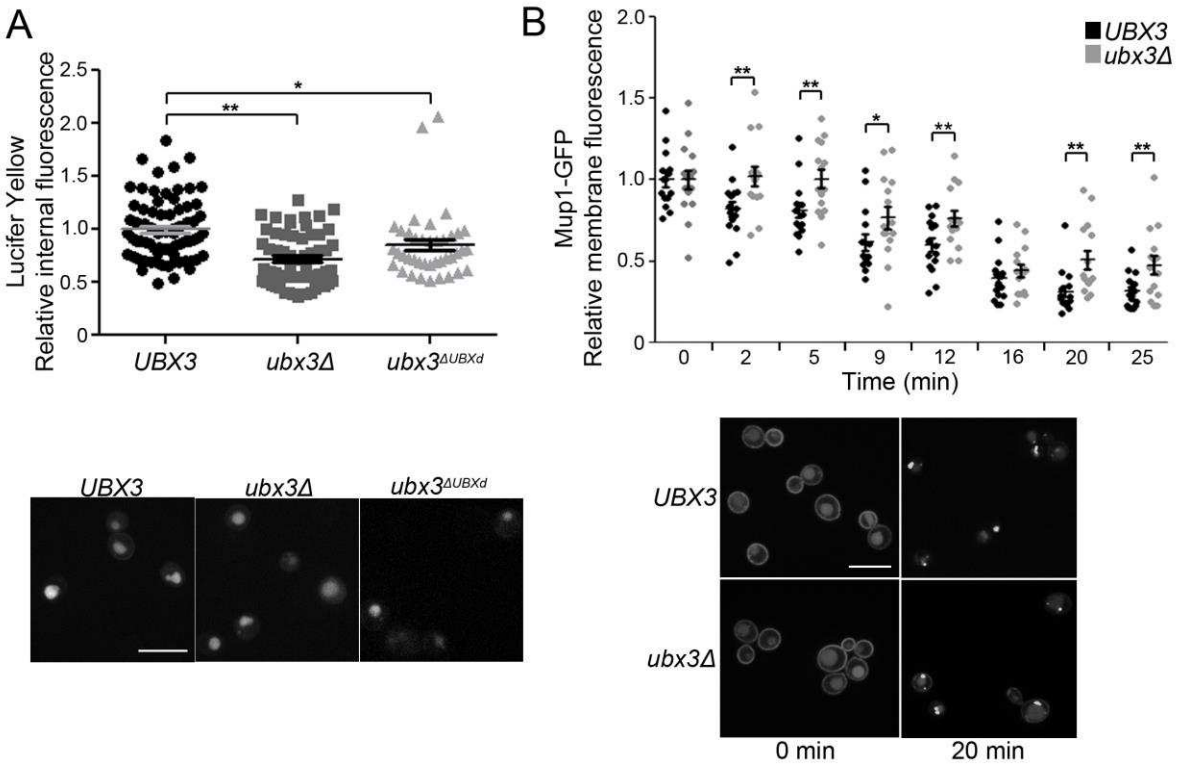

Figure 2.4: Ubx3 is needed for optimal endocytosis. A) Wild type cells (*UBX3*), cells carrying a deletion of the UBX3 gene (*ubx3*Δ) and a deletion of the UBX domain in the UBX3 gene (*ubx3*$^{\Delta UBXd}$) were incubated with Lucifer Yellow and imaged by confocal fluorescence microscopy. The fluorescence intensity inside the cell was measured, normalized by the intensity of the background and expressed as the average relative fluorescence intensity (40 cells per strain, **p<0.001 *p<0.01). The experiment was performed two times with similar results. Lower panels, representative images of the cells. Bar= 10 μm. B) Endocytosis of the methionine transporter Mup1 tagged with GFP was analyzed in *UBX3* and *ubx3*Δ cells as described in Materials and Methods. Fluorescence in the plasma membrane was measured using a mask drawn on the cell periphery and normalized to the background (15 cells per strain and time point, **p<0.001 *p<0.01). The experiment was performed three times with similar results. Lower panels, representative images of cells at 0 and 20 min after change to media containing methionine. Bar= 10 μm.

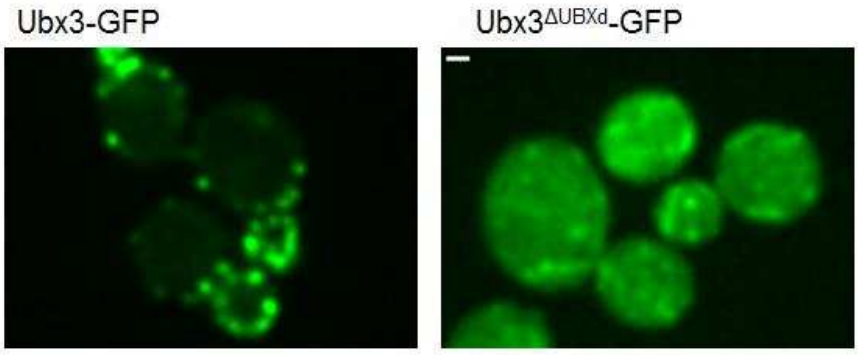

Figure 2.5: Ubx3 loses its endocytic localization upon UBX domain deletion. Ubx3-GFP is imaged with and without a UBX domain deletion. Scale bar = 1 μm.

Mup1 is a methionine transporter that is expressed at the plasma membrane when cells are starved for methionine, but quickly internalized via ubiquitin-dependent CME when cells are returned to methionine-rich media. Internalization of this cargo again portrayed a delay in *ubx3Δ* cells compared to wild-type cells (Figure 2.4.B). Together, these data demonstrate that Ubx3 is a new component of the clathrin-mediated endocytic machinery needed for optimal endocytosis.

2.3.4 Ubx3 regulates dynamics of the early arriving protein Ede1 but not later arriving coat proteins or actin assembly

In an effort to understand the mechanistic basis of Ubx3 function in CME, we examined the patch lifetimes of known endocytic proteins tagged with GFP in wild-type and *ubx3Δ* cells. We analyzed early (Ede1, Syp1), intermediate (End3, Ent2, Las17), and late (Myo5, Abp1, Rvs167) arriving components of the endocytic machinery [5, 10, 30-34]. Remarkably, Ede1–GFP had a significantly longer patch lifetime in *ubx3Δ* cells compared to wild-type cells while other endocytic proteins were unaffected (Figure 2.6.A–C). Ede1–GFP displayed a 34% increase in lifetime from 91 ± 4 sec to 123 ± 8 sec (mean ± SEM, $P<0.01$) (Figure 2.6.A–C). Analysis of *ubx3*$^{\Delta UBXd}$ cells demonstrated a similar increase in Ede1–GFP lifetime (129 ± 11 sec, mean ± SEM, $P<0.01$), again establishing that the UBX domain is required for Ubx3 function (Figure 2.6.B-C). The extension of the Ede1 patch lifetime occurs at the beginning of the endocytic process, as the time between arrival of Ede1–RFP and Sla1–GFP increases in *ubx3Δ* cells compared to wild-type cells (Figure 2.6.D–F). A similar delay was observed between the arrival of Ede1–RFP and Syp1–GFP in *ubx3Δ* cells compared to wildtype cells (Figure 2.6.D–F). The cause of this delay appeared to be a slower recruitment of Ede1–GFP to the endocytic site as we noted that in *ubx3Δ* cells and *ubx3*$^{\Delta UBXd}$ cells Ede1–GFP fluorescence intensity increased more

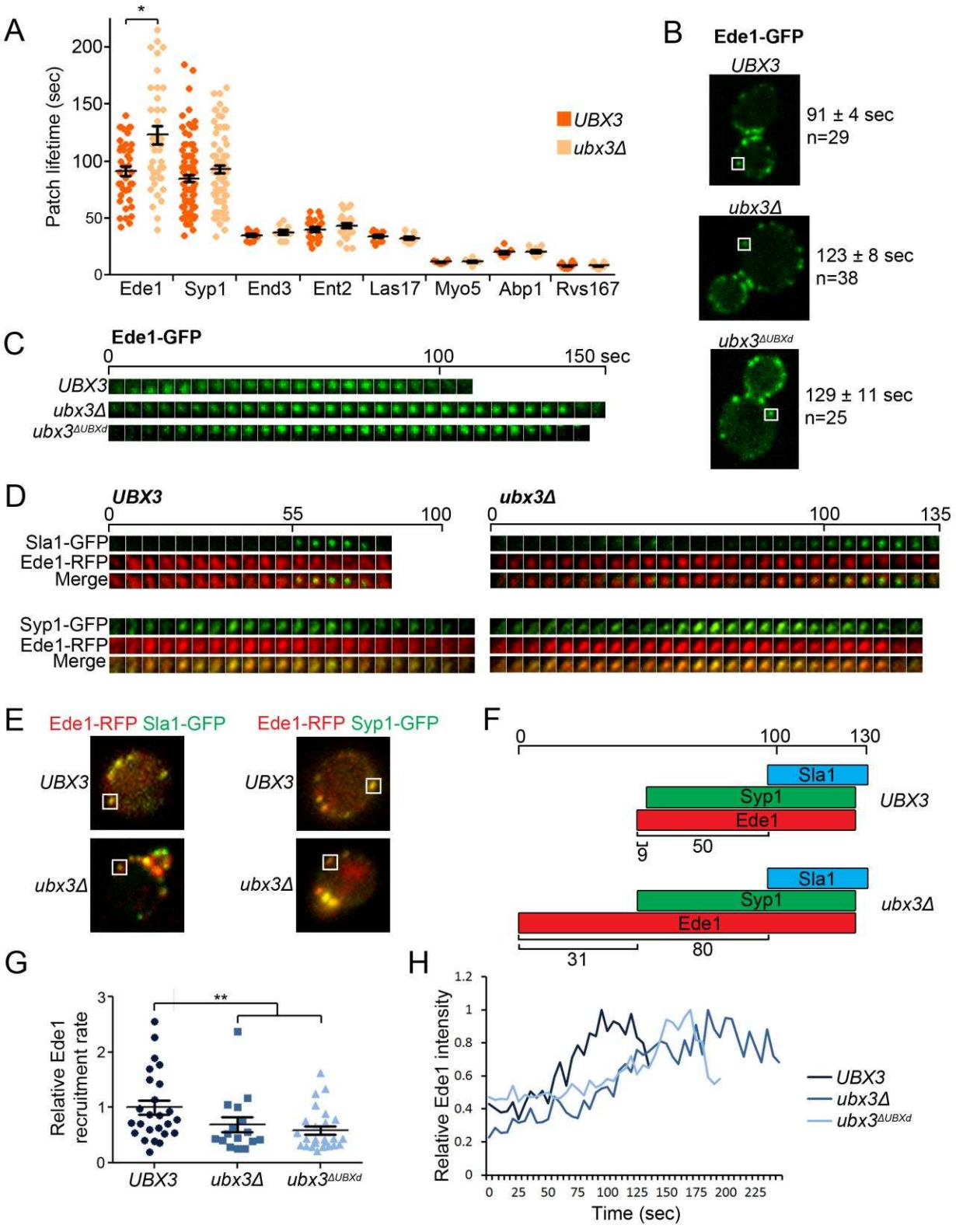

Figure 2.6: Ede1 dynamics at sites of endocytosis depend on Ubx3. A) Ede1-GFP has a large increase in endocytic patch lifetime in *ubx3Δ* cells, while other endocytic machinery proteins

tested are unaffected. Strains expressing the indicated GFP-tagged proteins either in *UBX3* or *ubx3*Δ background were analyzed by live cell fluorescence microscopy (10-58 patches per strain, *p<0.01). B) Panels represent a frame from movies of cells expressing Ede1-GFP in UBX3, *ubx3*Δ or $ubx3^{\Delta UBXd}$ background. Boxed patches are tracked in the kymographs shown in (C). Ede1-GFP patch lifetime and number of patches analyzed for each strain are shown on the right. C) Kymographs demonstrating the increase in Ede1-GFP lifetime in *ubx3*Δ cells and $ubx3^{\Delta UBXd}$ cells compared to *UBX3* cells. Each frame = 5 sec. D) Kymographs displaying the patch lifetime of Ede1-RFP is extended at the beginning of the endocytic process, before Syp1-GFP or Sla1-GFP arrive. Each frame = 5 sec. E) Panels represent a frame from the movies used to construct the kymographs shown in (D), with the corresponding endocytic patches indicated by white boxes. F) Cartoon representation of the Sla1, Syp1 and Ede1 relative timing of arrival to endocytic sites in *UBX3* and *ubx3*Δ cells. G-H) The recruitment rate of Ede1-GFP, measured from first appearance to peak patch intensity, is slower in *ubx3*Δ and $ubx3^{\Delta UBXd}$ cells compared to *UBX3* cells (25 patches per strain, **p<0.0001). The peak fluorescence intensity between strains was unchanged.

slowly before reaching the peak (Figure 2.6.C). Indeed, quantification of the Ede1–GFP relative recruitment rate demonstrated a significant defect in *ubx3Δ* cells and *ubx3*$^{\Delta UBXd}$ cells compared to wild-type cells (Figure 2.6.G-H). Slower Ede1 recruitment and prolonged endocytic patch lifetime in *ubx3Δ* cells and *ubx3*$^{\Delta UBXd}$ cells further link Ubx3 to the CME machinery and is consistent with the Lucifer yellow and Mup1–GFP endocytosis defects shown above.

Given the effect of *UBX3* gene deletion on the dynamics and patch lifetime of Ede1–GFP, we examined the converse relationship. The Ubx3–GFP patch lifetime was determined in wild-type and *ede1Δ* cells. Ubx3–GFP displayed a significant decrease in patch lifetime from 43 ± 2 sec to 31 ± 3 sec (mean ± SEM, $P<0.01$) suggesting a functional connection between Ubx3 and Ede1 (Figure 2.7).

Interestingly, UBX domain-containing proteins constitute a major family of cofactors for the ubiquitin-editing complex Cdc48 that determine its location and targets [23, 24, 35]. A previous study reported that all seven *S. cerevisiae* UBX domain-containing proteins bind Cdc48 by yeast-two-hybrid analysis [23]. We confirmed a physical interaction between Ubx3 and Cdc48 using a GST-pulldown assay (Figure 2.8.A). To test for a function of Cdc48 in endocytosis we used the Lucifer yellow uptake assay with wild-type cells (*CDC48*) and cells carrying a temperature-sensitive allele (*cdc48-3*) [36]. A severe defect in Lucifer yellow uptake was observed at 37˚, indicating a function for Cdc48 in endocytosis (Figure 2.8.B).

We further examined effects on Ede1 with Cdc48 inactivation. Ede1-GFP patch lifetime is increased to a similar extent in cells with heat inactivated Cdc48 (*cdc48-3)* (Figure 2.9.A) compared to *ubx3Δ*, endorsing that the effect on Ede1 in *ubx3Δ* cells and *ubx3*$^{\Delta UBXd}$ cells is caused by lack of Cdc48 recruitment to the endocytic site. Furthermore, we observed large

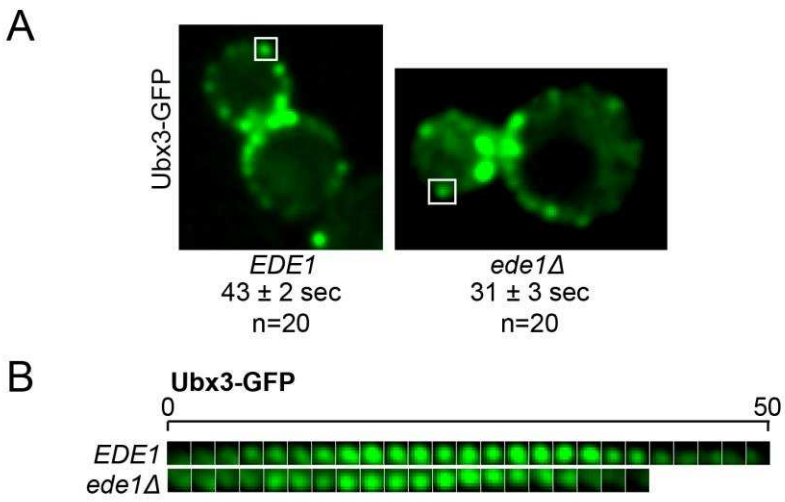

Figure 2.7: Ubx3 dynamics at sites of endocytosis depend on Ede1. A) Cells with white boxes demonstrating patches used in kymographs (B). Ubx3-GFP has a decrease in endocytic patch lifetime in *ede1Δ* cells. Strains expressing Ubx3-GFP either in *EDE1* or *ede1Δ* background were analyzed by live cell fluorescence microscopy (20 patches per strain, $p<0.01$). Each frame = 2 sec.

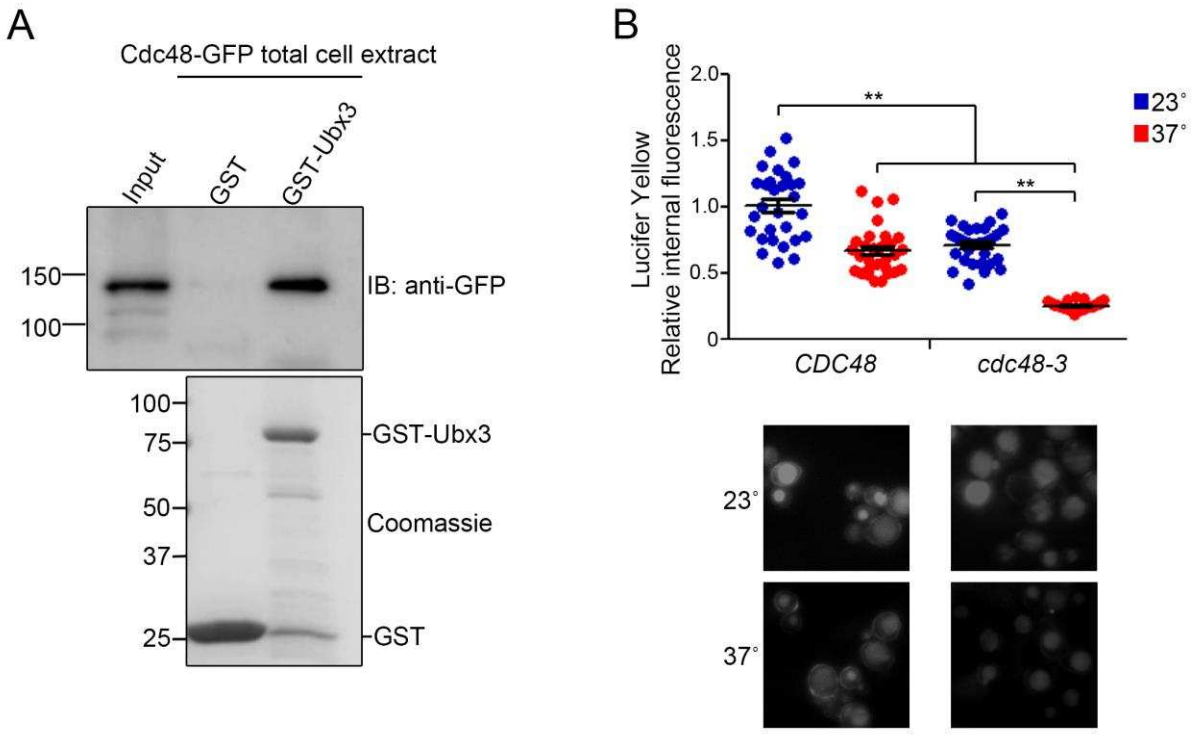

Figure 2.8: Ubx3 interacts physically with Cdc48 and endocytosis depends on Cdc48. A) Ubx3 binds Cdc48. GST-Ubx3 and GST alone were bound to glutathione-Sepharose beads and incubated with total cell extract prepared with a strain expressing Cdc48-GFP from the endogenous locus. The eluted proteins were analyzed by immunoblotting using an antibody to the GFP tag (anti-GFP). Lower panel shows a loading control coomassie stained gel of GST and GST-Ubx3 proteins bound to glutathione beads in the assay. B) Lucifer Yellow uptake was measured at room temperature and 37˚C in both wild type cells (*CDC48*), and cells carrying a temperature sensitive allele of the CDC48 gene (*cdc48-3*). The fluorescence intensity inside the cell was measured, normalized by the intensity of the background and expressed as the average relative fluorescence intensity (**p<0.0001). The lower panels show representative images of the cells.

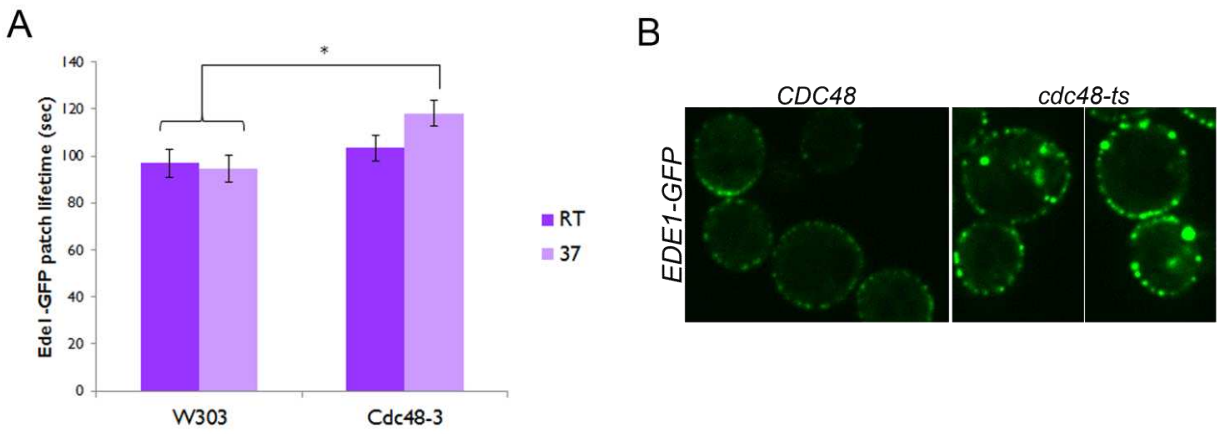

Figure 2.9: Ede1 is affected by Cdc48 inactivation. A) Inactivation of Cdc48 by incubation of *cdc48-3* strain at 37˚ increases Ede1-GFP patch lifetime while temperature does not affect Ede1 in wild type (*W303)* cells. Bars indicate average ± SEM. *$p<0.05$. B) Images of Ede1-GFP expressed at endogenous levels from a plasmid in wildtype cells (*CDC48*, left) and heat treated *cdc48-3* cells (right). Both internal and membrane proximal aggregates of Ede1-GFP are present when Cdc48 is inactivated.

aggregates of Ede1-GFP in cells with heat inactivated Cdc48 (Figure 2.9.B), suggesting a role for Cdc48 is disassembling protein aggregates at the endocytic site, as has been demonstrated as a role for Cdc48 in other cell processes. Therefore, Ubx3 function in endocytosis may be linked to the ubiquitin-editing and complex-segregating protein Cdc48.

2.4 Discussion

We utilized a new microscopy-based screening method to detect highly likely novel components of the CME machinery in *S. cerevisiae*. The proteins found here were not identified in previous screenings for endocytic proteins [13, 15]. Results from the screen should provide a valuable resource for the endocytosis and membrane transport community. Among proteins with unknown function, the top-scoring one, Ubx3, was confirmed as a new regulator of endocytosis using several approaches. The relatively modest nature of the endocytic defects observed in *ubx3Δ* cells may explain why this protein has not been identified in previous screenings. It is also possible that while not normally localized to CME sites, other UBX proteins do play a compensatory role in *ubx3Δ* cells. Additional proteins with unknown function, particularly those displaying high PCC in the screen, are likely bona fide regulators of endocytosis. Indeed we have confirmed that the third highest scoring protein, YER071C, is a new CME machinery component as described in Chapter 3. Characterization of the other top-scoring proteins identified here will likely shed new light on the CME regulatory mechanisms in *S. cerevisiae*. Given the high conservation of the CME machinery during evolution, the new proteins identified here likely regulate endocytosis not only in yeast but also in other eukaryotes.

Our data revealed Ubx3 as the first member of the conserved UBX domain protein family with a function in endocytosis. Ubx3 is a component of the coat that interacts physically and

functionally with clathrin and regulates endocytosis. Of note, Ubx3 represents the first example of a non-mammalian protein containing a W-box indicating that this clathrin-binding mode is ancient. Because deletion of the *UBX3* gene affected both bulk endocytosis (Lucifer yellow) and internalization of a specific cargo (Mup1–GFP), we favor a model in which Ubx3 functions as a general CME factor rather than a cargo-specific adaptor.

At a mechanistic level, Ubx3 regulates the patch dynamics of Ede1, one of the earliest arriving components and known to regulate endocytic site initiation [30, 34, 37]. Different scenarios could explain this result. First, it is possible that Ubx3 is present early on with Ede1 at endocytic sites at levels low enough that it is not detected until later when more molecules accumulate. We consider this possibility unlikely, but cannot rule it out. Second, Ede1 may begin to assemble normally, but only later stages of recruitment depend on Ubx3. Third, Ubx3 may act indirectly on Ede1 dynamics. Ede1 is subjected to ubiquitination and de-ubiquitination and alteration of this dynamic was previously shown to affect Ede1 recruitment to the membrane [37, 38]. Thus, we speculate that Ubx3 may regulate the balance of Ede1 ubiquitination/de-ubiquitination and consequently Ede1 dynamics at CME sites. Fourth, Ubx3 may function in endocytosis by regulating the ubiquitination of integral membrane protein cargo at endocytic sites or even downstream at endosomes. In such a scenario the extension of Ede1 patch lifetime in *ubx3Δ* cells would be secondary to cargo misregulation. In either of the last two scenarios, ubiquitin modifications of Ede1 or cargo are involved. The fact that Ubx3 binds to the ubiquitin-editing complex Cdc48 and that inactivation of Cdc48 affects endocytosis supports a function of Ubx3 in ubiquitin regulation at endocytic sites. Demonstration of Ede1 patch lifetime increase and Ede1-GFP aggregates with Cdc48 inactivation further contributes to the theory that the function of Ubx3 at endocytic sites is to recruit Cdc48. Increase of Ede1 patch lifetime could be

a result of unavailability of Ede1 due to these aggregates, thus explaining the reduced recruitment rate. However, elucidating exactly how Ubx3 regulates endocytosis warrants future experimentation.

In summary, through our screening we have provided evidence for novel, uncharacterized proteins as components of the CME machinery. Furthermore, these studies establish a new paradigm for UBX domain protein function as a regulator of endocytic site progression.

2.5 Experimental Procedures

2.5.1 Plasmids, yeast strains and GFP library screening

Recombinant GST-fusion Ubx3 protein and fragment containing residues 337-350 (W-box) were created by PCR amplification of full length ORF of genomic DNA or the corresponding fragment and cloning into pGEX-5X-1 (Amersham Biosciences). Recombinant polyhistidine-tagged clathrin heavy chain N-terminal domain was created by PCR amplification of bp 1-1449 of the *CHC1* ORF and cloning into pET-30a+ (Novagen). Site-directed mutagenesis was accomplished using the QuikChange system (Stratagene).

The full *Saccharomyces cerevisiae* GFP collection and a strain carrying a deletion of the UBX3 gene were obtained from Invitrogen [15]. The 319 GFP collection strains selected for the screen were grown in 96-well plates supplied with minimal media. SDY356 *(MATα ura3-52, leu2-3,112 his3-Δ200, trp1-Δ901, lys2-801, suc2-Δ9 GAL -MEL chc1-521::URA3 SLA1-RFP::KAN)* cells were introduced into each well using a replica plater. Mating was allowed for 2 hours at 30˚C. The replica plater was then used to stamp mated cells from the 96 well plate onto selective media agar plates. Mated cells were allowed to grow for 3 days, then returned to liquid media with 15% glycerol and stored at -80˚C until imaging as described below.

StrainYYH75 *(MATa ura3-52, leu2-3, cdc48-3)* carrying the temperature sensitive allele of the CDC48 gene and parental strain were a gift from Dr. Tingting Yao. All other strains carrying gene deletions or fluorescent tags were generated following standard approaches: SDY 356 and SDY427 (*MATα ura3-52, leu2-3,112 his3-Δ200, trp1-Δ901, lys2-801, suc2-Δ9 GAL -MEL chc1-521::URA3 UBX3-GFP::HIS3*) were employed for imaging in Figure 2.2.C. SDY500 (*MATα his3Δ1, leu2Δ0, met15-Δ0, ura3 Δ0, trp1-Δ901 ubx3Δ::URA3*) was created, mated with various strains from the GFP library and subsequently sporulated and subjected to tetrad dissection to generate haploid strains SDY586 (*MATa his3Δ1, leu2Δ0, met15-Δ0, ura3 Δ0 ubx3Δ::URA3, MUP1-GFP::HIS3*), SDY567 (*MATa his3Δ1, leu2Δ0, met15-Δ0, ura3 Δ0 ubx3Δ::URA3, EDE1-GFP::HIS3*), SDY569 (*MATa his3Δ1, leu2Δ0, met15-Δ0, ura3 Δ0 ubx3Δ::URA3, ENT2-GFP::HIS3*), SDY570 (*MATa his3Δ1, leu2Δ0, met15-Δ0, ura3 Δ0 ubx3Δ::URA3, RVS167-GFP::HIS3*), and SDY585 (*MATa his3Δ1, leu2Δ0, met15-Δ0, ura3 Δ0 ubx3Δ::URA3, SYP1-GFP::HIS3*), SDY667 (*MATa his3Δ1, leu2Δ0, met15-Δ0, ura3 Δ0 ubx3Δ::URA3, END3-GFP::HIS3*), SDY668 (*MATa his3Δ1, leu2Δ0, met15-Δ0, ura3 Δ0 ubx3Δ::URA3, LAS17-GFP::HIS3*), SDY669 (*MATa his3Δ1, leu2Δ0, met15-Δ0, ura3 Δ0 ubx3Δ::URA3, MYO5-GFP::HIS3*), and SDY670 (*MATa his3Δ1, leu2Δ0, met15-Δ0, ura3 Δ0 ubx3Δ::URA3, ABP1-GFP::HIS3*). These strains were utilized for fluorescence microscopy in Figure 2.4.A. SDY584 (*MATα his3Δ1, leu2Δ0, met15-Δ0, ura3 Δ0, EDE1-RFP::KANMX4)* was mated with the Syp1-GFP strain from the GFP library (*MAT*a *his3Δ1, leu2Δ0, met15-Δ0, ura3 Δ0 SYP1-GFP::HIS*) to create diploid strain SDY595 (*MAT*a/*MATα his3Δ1, leu2Δ0, met15-Δ0, ura3 Δ0 EDE1-RFP::KANMX4 SYP1-GFP::HIS*) which was subjected to sporulation and tetrad dissection, and resulting haploid segregant matted with SDY500. The resulting diploid strain was subjected to tetrad dissection to create SDY596 (*MATa his3Δ1, leu2Δ0, met15-Δ0, ura3 Δ0 ubx3Δ::URA3,*

EDE1-RFP::KANMX4, SYP1-GFP::HIS3). SDY622 (*MATa ura3-52, his3Δ1, leu2Δ0, trp1-Δ901 EDE1-RFP::KANMX4, SLA1-GFP::TRP1)* was mated with SDY500, sporulated and subjected to tetrad dissection to create SDY633 (*MAT*a *ura3-52, his3Δ1, leu2Δ0, trp1-Δ901 Δubx3::URA3, EDE1-RFP::KANMX4, SLA1-GFP::TRP1).* Strain harboring a deletion of the UBX domain in the endogenous *UBX3* gene was created, SDY648 (*MATa his3Δ1, leu2Δ0, met15-Δ0, ura3 Δ0 EDE1-GFP::HIS3 ubx3*$^{\Delta UBXd}$ *::URA3).* Strains expressing Ubx1-7 –GFP from the endogenous locus were obtained from the GFP library.

2.5.2 Biochemical methods

Total yeast cell extracts were prepared as described previously [17, 39]. GST- and polyhistidine-fusion proteins were expressed in *E. coli* and purified as described [19, 39]. GST pulldowns were performed by loading Glutathione-sepharose beads with GST-fusion protein for 30 min at room temperature. Beads were washed 2 times to remove excess GST-fusion protein, then cell extract or purified protein in PBS (or 50 mM HEPES, 100 mM NaCl, pH 7.4) containing 1% TritonX-100 was added to beads and rotated for 1 hour at 4˚C. Beads were washed 3 times with the same buffer and 1 time with buffer without TritonX-100. Western blotting was performed with Anti-6His (Sigma) or anti-GFP (Payne lab).

2.5.3 Fluorescence microscopy and endocytosis assays

Fluorescence microscopy was performed as described using an Olympus inverted IX81 confocal microscope with a Yokogawa spinning disc, as described previously [18]. Images were obtained with a 100X objective. Cells were grown to early log phase and imaged at room temperature except in case of heat shock (37˚C). Time-lapse images were collected every 2 sec

(Figure 2) or 5 sec (Figure 4). Slidebook 6 software (3I, Denver, CO) was used for image collection and analysis. Gaussian blur filters were applied to images in figures for ease of viewing. Pearson correlation coefficient was calculated using Slidebook 6 software. The standard deviation for PCCs was calculated between the individual PCC for multiple separate images, and is displayed in Table 2.1. Lucifer yellow uptake experiments were performed as described [40], incubating cells in dye for 2 hours at room temperature (excepting heat shock strains at 37˚C). Fluorescence was measured with a mask drawn on the vacuole and normalized to the background. Mup1-GFP cells were grown in minimal media with methionine to early log phase, moved to minimal media lacking methionine for 2 hours, and imaged at each time point after return to methionine-rich media. Fluorescence in the membrane was measured using a mask drawn on the cell periphery and normalized to the background. Student's t-test was calculated using Graph Pad software to determine statistical significance. Graphs displaying multiple data points, average, and standard deviation bars were also generated using Graph Pad software.

2.5.4 Acknowledgements

We acknowledge Caitlin Grossman for work on various experiments surrounding Ubx3, Al Aradi for help with protein purification, Colette Worcester for help with PCR, Tingting Yao for the *cdc48-3* strain, Laurie Stargell for *ubx3*Δ cells, and Greg Payne for anti-GFP antibody. This work was supported by National Science Foundation grant 1052188. K.B.F. acknowledges American Heart Association predoctoral fellowship. Microscopes used in this work are supported in part by the Microscope Imaging Network core infrastructure grant from Colorado State University.

REFERENCES

1. Farrell, K.B., C. Grossman, and S.M. Di Pietro, *New regulators of clathrin-mediated endocytosis identified in Saccharomyces cerevisiae by systematic quantitative fluorescence microscopy.* Genetics, 2015. **201**(3): p. 1061-70.
2. Robertson, A.S., E. Smythe, and K.R. Ayscough, *Functions of actin in endocytosis.* Cell Mol Life Sci, 2009. **66**(13): p. 2049-65.
3. McMahon, H.T. and E. Boucrot, *Molecular mechanism and physiological functions of clathrin-mediated endocytosis.* Nat Rev Mol Cell Biol, 2011. **12**(8): p. 517-33.
4. Reider, A. and B. Wendland, *Endocytic adaptors--social networking at the plasma membrane.* J Cell Sci, 2011. **124**(Pt 10): p. 1613-22.
5. Weinberg, J. and D.G. Drubin, *Clathrin-mediated endocytosis in budding yeast.* Trends Cell Biol, 2012. **22**(1): p. 1-13.
6. Boettner, D.R., R.J. Chi, and S.K. Lemmon, *Lessons from yeast for clathrin-mediated endocytosis.* Nat Cell Biol, 2012. **14**(1): p. 2-10.
7. Kirchhausen, T., D. Owen, and S.C. Harrison, *Molecular structure, function, and dynamics of clathrin-mediated membrane traffic.* Cold Spring Harb Perspect Biol, 2014. **6**(5): p. a016725.
8. Merrifield, C.J. and M. Kaksonen, *Endocytic accessory factors and regulation of clathrin-mediated endocytosis.* Cold Spring Harb Perspect Biol, 2014. **6**(11): p. a016733.
9. Kaksonen, M., Y. Sun, and D.G. Drubin, *A pathway for association of receptors, adaptors, and actin during endocytic internalization.* Cell, 2003. **115**(4): p. 475-87.
10. Kaksonen, M., C.P. Toret, and D.G. Drubin, *A modular design for the clathrin- and actin-mediated endocytosis machinery.* Cell, 2005. **123**(2): p. 305-20.
11. Idrissi, F.Z., A. Blasco, A. Espinal, and M.I. Geli, *Ultrastructural dynamics of proteins involved in endocytic budding.* Proc Natl Acad Sci U S A, 2012. **109**(39): p. E2587-94.
12. Kukulski, W., M. Schorb, M. Kaksonen, and J.A. Briggs, *Plasma membrane reshaping during endocytosis is revealed by time-resolved electron tomography.* Cell, 2012. **150**(3): p. 508-20.
13. Burston, H.E., L. Maldonado-Baez, M. Davey, B. Montpetit, C. Schluter, B. Wendland, and E. Conibear, *Regulators of yeast endocytosis identified by systematic quantitative analysis.* J Cell Biol, 2009. **185**(6): p. 1097-110.
14. Carroll, S.Y., P.C. Stirling, H.E. Stimpson, E. Giesselmann, M.J. Schmitt, and D.G. Drubin, *A yeast killer toxin screen provides insights into a/b toxin entry, trafficking, and killing mechanisms.* Dev Cell, 2009. **17**(4): p. 552-60.
15. Huh, W.K., J.V. Falvo, L.C. Gerke, A.S. Carroll, R.W. Howson, J.S. Weissman, and E.K. O'Shea, *Global analysis of protein localization in budding yeast.* Nature, 2003. **425**(6959): p. 686-91.
16. Ayscough, K.R., J.J. Eby, T. Lila, H. Dewar, K.G. Kozminski, and D.G. Drubin, *Sla1p is a functionally modular component of the yeast cortical actin cytoskeleton required for correct localization of both Rho1p-GTPase and Sla2p, a protein with talin homology.* Mol Biol Cell, 1999. **10**(4): p. 1061-75.

17. Di Pietro, S.M., D. Cascio, D. Feliciano, J.U. Bowie, and G.S. Payne, *Regulation of clathrin adaptor function in endocytosis: novel role for the SAM domain.* EMBO J, 2010. **29**(6): p. 1033-44.
18. Feliciano, D. and S.M. Di Pietro, *SLAC, a complex between Sla1 and Las17, regulates actin polymerization during clathrin-mediated endocytosis.* Mol Biol Cell, 2012. **23**(21): p. 4256-72.
19. Feliciano, D., T.O. Tolsma, K.B. Farrell, A. Aradi, and S.M. Di Pietro, *A second Las17 monomeric actin-binding motif functions in Arp2/3-dependent actin polymerization during endocytosis.* Traffic, 2015. **16**(4): p. 379-97.
20. Cherry, J.M., E.L. Hong, C. Amundsen, R. Balakrishnan, G. Binkley, E.T. Chan, K.R. Christie, M.C. Costanzo, S.S. Dwight, S.R. Engel, et al., *Saccharomyces Genome Database: the genomics resource of budding yeast.* Nucleic Acids Res, 2012. **40**(Database issue): p. D700-5.
21. Chapa-y-Lazo, B., E.G. Allwood, R. Smaczynska-de, II, M.L. Snape, and K.R. Ayscough, *Yeast endocytic adaptor AP-2 binds the stress sensor Mid2 and functions in polarized cell responses.* Traffic, 2014. **15**(5): p. 546-57.
22. Dreveny, I., H. Kondo, K. Uchiyama, A. Shaw, X. Zhang, and P.S. Freemont, *Structural basis of the interaction between the AAA ATPase p97/VCP and its adaptor protein p47.* EMBO J, 2004. **23**(5): p. 1030-9.
23. Schuberth, C., H. Richly, S. Rumpf, and A. Buchberger, *Shp1 and Ubx2 are adaptors of Cdc48 involved in ubiquitin-dependent protein degradation.* EMBO Rep, 2004. **5**(8): p. 818-24.
24. Schuberth, C. and A. Buchberger, *UBX domain proteins: major regulators of the AAA ATPase Cdc48/p97.* Cell Mol Life Sci, 2008. **65**(15): p. 2360-71.
25. Kelley, L.A., S. Mezulis, C.M. Yates, M.N. Wass, and M.J. Sternberg, *The Phyre2 web portal for protein modeling, prediction and analysis.* Nat Protoc, 2015. **10**(6): p. 845-58.
26. Bensen, E.S., G. Costaguta, and G.S. Payne, *Synthetic genetic interactions with temperature-sensitive clathrin in Saccharomyces cerevisiae. Roles for synaptojanin-like Inp53p and dynamin-related Vps1p in clathrin-dependent protein sorting at the trans-Golgi network.* Genetics, 2000. **154**(1): p. 83-97.
27. Dell'Angelica, E.C., J. Klumperman, W. Stoorvogel, and J.S. Bonifacino, *Association of the AP-3 adaptor complex with clathrin.* Science, 1998. **280**(5362): p. 431-4.
28. Ramjaun, A.R. and P.S. McPherson, *Multiple amphiphysin II splice variants display differential clathrin binding: identification of two distinct clathrin-binding sites.* J Neurochem, 1998. **70**(6): p. 2369-76.
29. Miele, A.E., P.J. Watson, P.R. Evans, L.M. Traub, and D.J. Owen, *Two distinct interaction motifs in amphiphysin bind two independent sites on the clathrin terminal domain beta-propeller.* Nat Struct Mol Biol, 2004. **11**(3): p. 242-8.
30. Toshima, J.Y., J. Toshima, M. Kaksonen, A.C. Martin, D.S. King, and D.G. Drubin, *Spatial dynamics of receptor-mediated endocytic trafficking in budding yeast revealed by using fluorescent alpha-factor derivatives.* Proc Natl Acad Sci U S A, 2006. **103**(15): p. 5793-8.
31. Boettner, D.R., J.L. D'Agostino, O.T. Torres, K. Daugherty-Clarke, A. Uygur, A. Reider, B. Wendland, S.K. Lemmon, and B.L. Goode, *The F-BAR protein Syp1 negatively regulates WASp-Arp2/3 complex activity during endocytic patch formation.* Curr Biol, 2009. **19**(23): p. 1979-87.

32. Reider, A., S.L. Barker, S.K. Mishra, Y.J. Im, L. Maldonado-Baez, J.H. Hurley, L.M. Traub, and B. Wendland, *Syp1 is a conserved endocytic adaptor that contains domains involved in cargo selection and membrane tubulation.* EMBO J, 2009. **28**(20): p. 3103-16.
33. Stimpson, H.E., C.P. Toret, A.T. Cheng, B.S. Pauly, and D.G. Drubin, *Early-arriving Syp1p and Ede1p function in endocytic site placement and formation in budding yeast.* Mol Biol Cell, 2009. **20**(22): p. 4640-51.
34. Brach, T., C. Godlee, I. Moeller-Hansen, D. Boeke, and M. Kaksonen, *The initiation of clathrin-mediated endocytosis is mechanistically highly flexible.* Curr Biol, 2014. **24**(5): p. 548-54.
35. Stolz, A., W. Hilt, A. Buchberger, and D.H. Wolf, *Cdc48: a power machine in protein degradation.* Trends Biochem Sci, 2011. **36**(10): p. 515-23.
36. Ye, Y., H.H. Meyer, and T.A. Rapoport, *The AAA ATPase Cdc48/p97 and its partners transport proteins from the ER into the cytosol.* Nature, 2001. **414**(6864): p. 652-6.
37. Dores, M.R., J.D. Schnell, L. Maldonado-Baez, B. Wendland, and L. Hicke, *The function of yeast epsin and Ede1 ubiquitin-binding domains during receptor internalization.* Traffic, 2010. **11**(1): p. 151-60.
38. Weinberg, J.S. and D.G. Drubin, *Regulation of clathrin-mediated endocytosis by dynamic ubiquitination and deubiquitination.* Curr Biol, 2014. **24**(9): p. 951-9.
39. Feliciano, D., J.J. Bultema, A.L. Ambrosio, and S.M. Di Pietro, *In vivo andin vitro studies of adaptor-clathrin interaction.* J Vis Exp, 2011(47).
40. Duncan, M.C., M.J. Cope, B.L. Goode, B. Wendland, and D.G. Drubin, *Yeast Eps15-like endocytic protein, Pan1p, activates the Arp2/3 complex.* Nat Cell Biol, 2001. **3**(7): p. 687-90.

CHAPTER 3

TDA2 IS A TCTEX TYPE DYNIEN LIGHT CHAIN WITH A ROLE IN THE ACTIN CYTOSKELETON DURING CLATHRIN-MEDIATED ENDOCYTOSIS

3.1 Summary

Clathrin-mediated endocytosis is a critical process for many aspects of normal cell function. Membrane bound cargo is collected in protein coated membrane regions which invaginate and pinch off to form cytosolic vesicles. In yeast, actin polymerization is required for membrane bending in this process. Close to sixty endocytic proteins have been identified in yeast, yet questions in the process still remain. Here we demonstrate that Tda2 is a novel protein of the endocytic machinery. Tda2 localizes to late stage endocytic sites similar to actin associated proteins and *tda2Δ* shows a small endocytic defect. Crystal structure reveals that Tda2 is a TcTex type dynein light chain, the first to be identified in yeast, but it functions independently of the dynein motor complex. Tda2 is not recruited to endocytic sites with LatA treatment and localizes with Cap1 and Abp1 to actin filaments. *tda2Δ* cells display an extended patch lifetime of actin capping protein Cap1 and a reduced fluorescence of actin-associated protein Aim21 at the endocytic site. *cap1Δ* cells show more Tda2 recruited to the endocytic site and for a longer lifetime, as expected for actin-associated proteins. Tda2 forms a complex with Aim21 and depends on Aim21 for endocytic localization. Tda2 is a motor independent dynein light chain and a novel component of the actin cytoskeleton at the endocytic site.

3.2 Introduction

Clathrin mediated endocytosis (CME) is an essential process spanning all eukaryotes. CME has roles in maintenance of membrane composition, signaling, protein trafficking, virus uptake, and nutrient and drug internalization, among others [1-3]. Applications of CME extend from basic eukaryotic cell biology to physiology and human disease. CME is highly conserved between yeast and mammalian cells in protein composition, progression, and function [4-6]. In yeast, close to sixty proteins have been identified with roles in CME, and fluorescent microscopy as well as recent advances in super resolution and correlative fluorescent and electron microscopy have allowed in depth study of many of these proteins [1, 2]. However, many aspects of the process are still not well understood. Early in CME, cargo and coat proteins gather at the membrane in an immobile but variable timed phase. Intermediate coat proteins and actin regulators then arrive at the endocytic site. Later, actin polymerization and actin associated proteins are seen. Lastly, scission and uncoating processes free the vesicle and allow recycling of machinery and coat components [2, 3, 6, 7].

Actin polymerization during CME is essential to overcome high membrane tension in yeast to produce membrane bending [8]. When actin polymerization is disrupted such as with actin monomer sequestering agent Latrunculin A, early endocytic proteins are recruited to the membrane but invagination does not occur [6, 7]. Similarly, when the link between actin and membrane is broken, such as in *sla2Δ* cells, large "comet tails" of actin are present but the membrane does not internalize [6]. Actin polymerization is a highly regulated process with numerous nucleation promoting factors (NPF) including Las17, Pan1 and Myo3/5, as well as proteins required for recruitment and inhibition of the NPFs, such as Sla1 and Bzz1. As CME utilizes a branched actin structure, the seven proteins of the Arp2/3 complex are present, as well

as capping (Cap1/2/Aip1), crosslinking and stabilizing (Abp1/Sac6), and depolymerizing (Cof1/Crn1) proteins [2]. The intricacies of this network of actin-associated proteins are still being uncovered.

We have identified Tda2, a previously uncharacterized protein, as a novel candidate protein of the endocytic machinery through a screening of the yeast GFP library [9]. Here we describe Tda2 as a new component of late stage CME and the actin cytoskeleton. X-ray crystallography revealed Tda2 to be a TcTex type dynein light chain, the first to be identified in yeast, yet Tda2 has a dynein motor-independent role in CME. Tda2 localizes to the endocytic site during actin polymerization, is functionally connected with Cap1/2, and exists as a stable complex with Aim21.

3.3 Results

3.3.1 Tda2 is a novel late stage endocytic protein

Tda2 colocalizes with endocytic clathrin adaptor Sla1 with a Pearson correlation coefficient of 0.49 ± 0.13 (Figure 3.1.A). In time lapse imaging, Tda2 appears at 96% of Sla1 patches. Tda2 has a patch lifetime of 12.6 ± 4.0 sec and appears only at the late stages of Sla1 fluorescence (Figure 3.1.B). Tda2 overlaps Sla1 fluorescence by several seconds, and persists after Sla1 disappearance. When expressed in cells with a temperature sensitive clathrin heavy chain (*chc1-ts*), Tda2 shows no patch lifetime effect when clathrin is destabilized by high temperature, while coat proteins such as Sla1 have a significantly decreased patch lifetime (Figure 3.1.C-D). Timing, localization, dynamics, and independence from the clathrin coat suggest Tda2 is a part of the late stage endocytic machinery.

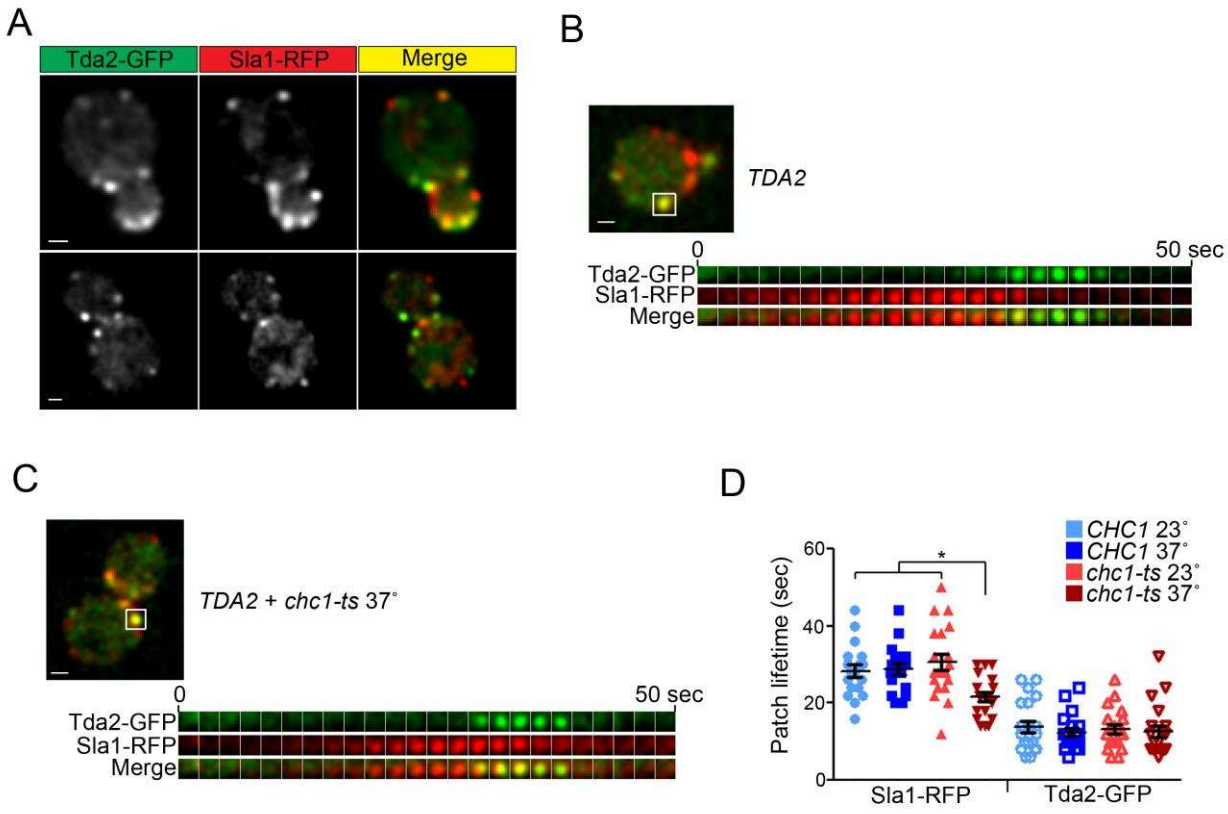

Figure 3.1: Tda2 localizes to sites of clathrin-mediated endocytosis. A) Tda2 colocalizes with Sla1. B) Tda2 localizes to late stages of endocytosis as Tda2-GFP fluorescence only overlaps during final seconds of Sla1-RFP fluorescence. C-D) Clathrin disruption by temperature sensitive allele *chc1-ts* reduces patch lifetime in Sla1 but not Tda2. Wild type (*CHC1*) cells are not affected by temperature and *chc1-ts* cells are not affected by permissive temperature. Plot bars indicate average ± SD. Kymographs show one frame every 2 seconds. Bar = 1μm. *$p<0.05$

To analyze endocytic dependence on Tda2, endocytic assays were performed with a *tda2Δ* strain. A small but significant defect in fluid phase endocytosis was measured in *tda2Δ* cells using fluorescent dye Lucifer yellow (Figure 3.2.A). This defect is minor when compared with *sla1Δ*, which severely affects CME. An endocytic defect was also demonstrated in the *tda2Δ* strain when measuring cargo specific intake. Mup1-GFP, which is localized to the membrane in methionine starved cells, is quickly internalized via ubiquitin-dependent CME after return to methionine-rich media. A delay in Mup1-GFP cargo internalization was observed in *tda2Δ* cells (Figure 3.2.B). These endocytic defects suggest Tda2 is an important, but not essential part of the CME machinery.

3.3.2 Tda2 is a TcTex type dynein light chain

Tda2 was a previously uncharacterized protein and amino acid sequence indicated no predicted domains or homology to known proteins with which to infer function. However, structural prediction program PHYRE2 [10] indicated a dynein light chain and the actin depolymerizing factor homology domain (ADFH) as possible folds. To determine the stucture, recombinant Tda2 was purified with a 6His tag from BL21 codon plus *E. Coli*, concentrated to 25 mg/ml, and crystals were obtained after 4 days using the hanging drop method. Several X-ray diffraction data sets were collected at the Berkeley synchrotron. The molecular replacement method did not work to solve the structure with either dynein light chain or the ADFH domain. Structure was solved after Bromine soaking for phase determination and revealed the 14.5 kDa protein associates into a stable dimer of 29 kDa. The two monomers perform domain exchange to form a strand in the β-sheet of the opposing peptide's structure (Figure 3.3.A).

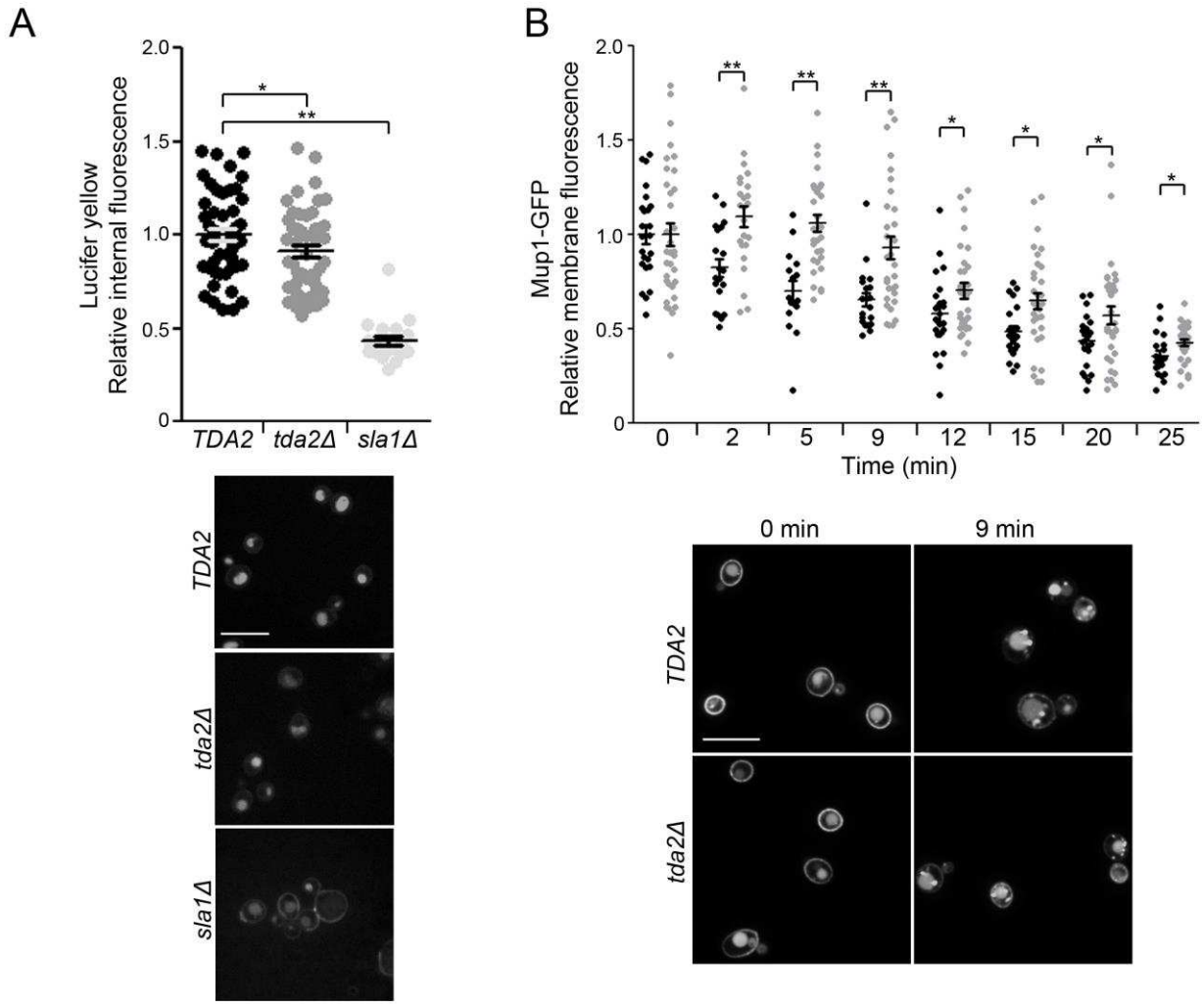

Figure 3.2: Tda2 deletion causes an endocytic defect. A) Fluorescent dye Lucifer Yellow is internalized at a modestly reduced rate in *tda2Δ* cells. *sla1Δ* cells portray a severe defect. Vacuoles containing Lucifer yellow are seen after two hours of incubation, pictured below. B) Mup1-GFP internalization is delayed in *tda2Δ* cells. Plasma membrane fluorescence is measured at indicated time points after returning cells to methionine rich media. Representative images at indicated time points are pictured below. Plot bars indicate average ± SD. Bar = 10 μm *p<0.05 **p<0.01

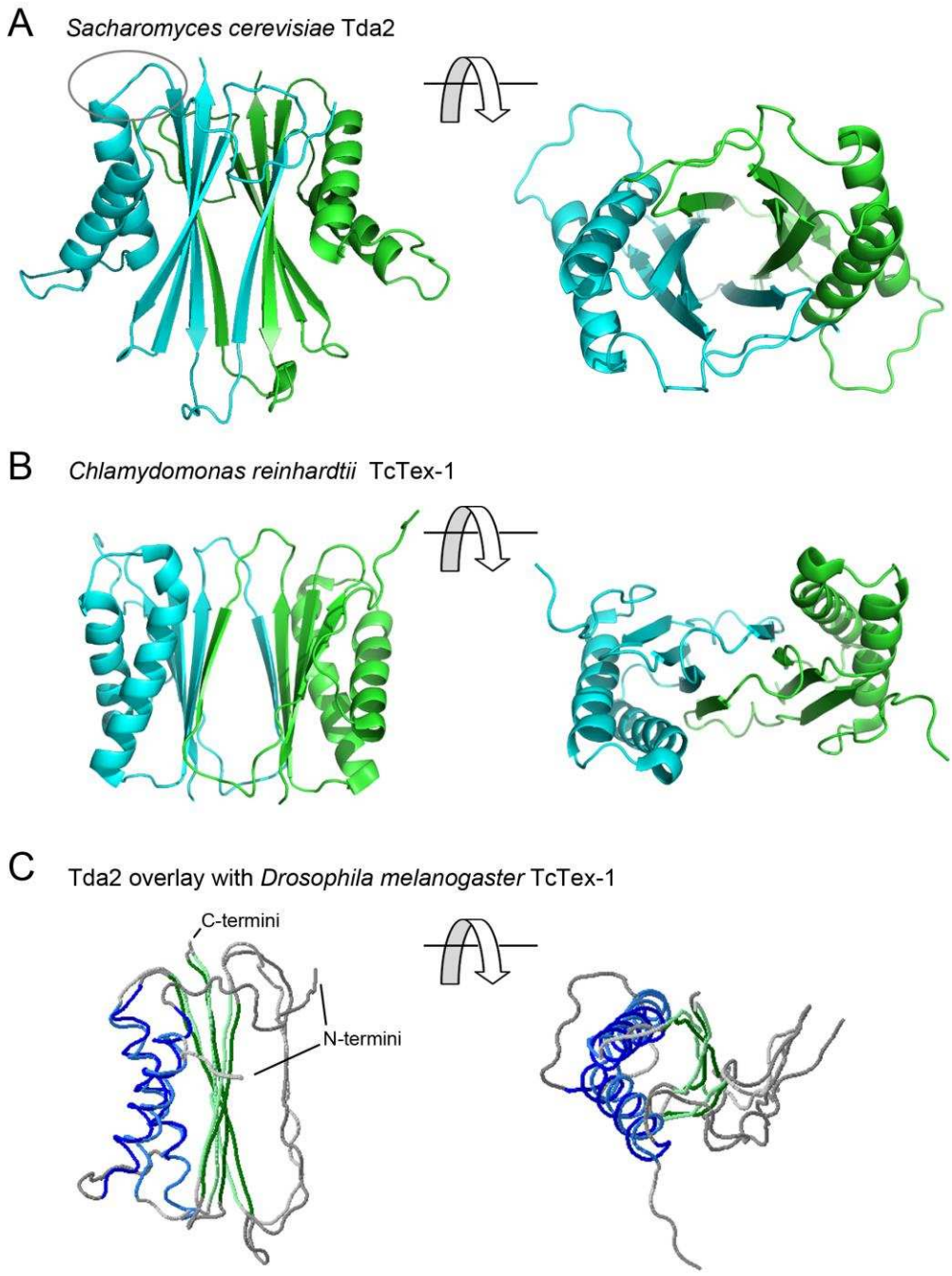

Figure 3.3: Crystal structure of Tda2 reveals a TcTex dynein light chain homolog. A) Tda2 associates into a stable dimer with domain exchange between monomers sharing a strand of β-sheet. One molecule is shown in cyan, one is shown in green. Structure is rotated 90˚ for another view. B) Structure of a single molecule of *Chlamydomonas* TcTex-1 shows a similar dimer with domain exchange. One molecule is shown in cyan, one is shown in green. (PDB entry 1XDX [11]). C) Trace overlay of single molecules of Tda2 (darker colors) and *Drosophila melanogaster* TcTex-1 (lighter colors). α-helices are in blue and β-sheets are in green. (PDB entry 1YGT [12]).

Structural analysis revealed Tda2 as a homolog of a dynein light chain, TcTex-1 (Figure 3.3.B). Tda2 structure can be overlaid with TcTex-1 with a r.m.s.d of 1.79 (Figure 3.3.C) with the largest diversity at the N-terminus. TcTex is one of three dynein light chain families in mammalian cells including LC8 and roadblock, whereas only the LC8 light chain has previously been identified in yeast based on sequence homology [13]. However, BLAST search and subsequent alignment of numerous fungal Tda2-like proteins reveals a conserved protein throughout many species (Figure 3.4.A-B), thus the TcTex dynein light chain is revealed as a protein of ancient function. The Tda2-like and TcTex sequences contain a conserved YKYϕϕ, where ϕ indicates a bulky hydrophobic, not present in the LC8 light chain. In fungal species, the entire conserved region includes HSSXYKYϕϕ (underlined in Figure 3.4.A), while the first three residues vary in other species (Figure 3.4.B). This sequence is located in the unstructured loop between alpha helix and beta strand (indicated in grey ellipse in Figure 3.3.A) with the hydrophobic residues continuing into the beta strand (Figure 3.3.A). Human TcTex-1 and yeast Tda2 have a sequence identity of 16% (Figure 3.4.B) while the LC8 dynein light chains have a sequence identity of 47% between species, explaining why Tda2 has previously been unrecognized as a TcTex-1 homolog. When comparing yeast LC8 and Tda2, only 9% sequence identity is present and r.m.s.d of Tda2 with LC8 structures are around 2.2-2.4. Sequence phylogeny confirms the yeast LC8 is more closely related to human LC8 than the other fungal TcTex proteins (Figure 3.4.C). Phylogeny also groups the fungal TcTex proteins together and non-fungal proteins together, including algal *Chlamydomonas*, suggesting a deviation of TcTex after branching off of the fungal ancestor.

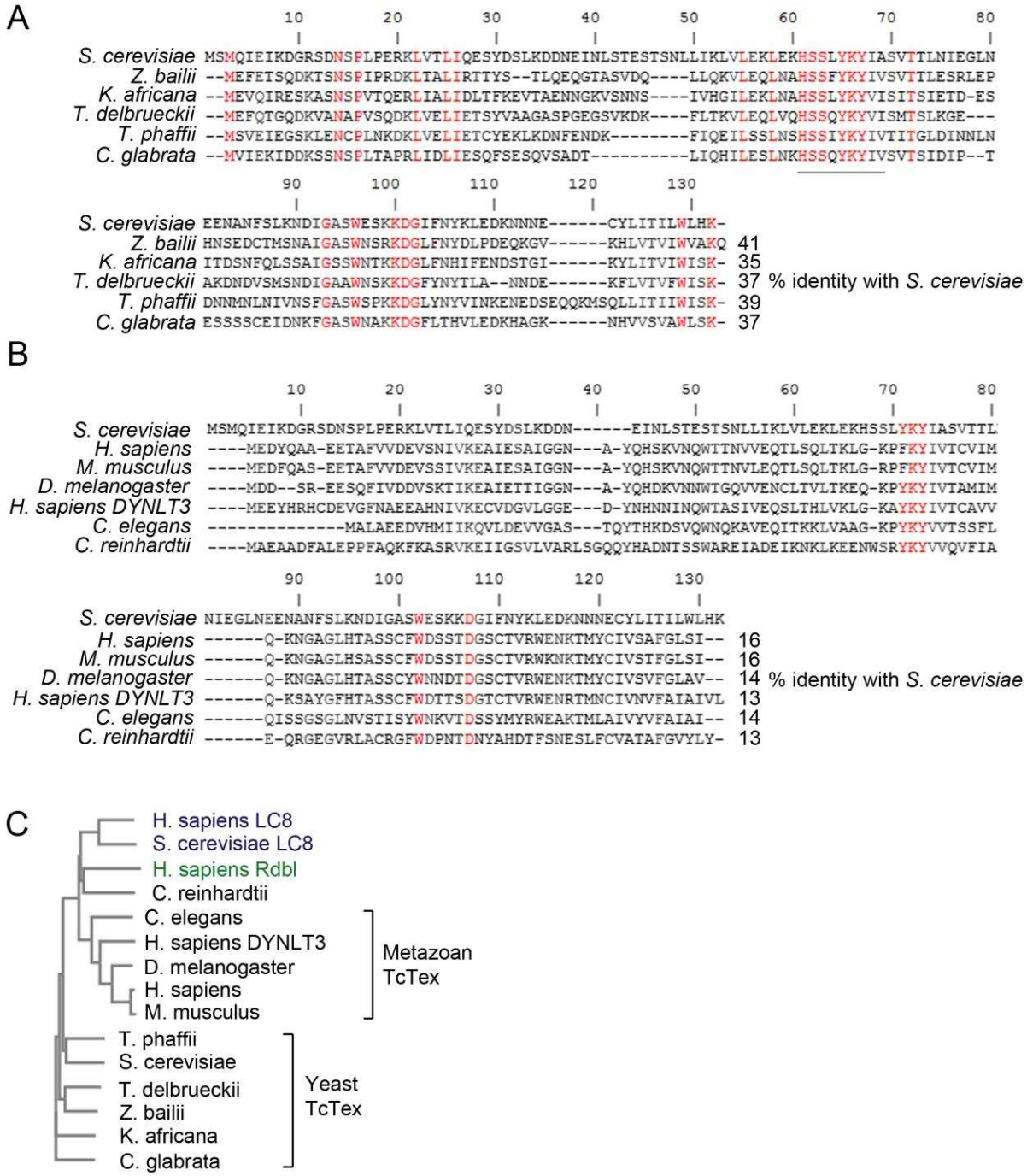

Figure 3.4: Sequence homology of Tda2 and TcTex-1 homologs. A) Sequence alignment of Tda2-like proteins in 6 yeasts and % sequence identity with *S. cerevisiae* Tda2. Residues conserved throughout the alignment are displayed in red. B) Sequence alignment of Tda2 with TcTex-1 of other various species, as well as TcTex-3 in humans and % sequence identity with *S. cerevisiae* Tda2. Residues conserved throughout the alignment are displayed in red. C) Phylogenetic tree of species represented in (A-B) as well as yeast and human LC8 dynein light chains (blue) and human roadblock light chain (green).

3.3.3 Tda2 is dynein motor independent

Identification of Tda2 as a member of the dynein light chain family was unexpected as microtubules and the dynein motor complex are not known to have roles in endocytosis. To investigate whether Tda2 is associated with the dynein complex, cells were treated with the microtubule-destabilizer Nocodazole. Known endocytic proteins did not show any change in patch lifetimes under conditions in which microtubules are disrupted. Similarly, Tda2 lifetime was unaffected, suggesting microtubules are not an essential component of endocytic sites and Tda2 recruitment does not require microtubules (Figure 3.5.A-C). A *tda2Δ* strain also did not show any obvious defects in microtubules labeled with Tub1-GFP or growth defects under normal or high temperature conditions (Figure 3.5.C).

To allow further investigation into endogenous Tda2, a rabbit anti-Tda2 antibody was created and verified in cytosolic extracts and with purified protein (Figure 3.6). To confirm Tda2 is not associated with the dynein complex, a TAP-tagged strain of the dynein heavy chain (*DYN1-TAP)* was used to purify the dynein motor complex. Tda2 was present in total cell extracts but did not co-purify with the motor dynein complex (Figure 3.5.D). Size exclusion chromatography was then performed to examine the behavior of Tda2 in the cytosol (Figure 3.6). Recombinant purified Tda2 eluted at the size expected for the stable homodimer demonstrated in the crystal structure. In cytosolic extract prepared from wild type cells, a portion of Tda2 elutes as the stable dimer, but also as a larger complex, estimated with column standards to have a Stokes radius of 61Å or a molecular weight of 244 kDa for a globular complex. A cytosolic extract from a *tda2Δ* strain shows no signal, confirming the specificity of our antibody (Figure 3.6). The predicted size of the cytosolic Tda2 complex is much smaller than the large dynein motor protein complex of over 1000 kDa, which elutes with the exclusion volume (fraction 8),

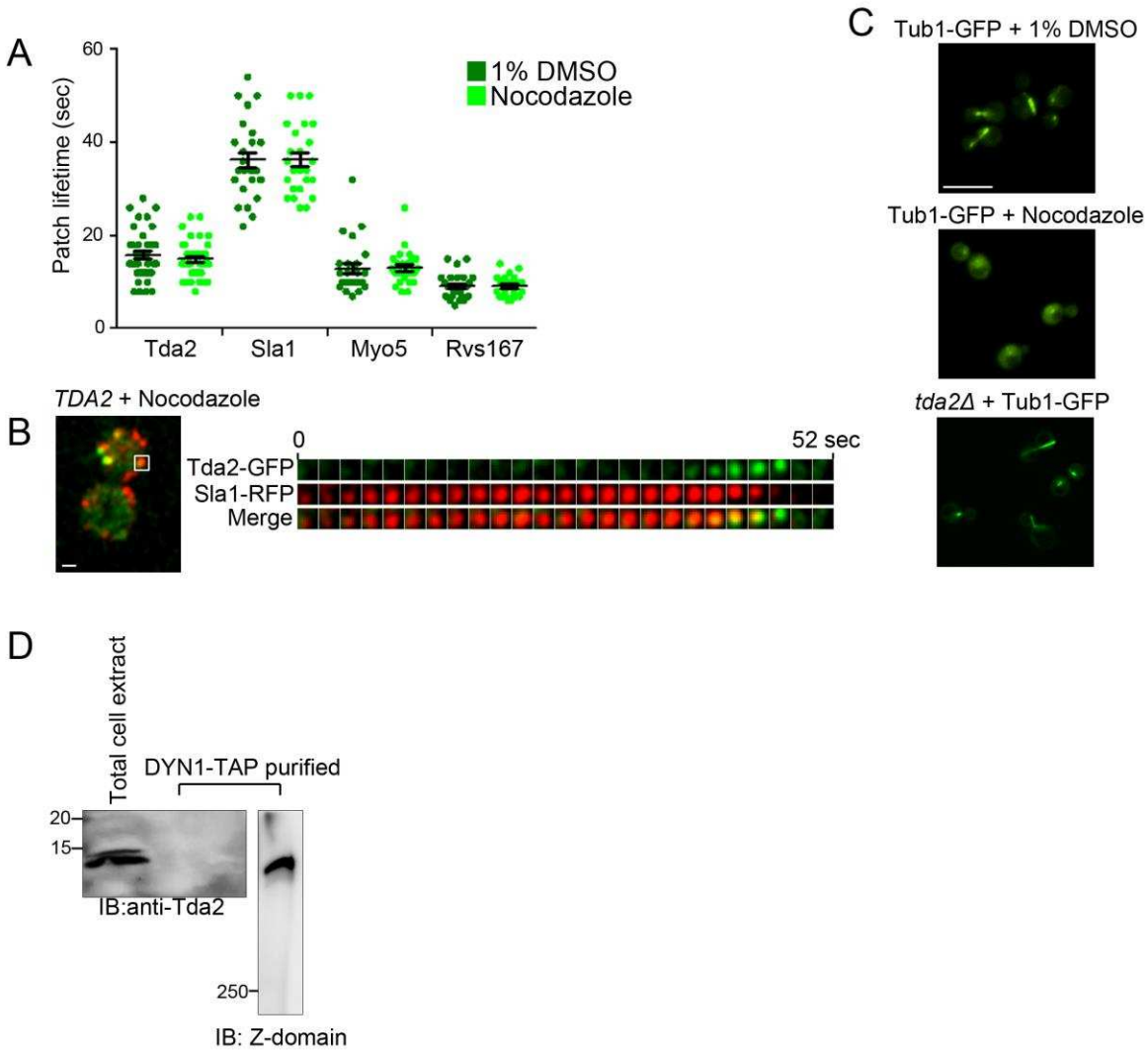

Figure 3.5: Tda2 is not associated with the dynein motor protein complex. A) Nocodazole treatment does not affect known proteins of the endocytic machinery, nor Tda2 patch lifetime. Plot bars indicate average ± SD. B) Kymograph indicating no change in Sla1 or Tda2 patch lifetime. Bar = 1 μm. Kymographs show one frame every 2 seconds. C) GFP-tagged tubulin is seen in wild type, nocodazole treated, and *tda2Δ* cells. Microtubules are dissembled with Nocodazole treatment and no changes are seen between wild type and *tda2Δ*. Bar = 10 μm. D) TAP-tagged dynein heavy chain does not show Tda2 as part of the purified complex though it is present in the unpurified cell extract (left). An IgG blot for the Z-domain of the TAP-tag in DYN1-TAP confirms dynein is present in the purification.

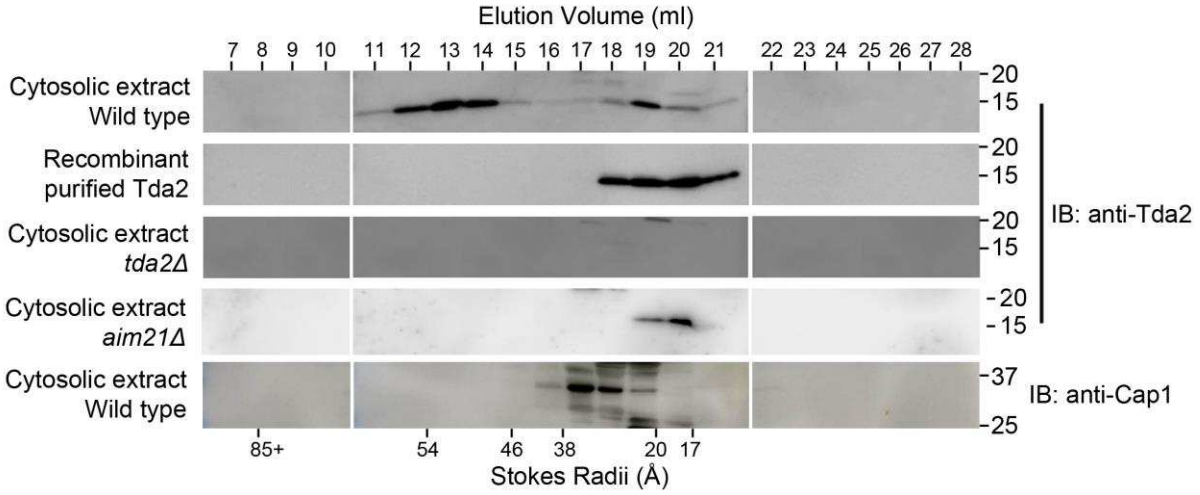

Figure 3.6: Tda2 exists as a dimer and in a large stable complex. Gel filtration demonstrates expected elution size for purified recombinant Tda2 as a homodimer (fraction 18-21). Cytosolic cellular extracts portray no Tda2 in the *tda2Δ* strain, confirming the specificity of our antibody. Wild type cells show Tda2 as a dimer (fraction 19-20) as well as a larger complex (fraction 12-14). Deletion of the Aim21 gene (*aim21Δ)* abolishes evidence of this complex in the cytosol. In wild type cells, Cap1 elutes in different fractions than the Tda2-Aim21 complex (fraction 17-18). The Stokes radii of standard proteins are indicated at the bottom.

further supporting Tda2 as separate from the dynein motor complex. Tda2 is not stably associated with the dynein motor complex despite identification of its mammalian homolog as TcTex-1 dynein light chain.

3.3.4 Tda2 is associated with the actin cytoskeleton

Due to the late recruitment of Tda2 to the endocytic site, its dynamics and lifetime appeared similar to actin-associated proteins. Tda2 dynamics appeared similar to Abp1, but Abp1 has a slightly longer patch lifetime (Figure 3.7.A). Upon treatment of cells with the actin depolymerizing agent Latrunculin A, Tda2 is no longer recruited to endocytic patches (Figure 3.7.B). This behavior is typical of proteins dependent on filamentous actin for recruitment to the endocytic site [6]. On the other hand, coat proteins such as Sla1 are recruited but immobile (Figure 3.7.B) [6]. In untreated cells, Tda2 fluorescence persists a few seconds after Sla1 disappearance, which is also characteristic of actin-associated proteins as actin continues to propel the vesicle after scission (Figure 3.1.B) [6].

Interestingly, the fluorescent localization of Tda2 appeared slightly offset from Abp1, with Tda2 appearing closer to the membrane than Abp1 fluorescence. Upon quantification, the peak patch intensity of Tda2 was found to be 0.13 ± 0.06 µm closer to the membrane than the peak patch intensity of Abp1 (Figure 3.7.C-D). This offset in localization has been previously demonstrated between Cap1/2 and Abp1, with capping proteins localizing closer to the membrane [14]. When Tda2 fluorescence was compared with Cap1, there was no shift in location of peak patch intensity (Figure 3.7.E-F). This was also confirmed in cells with fluorescent tags reversed (Figure 3.8). Thus, Tda2 has a similar localization to Cap1, an actin plus end-binding protein. A previous TAP-tag screening associated Tda2 with both Cap1/2 and

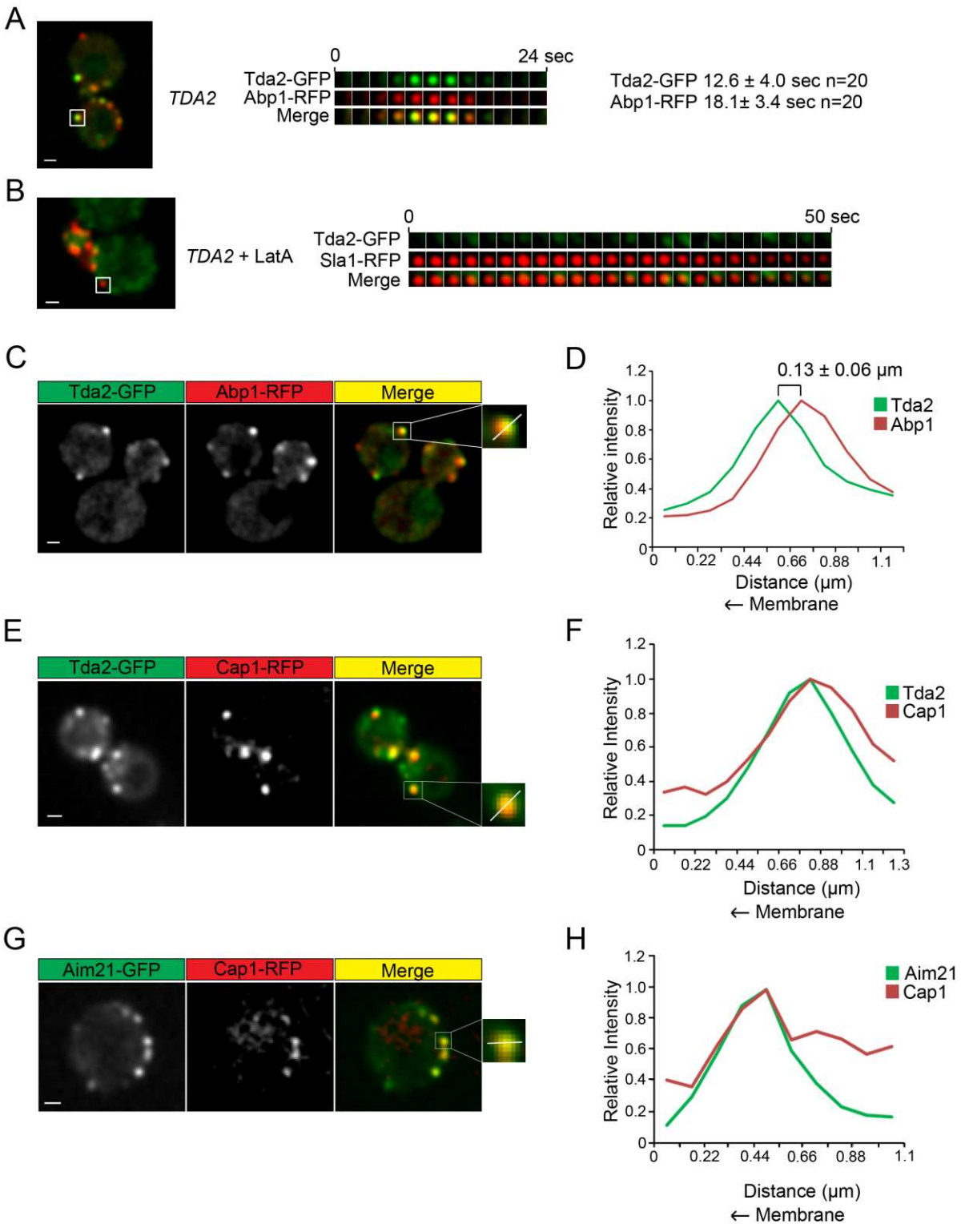

Figure 3.7: Tda2 localizes to the actin cytoskeleton. A) Tda2 and Abp1 have similar dynamics while Abp1 has a longer patch lifetime. B) When cells are treated with Latrunculin A, Tda2 is not recruited to endocytic sites while Sla1 is recruited but immobile. C) Tda2 and Abp1 have a

high degree of colocalization, but fluorescent peaks appear separated (inset). D) Graph of relative intensity from linescan of one representative patch pictured in C. Quantification of 20 patches ± SD. E) Tda2 and Cap1 have a high degree of colocalization, and fluorescent peaks do not appear separated (inset). F) Graph of relative intensity from linescan of one representative patch pictured in E. Quantification of 20 patches shows no significant difference in peaks. Distances between Tda2-Abp1 are significantly different from distances between Tda2-Cap1 ($p<0.0001$). G) Aim21 and Cap1 have a high degree of colocalization, and fluorescent peaks do not appear separated (inset). H) Graph of relative intensity from linescan of one representative patch picture in G. Quantification of 20 patches shows no significant difference in peaks. Bar = 1 µm.

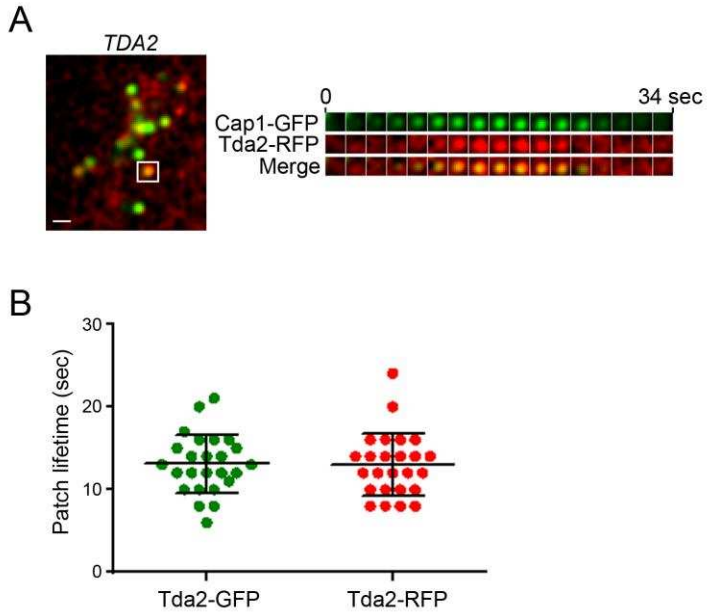

Figure 3.8: Tda2 has similar patch lifetime and dynamics when tagged with RFP. A) Tda2-RFP imaged with Cap1-GFP shows no shift in localization, as with Tda2-GFP and Cap1-RFP. B) No significant difference in patch lifetime was detected between Tda2-GFP and Tda2-RFP. Kymograph shows one frame every 2 seconds. Plot bars indicate average ± SD.

Aim21, suggesting interaction between these proteins [15]. Cap1 was also found to have no shift in localization when compared with actin-associated protein Aim21, suggesting Aim21 also has similar localization to Tda2 and Cap1 (Figure 3.7.G-H).

3.3.5 Tda2 is in a stable complex with Aim21

To further demonstrate the role of Tda2 in CME, the patch lifetimes of known endocytic proteins in cells lacking Tda2 were measured. Of particular interest were actin-associated proteins. Cap1-GFP displayed a slightly longer patch lifetime in cells lacking Tda2, with a statistically significant increase from 19 ± 3 to 22 ± 5 sec (Figure 3.9.A). Las17-GFP and Abp1-GFP also trended towards longer patch lifetimes, but were not statistically significant. Early stage endocytic proteins and other late stage proteins did not have a significant change in patch lifetime. Cap1-GFP showed a reduction in its intensity at endocytic patches (Figure 3.9.B,D). Additionally, Aim21-GFP had a large reduction in its intensity at endocytic patches in *tda2Δ* strain, to approximately half the intensity of wild type cells (Figure 3.9.C,E).

Conversely, when Tda2-GFP was observed in *cap1Δ* cells, slightly more Tda2 appeared at the endocytic site and the patch lifetime of Tda2-GFP was increased (Figure 3.9.F-H). These effects are consistent with actin-associated proteins in a *cap1Δ* strain as more actin is polymerized at the endocytic site [6]. Interestingly, when we looked at Tda2-GFP in an *aim21Δ* strain, we observed no Tda2 recruited to endocytic sites (Figure 3.9.F). These findings suggest Tda2 is dependent on Aim21 for recruitment to the endocytic site. Tda2 is also important for recruitment or maintenance of Aim21 at the endocytic patch, though some Aim21 is still recruited without Tda2. Aim21-GFP also displayed no shift in localization when compared with

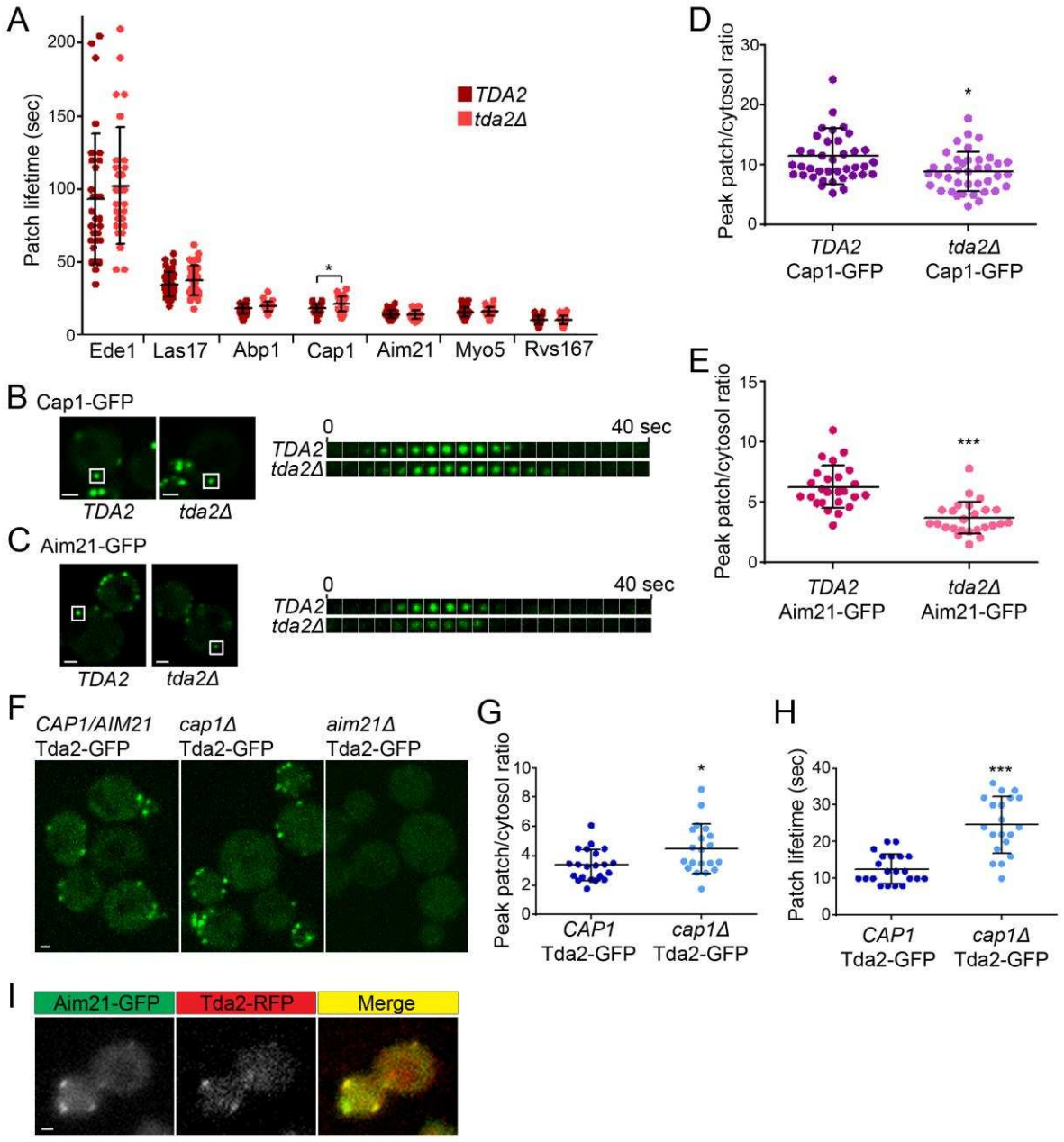

Figure 3.9: Tda2 deletion affects actin associated proteins. A) *tda2Δ* shows no effect on Ede1, Las17, Abp1, Myo5, or Rvs167. Cap1-GFP shows an increase in patch lifetime. B) Kymographs demonstrating increase in Cap1-GFP patch lifetime and reduction in intensity, quantified in (D). C) Kymographs demonstrating similar Aim21-GFP patch lifetime in *tda2Δ* but severe reduction in intensity, quantified in (E). D) Cap1 shows reduced intensity at endocytic sites in *tda2Δ*. E) Aim21 shows reduced intensity at endocytic sites in *tda2Δ*. F) Images of Tda2-GFP in wild type cells, *cap1Δ*, and *aim21Δ* cells. G) Increased intensity of Tda2 in *cap1Δ* cells. H) Increased patch lifetime of Tda2 in *cap1Δ* cells. I) Tda2 and Aim21 have a high degree of colocalization with no apparent shift in localization. Bars indicate average ± SD. Kymographs show one frame every 2 seconds. *p<0.05 **p<0.01 ***p<0.001

Cap1 (Figure 3.7.G-H) or Tda2 (Figure 3.9.I), suggesting all three proteins have similar localization with an offset relative to Abp1.

As demonstrated in Figure 3.6, the majority of Tda2 elutes in a large cytosolic complex by size exclusion chromatography. In *aim21Δ* cells, this complex is no longer present (Figure 3.6), suggesting Aim21 is an essential component of this complex. In order to test if the Tda2 complex contained capping protein, we obtained an antibody against yeast Cap1 (generous gift from John Cooper, Washington University). A blot for endogenous Cap1 in the same cytosolic extract chromatography fractions from wild type cells reveals it is not a stable part of this complex (Figure 3.6).

We propose that Aim21 and Tda2 are in a stable complex, possibly with a Tda2 dimer and two copies of Aim21 to approximate the predicted size of the cytosolic gel filtration complex (see Discussion). The Tda2-Aim21 complex is recruited to the endocytic site and Tda2 alone does not have endocytic localization. The complex may associate with Cap1 and the actin cytoskeleton towards the plus end of the actin filaments, though capping proteins are not required for recruitment nor exist as a stable part of the complex (Figure 3.10).

3.4 Discussion

We have demonstrated that Tda2 is a novel endocytic protein associated with the actin cytoskeleton and the first TcTex dynein light chain identified in yeast and to our knowledge, the first dynein motor complex independent light chain in yeast. Tda2 has high levels of colocalization with endocytic proteins Sla1, Abp1, Cap1, and Aim21. Tda2 is not recruited to the endocytic site when treated with LatA and is unaffected by clathrin disruption, suggesting it is not part of the endocytic coat but associated with the actin cytoskeleton. Tda2 has a similar

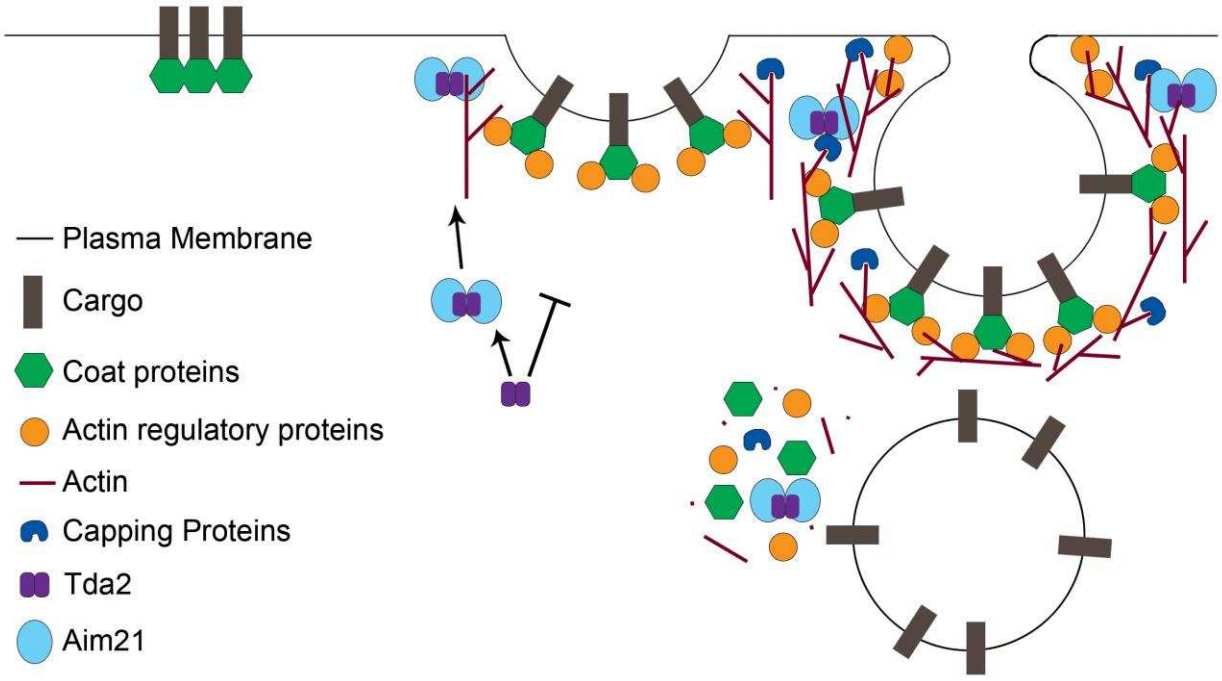

Figure 3.10: Model of Tda2 function in clathrin-mediated endocytosis. Tda2, a TcTex dynein light chain homolog, exists as a stable dimer. Tda2 associates with Aim21 into a stable complex, which is recruited to endocytic sites. Without Aim21, Tda2 is not recruited to endocytic sites. The complex is localized towards the membrane, similar to plus-end actin binding proteins Cap1/2. The Tda2-Aim21 complex is not dependent on Cap1 for recruitment, but Cap1 recruitment is enhanced by the presence of Tda2-Aim21.

localization to the actin capping proteins Cap1/2 with an offset from Abp1 but shares dynamics with Abp1 and other actin associated proteins involved in CME. Without Tda2, Cap1 and Aim21 have reduced recruitment to the endocytic site. Without Aim21, Tda2 is not recruited to the endocytic patch. By X-ray crystallography, Tda2 was revealed as a TcTex type dynein light chain, which is its first identification in yeast and reveals TcTex-1 as a protein of ancient function. However, Tda2 does not appear to be associated with dynein or microtubules, but is present as a dimer and in a stable complex with Aim21 in cells.

Little is known about the function of Aim21 besides its localization to membrane actin patches and involvement in mitochondrial migration along actin filaments [16, 17]. Aim21 is predicted to be a disordered protein with no predicted structure or conserved domains. In fact, Aim21 is proline-rich with numerous poly-proline motifs that are predicted to bind many SH3 domains of the endocytic machinery [18], which may explain why some Aim21 is still present at the endocytic site in *tda2Δ* cells. Additionally, though predicted to be disordered, Aim21 does not appear to be degraded in a *tda2Δ* strain (Figure 3.11.A-B). Aim21 may be associated with other cellular proteins as well, giving Aim21 its mitochondria migration phenotype, yet we do not observe Tda2 or Aim21 fluorescence localizing anywhere except endocytic sites. Based on predicted molecular weight from size exclusion chromatography standards, there may be two Aim21 molecules per Tda2 dimer in the complex. The molecular weight of these four peptides (179 kDa) is below the predicted complex weight (244 kDa), which is consistent with an imperfectly globular complex. Alternatively, there may be one only Aim21 molecule with the complex existing in a non-globular conformation. We also cannot rule out the possibility of additional proteins in the complex that were not identified in the scope of this study.

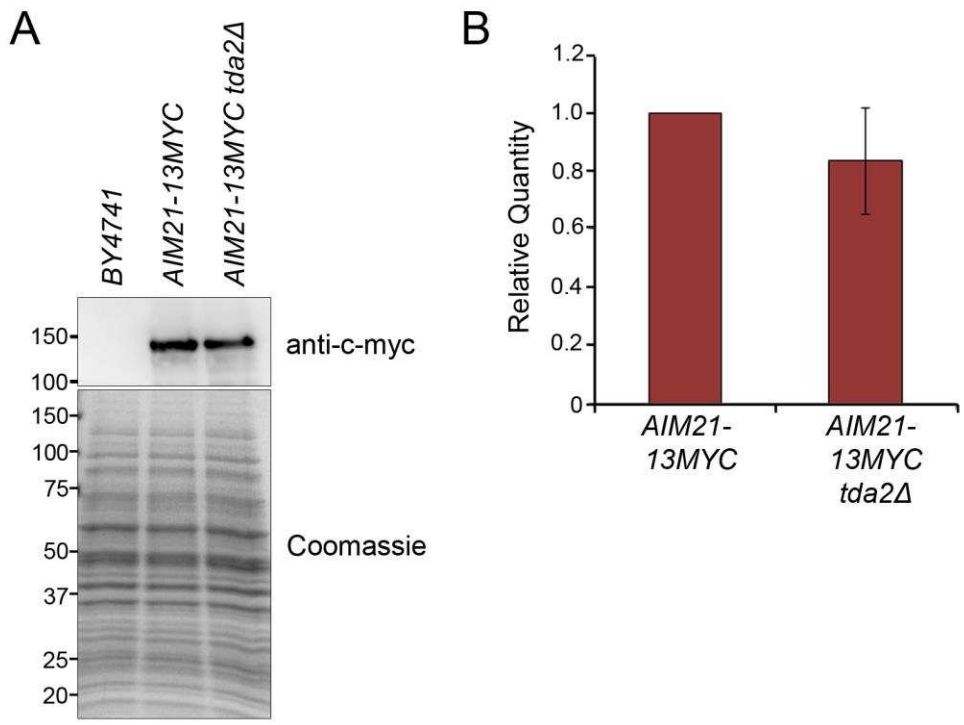

Figure 3.11: Aim21 is not degraded in *tda2Δ* cells. A) Representative western blot of total cell extracts for Aim21-13Myc in wild type and *tda2Δ* shows no change in Aim21 levels. Coomassie stain demonstrates equal amounts of each cell extract were loaded. B) Quantification of 4 blots for Aim21 in wild type and *tda2Δ* cells shows no significant difference in relative protein quantity. Bars indicate average ± SD.

In mammalian cells, TcTex is one of three dynein light chain families; the others include the well-studied LC8 as well as the roadblock light chains. TcTex-1 co-purifies with the dynein motor complex in mammals and is demonstrated to bind the dynein intermediate chain via hydrophobic regions [19] and has been predicted to link cargo to the motor complex [20], though cargo linking is now under debate. Additionally, light chains have also been observed in roles outside solely the dynein motor protein [21-23]. As light chains such as LC8 and TcTex-1 are such strong dimers, a predicted activity for these molecules is a sort of "dimerization chaperone", encouraging two molecules to dimerize by pulling them into close proximity, even proteins outside a traditional dynein role [24]. Yeast Tda2 may be performing a similar dimerization role with Aim21. Since yeast Tda2 does not associate with dynein, the light chain role of this protein family may have been gained later in the evolutionary tree, with a dynein-independent role as its early function. LC8 and TcTex-1 are structurally similar, yet have very little sequence identity and different binding partners [24]. The gain of dynein function for TcTex may also explain this phenomenon as a functional convergence rather than sequence divergence of two functionally similar proteins.

While Cap1/2 do not appear to be in a stable complex with Tda2, they may associate transiently based on increased Cap1-GFP patch lifetime and reduced intensity in *tda2Δ*. Additionally, the localization of Tda2 is similar to the capping protein localization [14]. However, Cap1 did not bind Tda2 directly or with enough affinity to be detected via GST-pulldown, but a physical interaction between these proteins has been predicted in the past by TAP-tag purification of Cap1, which revealed Tda2 and Aim21 in association with Cap1 [15]. The exact role of Tda2 and Aim21 and their interaction with capping protein in the actin cytoskeleton during CME will require further investigation.

The identification of Tda2 as a potential endocytic protein was achieved by screening the yeast GFP library [9]. Confirmation of this previously uncharacterized protein as a bona fide component of the endocytic machinery and novel dynein light chain exposes how much is still unknown about this essential cell process.

3.5 Experimental Procedures

3.5.1 Plasmids and yeast strains

Recombinant polyhistidine-fusion protein Tda2 was created by PCR amplification of full length ORF Tda2 from genomic DNA and cloned into pET30a(+) vector using NdeI and SalI to produce one poly-histidine tag. GFP-Tub1(Leu) plasmid was a gift from the laboratory of Steven Markus. 13-Myc-tagging of Aim21 and RFP-tagging of Cap1 and Tda2 were performed by PCR amplification of pFA6a plasmids and homologous recombination.

Background strains of *Saccharomyces cerevisiae* BY4741 and BY4742 were used for this study. Figure 1 images were obtained from SDY423 (*MATα ura3-52, leu2-3,112, his3-Δ200, trp1-Δ901, lys2-801, suc2-Δ9, GAL - MEL chc1-521::URA3, UBX3-GFP::HIS3, SLA1-RFP::KanMX6*). Wild-type GFP-expressing strains (Tda2-GFP, Mup1-GFP, Sla1-GFP, Ede1-GFP, Las17-GFP, Abp1-GFP, Cap1-GFP, Aim21-GFP, Myo5-GFP, Rvs167-GFP) were obtained from the yeast GFP library (Invitrogen). Tda2-GFP was mated and dissected to obtain SDY425 *(MATα his3Δ1, leu2Δ0, met15-Δ0, ura3Δ0, TDA2-GFP::HIS3)*. SDY425 was mated with knockout library strains ΔCap1 and ΔAim21 to obtain SDY741 *(MATa his3Δ1, leu2Δ0, met15-Δ0, ura3Δ0, cap1Δ::KanMX4, TDA2-GFP::HIS3)* and SDY754 *(MATa his3Δ1, leu2Δ0, met15-Δ0, ura3Δ0, aim21Δ::KanMX4, TDA2-GFP::HIS3)*. SDY425 was mated with SDY360 to create SDY710 (*MATa his3Δ1, leu2Δ0, met15-Δ0, ura3Δ0, ABP1-RFP::TRP1, TDA2-*

GFP::HIS3). The Tda2 ORF was then tagged with RFP using homologous recombination from a pFA6a-mRFP-KanMX6 PCR product to create SDY740 *(MATα his3Δ1, leu2Δ0, met15-Δ0, ura3Δ0, TDA2-RFP::KanMX6)*. SDY740 was then mated with GFP library strains to obtain SDY751 *(MATa his3Δ1, leu2Δ0, met15-Δ0, ura3Δ0, CAP1-GFP::HIS3, TDA2-RFP::KanMX6)* and SDY781 *(MATa his3Δ1, leu2Δ0, met15-Δ0, ura3Δ0, AIM21-GFP::HIS3, TDA2-RFP::KanMX6)*. Δ strains (ΔTda2, ΔSla1, ΔCap1 and ΔAim21) were obtained from the yeast knockout library (GE). ΔTda2 was mated and dissected to create SDY722 *(MATα his3Δ1, leu2Δ0, met15-Δ0, ura3Δ0, tda2Δ::KanMX4)*. SDY722 was mated with GFP library strains to create SDY656 *(MATα his3Δ1, leu2Δ0, met15-Δ0, ura3Δ0, tda2Δ::KanMX4, MUP1-GFP::HIS3)*, SDY723 *(MATa his3Δ1, leu2Δ0, met15-Δ0, ura3Δ0, tda2Δ::KanMX4, EDE1-GFP::HIS3)*, SDY735 *(MATa his3Δ1, leu2Δ0, met15-Δ0, ura3Δ0, tda2Δ::KanMX4, LAS17-GFP::HIS3)*, SDY731 *(MATa his3Δ1, leu2Δ0, met15-Δ0, ura3Δ0, tda2Δ::KanMX4, ABP1-GFP::HIS3)*, SDY725 *(MATa his3Δ1, leu2Δ0, met15-Δ0, ura3Δ0, tda2Δ::KanMX4, CAP1-GFP::HIS3)*, SDY727 *(MATa his3Δ1, leu2Δ0, met15-Δ0, ura3Δ0, tda2Δ::KanMX4, AIM21-GFP::HIS3)*, SDY729 *(MATa his3Δ1, leu2Δ0, met15-Δ0, ura3Δ0, tda2Δ::KanMX4, MYO5-GFP::HIS3)*, and SDY733 (*MATa his3Δ1, leu2Δ0, met15-Δ0, ura3Δ0, tda2Δ::KanMX4, RVS167-GFP::HIS3)*. DYN1-TAP strain with overexpression was a gift from the laboratory of Steven Markus.

3.5.2 Biochemical methods

Total yeast cell extracts were prepared as described previously [25, 26]. Extracts were separated by spinning at 300,000xg for 20 min to obtain cytosolic fractions. Gel filtration was performed on a Superose 6 10/300 GL column (GE) equilibrated with PBS with fractions

collected every 1 ml. Proteins and standards used include: BSA, Cytochrome C, Carbonic anhydrase, Alcohol dehydrogenase, β-amylase, Apoferritin, Thyroglobulin, and dextran blue. Recombinant Tda2 polyhistidine-fusion protein was expressed in BL21 codon plus *Escherichea coli* and purified as described previously [26, 27]. Tda2 antibody was induced with purified polyhistidine-fusion Tda2 in rabbit by Cocalico Biologicals (Reamstown, PA). Antibody was affinity purified from serum using polyhistidine-fusion Tda2 covalently attached to Affi-Gel 15 activated media and validated using yeast total cell extracts from wild type, Tda2-GFP, and tda2Δ strains. The yeast Cap1 antibody was a generous gift from the laboratory of John Cooper (Washington University).

3.5.3 Fluorescence microscopy and endocytosis assays

Fluorescence microscopy was performed as described using an Olympus inverted IX81 confocal microscope with a Yokogawa spinning disc, as described previously [28]. Images were obtained with a 100X objective. Cells were grown to early log phase and imaged at room temperature except in case of heat shock (37˚C). Time lapse images were collected every 2 seconds except for Ede1-GFP which was imaged every 5 seconds. Lucifer yellow and Mup1-GFP endocytic assays were performed as described previously [9]. Latrunculin A treatment was performed as described previously [29]. Slidebook 6 software (3I, Denver, CO) was used for image collection and analysis. Student's t-test was calculated using Graph Pad software to determine statistical significance. Graphs displaying multiple data points, average, and standard deviation bars were also generated using Graph Pad software.

3.5.4 Crystallography and sequence analysis

Purified Tda2-6His was concentrated in 10 mM HEPES (pH 7.0), 100 mM NaCl, 5% glycerol. Hanging drop method was performed by mixing 1µl protein solution with 1µl precipitating solution (0.1 Sodium Acetate (pH 5.0), 1.6 M Ammonium Sulfate, 15% Xylitol) with 0.5ml of precipitating solution in the reservoir and trays were incubated at 16˚C. Crystals appeared after 4 days and were soaked in bromine. Crystallization and structure determination were performed by Seth McDonald and Olve Peersen. Sequence alignment and phylogenetic analysis were performed using Multalin and Clustal Omega (EMBL-EBI). Structural overlay was performed with PDBeFold (EMBL-EBI).

3.5.5 Acknowledgements

We acknowledge Colette Worchester for her work on strain production and microscopy, Caitlin Grossman for her work on protein purification in this project, and Al Aradi for protein purification and antibody purification and testing. We acknowledge Seth McDonald and Olve Peersen for setting up crystal trays, X-ray crystallography, and solving of the structure. Dynein strains, protocols, and helpful recommendations were provided by the laboratory of Steven Markus. Microscopes used in this work are supported in part by the Microscope Imaging Network core infrastructure grant from Colorado State University.

REFERENCES

1. Weinberg, J. and D.G. Drubin, *Clathrin-mediated endocytosis in budding yeast.* Trends Cell Biol, 2012. **22**(1): p. 1-13.
2. Goode, B.L., J.A. Eskin, and B. Wendland, *Actin and endocytosis in budding yeast.* Genetics, 2015. **199**(2): p. 315-58.
3. Boettner, D.R., R.J. Chi, and S.K. Lemmon, *Lessons from yeast for clathrin-mediated endocytosis.* Nat Cell Biol, 2012. **14**(1): p. 2-10.
4. Taylor, M.J., D. Perrais, and C.J. Merrifield, *A high precision survey of the molecular dynamics of mammalian clathrin-mediated endocytosis.* PLoS Biol, 2011. **9**(3): p. e1000604.
5. Doyon, J.B., B. Zeitler, J. Cheng, A.T. Cheng, J.M. Cherone, Y. Santiago, A.H. Lee, T.D. Vo, Y. Doyon, J.C. Miller, et al., *Rapid and efficient clathrin-mediated endocytosis revealed in genome-edited mammalian cells.* Nat Cell Biol, 2011. **13**(3): p. 331-7.
6. Kaksonen, M., C.P. Toret, and D.G. Drubin, *A modular design for the clathrin- and actin-mediated endocytosis machinery.* Cell, 2005. **123**(2): p. 305-20.
7. Kaksonen, M., Y. Sun, and D.G. Drubin, *A pathway for association of receptors, adaptors, and actin during endocytic internalization.* Cell, 2003. **115**(4): p. 475-87.
8. Mulholland, J., D. Preuss, A. Moon, A. Wong, D. Drubin, and D. Botstein, *Ultrastructure of the yeast actin cytoskeleton and its association with the plasma membrane.* J Cell Biol, 1994. **125**(2): p. 381-91.
9. Farrell, K.B., C. Grossman, and S.M. Di Pietro, *New regulators of clathrin-mediated endocytosis identified in Saccharomyces cerevisiae by systematic quantitative fluorescence microscopy.* Genetics, 2015. **201**(3): p. 1061-70.
10. Kelley, L.A., S. Mezulis, C.M. Yates, M.N. Wass, and M.J. Sternberg, *The Phyre2 web portal for protein modeling, prediction and analysis.* Nat Protoc, 2015. **10**(6): p. 845-58.
11. Wu, H., M.W. Maciejewski, S. Takebe, and S.M. King, *Solution structure of the Tctex1 dimer reveals a mechanism for dynein-cargo interactions.* Structure, 2005. **13**(2): p. 213-23.
12. Williams, J.C., H. Xie, and W.A. Hendrickson, *Crystal structure of dynein light chain TcTex-1.* J Biol Chem, 2005. **280**(23): p. 21981-6.
13. Wickstead, B. and K. Gull, *Dyneins across eukaryotes: a comparative genomic analysis.* Traffic, 2007. **8**(12): p. 1708-21.
14. Michelot, A., A. Grassart, V. Okreglak, M. Costanzo, C. Boone, and D.G. Drubin, *Actin filament elongation in Arp2/3-derived networks is controlled by three distinct mechanisms.* Dev Cell, 2013. **24**(2): p. 182-95.
15. Gavin, A.C., M. Bosche, R. Krause, P. Grandi, M. Marzioch, A. Bauer, J. Schultz, J.M. Rick, A.M. Michon, C.M. Cruciat, et al., *Functional organization of the yeast proteome by systematic analysis of protein complexes.* Nature, 2002. **415**(6868): p. 141-7.
16. Huh, W.K., J.V. Falvo, L.C. Gerke, A.S. Carroll, R.W. Howson, J.S. Weissman, and E.K. O'Shea, *Global analysis of protein localization in budding yeast.* Nature, 2003. **425**(6959): p. 686-91.
17. Hess, D.C., C.L. Myers, C. Huttenhower, M.A. Hibbs, A.P. Hayes, J. Paw, J.J. Clore, R.M. Mendoza, B.S. Luis, C. Nislow, et al., *Computationally driven, quantitative*

experiments discover genes required for mitochondrial biogenesis. PLoS Genet, 2009. **5**(3): p. e1000407.
18. Tonikian, R., X. Xin, C.P. Toret, D. Gfeller, C. Landgraf, S. Panni, S. Paoluzi, L. Castagnoli, B. Currell, S. Seshagiri, et al., *Bayesian modeling of the yeast SH3 domain interactome predicts spatiotemporal dynamics of endocytosis proteins.* PLoS Biol, 2009. **7**(10): p. e1000218.
19. Williams, J.C., P.L. Roulhac, A.G. Roy, R.B. Vallee, M.C. Fitzgerald, and W.A. Hendrickson, *Structural and thermodynamic characterization of a cytoplasmic dynein light chain-intermediate chain complex.* Proc Natl Acad Sci U S A, 2007. **104**(24): p. 10028-33.
20. Pfister, K.K., P.R. Shah, H. Hummerich, A. Russ, J. Cotton, A.A. Annuar, S.M. King, and E.M. Fisher, *Genetic analysis of the cytoplasmic dynein subunit families.* PLoS Genet, 2006. **2**(1): p. e1.
21. Sachdev, P., S. Menon, D.B. Kastner, J.Z. Chuang, T.Y. Yeh, C. Conde, A. Caceres, C.H. Sung, and T.P. Sakmar, *G protein beta gamma subunit interaction with the dynein light-chain component Tctex-1 regulates neurite outgrowth.* EMBO J, 2007. **26**(11): p. 2621-32.
22. Nagler, M., L. Palkowitsch, S. Rading, B. Moepps, and M. Karsak, *Cannabinoid receptor 2 expression modulates Gbeta1gamma2 protein interaction with the activator of G protein signalling 2/dynein light chain protein Tctex-1.* Biochem Pharmacol, 2016. **99**: p. 60-72.
23. Liu, C., J.Z. Chuang, C.H. Sung, and Y. Mao, *A dynein independent role of Tctex-1 at the kinetochore.* Cell Cycle, 2015. **14**(9): p. 1379-88.
24. Rapali, P., A. Szenes, L. Radnai, A. Bakos, G. Pal, and L. Nyitray, *DYNLL/LC8: a light chain subunit of the dynein motor complex and beyond.* FEBS J, 2011. **278**(17): p. 2980-96.
25. Di Pietro, S.M., D. Cascio, D. Feliciano, J.U. Bowie, and G.S. Payne, *Regulation of clathrin adaptor function in endocytosis: novel role for the SAM domain.* EMBO J, 2010. **29**(6): p. 1033-44.
26. Feliciano, D., J.J. Bultema, A.L. Ambrosio, and S.M. Di Pietro, *In vivo andin vitro studies of adaptor-clathrin interaction.* J Vis Exp, 2011(47).
27. Feliciano, D., T.O. Tolsma, K.B. Farrell, A. Aradi, and S.M. Di Pietro, *A second Las17 monomeric actin-binding motif functions in Arp2/3-dependent actin polymerization during endocytosis.* Traffic, 2015. **16**(4): p. 379-97.
28. Feliciano, D. and S.M. Di Pietro, *SLAC, a complex between Sla1 and Las17, regulates actin polymerization during clathrin-mediated endocytosis.* Mol Biol Cell, 2012. **23**(21): p. 4256-72.
29. Newpher, T.M., R.P. Smith, V. Lemmon, and S.K. Lemmon, *In vivo dynamics of clathrin and its adaptor-dependent recruitment to the actin-based endocytic machinery in yeast.* Dev Cell, 2005. **9**(1): p. 87-98.

CHAPTER 4

CONCLUSIONS AND IMPLICATIONS FROM THE IDENTIFICATION OF NEW PROTEINS OF THE ENDOCYTIC MACHINERY

4.1 Summary

Despite decades of research on clathrin-mediated endocytosis (CME), this essential cellular process remains incompletely understood. We have attempted to further investigate CME using a novel screening approach with fluorescent microscopy and the yeast GFP library. There have been previous screens for proteins involved in endocytosis using methods such as synthetic lethality and cargo accumulation in null and mutant strains. Our screening of the GFP library does not depend on a gene knockout or strong endocytic phenotype to identify new proteins. By looking at protein localization in wild type cells, we can identify novel endocytic proteins with redundant function, without strong phenotypes, and without excess stress on cells. This screening approach has potential for success with other cell processes that have distinct cellular localizations and known fluorescent markers. Through this visual screening approach, we have identified many potential previously uncharacterized proteins of the endocytic machinery. We have confirmed two of these proteins, Ubx3 and Tda2, and performed initial characterization of their function.

Ubx3, a previously uncharacterized protein, is the first UBX domain-containing protein identified with an endocytic role, despite the multiple roles of ubiquitin in CME. UBX domain-containing proteins are well-known regulators of AAA ATPase Cdc48. Cdc48 has many diverse roles in cellular maintenance ranging from membrane fusion to chromatin modification and

ubiquitin and proteasome processes, yet these functions center around the ability of Cdc48 to segregate protein complexes. UBX domain-containing proteins regulate and recruit Cdc48 to the correct locale for its varying functions. Our findings indicate a role for Ubx3 in recruitment of Cdc48 for regulation of the protein coat at sites of clathrin-mediated endocytosis.

Tda2 was also previously an uncharacterized protein with no predicted domains or conserved sequences. Structural prediction programs indicated that Tda2 may be similar to a dynein light chain or an actin delpolymerizing factor/cofilin protein and the former was shown to be true by X-ray crystallography. There are three dynein light chain families: LC8, TcTex, and roadblock. Tda2 is a TcTex-1 dynein light chain homolog, which was previously unidentified in yeast. Tda2 does not appear to associate with the dynein motor protein complex in yeast, where the only known role of dynein is spindle positioning during mitosis. However, dynein light chains have been demonstrated in roles outside of the traditional dynein motor complex role in mammalian cells. Tda2 behaves similarly to actin-associated proteins in clathrin-mediated endocytosis, based on localization, sensitivity to LatA, timing, effects of the knockout strain, and its association with Aim21. Thus we have identified a novel endocytic protein, identified a new dynein light chain in yeast, added to the growing evidence of roles for dynein light chains outside of the dynein motor, and revealed dynein independence as an ancient property.

Confirmation of these two new proteins involved in endocytosis suggests there is still much unknown about the process. Many transmembrane proteins have not been confirmed as endocytic cargo, and questions about cargo recruitment and adaptor recognition of cargo still remain. A screening using the GFP library is proposed for systematic identification of endocytic cargo. Additionally, during our screening of the yeast GFP library for endocytic machinery, we

identified 28 uncharacterized proteins that colocalized with endocytic adaptor Sla1. There is potential for confirmation of more these proteins as novel components of the CME machinery.

4.2 A screen of the GFP library successfully identified proteins of the endocytic machinery

4.2.1 Previous yeast screening methods

The simplicity of yeast genetics has allowed creation of the knockout, TAP-tag, overexpression, HA-tag, and GFP libraries, plasmid and interaction libraries, among others. Easy availability of any strain or complete library possessing the indicated change to almost any ORF in the yeast genome has encouraged many to perform genome-wide screenings in the past, including many for proteins involved in clathrin-mediated endocytosis.

The yeast deletion library has been screened for a huge range of phenotypes: cell and bud shape, pH resistance, heat, nutrient, toxin, and oxidation sensitivity, and more. Synthetic lethal screens are similar but show that two proteins, which can be knocked out individually with the cell remaining viable, are lethal to the cell when knocked out simultaneously. This suggests the two proteins work in analogous pathways or functions. Null screenings in CME rely on the knockout of a specific protein producing a measurable phenotype to indicate a result. Understandably, proteins essential to the cell cannot be deleted and are left out of such screenings. Established endocytic machinery protein Pan1 and actin depolymerization protein Cof1 are essential to the cell, and many other endocytic protein deletion strains have detrimental growth and toxin resistance defects, such as Sla1 or Las17 deletions. These complicate the results of knockout screenings.

Some of the earliest screenings for clathrin-mediated endocytosis center on the internalization of the yeast mating factor peptides, alpha factor or “a” factor [1]. These bind to

corresponding receptors on the opposite mating type cell and are internalized via CME, thus deficient internalization indicates the knockout of a required endocytic protein. Another of the earliest endocytic-specific protein screenings used FM4-64, a lipophilic fluorescent dye, and FACS to look for mutant cells with internalization defects [2]. Lucfier yellow fluorescent dye was also used to track endocytic internalization without modification of the cell or genome [3, 4], and more recently fluorescent alpha factor has expanded the use of the mating pheromone receptors to measure endocytosis [5].

Cargo-based endocytic screenings rely on the phenotype of reduced cargo protein internalization in the presence of a knockout or mutation. One such study used a chimeric protein of Snc1 and invertase as a synthetic cargo and introduced to genome-wide deletion collections. Increased invertase activity indicated a reduction in endocytosis, thus identifying the deleted gene as a vital component of endocytic machinery [6]. Another interesting study used a cargo phenotype without dependence on the knockout collection. The Wendland lab has introduced random mutations throughout the yeast genome in cells expressing a cargo protein with pH-sensitive GFP. In cells with normal internalization levels, cargo is internalized and reaches the vacuole where the GFP is quenched. However, cells with defective internalization have fluorescent cargo remaining on the surface, and can be sorted based on FACS. Cells were then sequenced to identify mutations, finding several new endocytic proteins as well as previously unknown important regions and motifs in established endocytic machinery [personal communication].

Toxin-based screens rely on the resistance or sensitivity of cells with endocytic defects to different toxins. Cells resistant to K28 toxin revealed endocytic proteins in a screen of the deletion collection as well as many genes not represented in deletion strains through use of

temperature sensitive alleles [7]. Antifungal molecules can also be used to identify endocytic proteins. Canavanine is a toxic arginine derivative internalized by Can1, the arginine permease in yeast. Cells defective in endocytosis accumulate Can1 at the membrane and are sensitive to Canavanine toxicity [8]. Caspofungin is another antifungal molecule which acts by inhibiting cell wall synthesis, and cells defective in endocytosis are more sensitive to the drug [9].

In vitro studies have also been utilized to find protein interactions related to clathrin-mediated endocytosis. One such study used phage display, yeast two-hybrid, and peptide array screens to predict the interactome of yeast SH3 domains [10], which have vital roles in CME as described in Chapter 1. This study identified potential new endocytic proteins and interactions, some of which have been confirmed by other studies. This study also indicated Aim21 may have some interactions with the SH3 domains of various endocytic proteins, but this has yet to be demonstrated outside of a predictive model. The yeast two-hybrid technique can also be used to screen entire libraries of genomic fragments for interactions, but depends on correct cellular localization, folding, and transcription activation, resulting in many false positives and negatives [11].

There have also been numerous studies which have attempted to categorize the entire yeast proteome, instead of a single process. One of these is the creation and high-throughput localization study of the yeast GFP library [12], described in further detail in Chapter 1. Another example includes the TAP-tag purification and mass spectrometry analysis of 589 protein assemblies [13]. The protein complexes defined by this group included the Cap1-TAP potential complex discussed in Chapter 3, where associated with Cap1 were Cap2, Tda2, and Aim21.

These techniques and past screenings have been successful in identification of many CME machinery proteins, though no screening finds all proteins in a process. Each screening method has benefits and drawbacks, identifying some proteins but lacking others.

4.2.2 Advantages and shortcomings of the GFP library screen

To our knowledge, a GFP localization-based screening, as described in Chapter 2, has not been previously performed to identify endocytic machinery. There were several advantages to this approach over endocytic screens previously performed. First, our GFP screen was performed without the use of knockout strains. The use of knockout strains limits the screen to non-essential genes, and addition of temperature sensitive alleles as in Carroll *et al.* (2009) [7] still does not complete the genome. Also, a knockout may not show a phenotype in proteins with redundant functions, which is common among proteins of the endocytic machinery. Compensation by other proteins may reduce the level of an endocytic defect. Additionally, knockout of an unrelated gene may stress the cell, showing an endocytic defect when the deleted gene is not directly a part of the endocytic machinery. Similarly, toxin-based screens can stress the cell and skew results. Our GFP library screening is performed without any gene disruption or toxin stress.

A weakness associated with cargo-based screens is the identification of false positive results in other trafficking processes. Mislocalization of a cargo protein identifies false positives associated with other trafficking processes or causing errors in protein production. Cargo-based screens also do not identify proteins without a strong phenotype upon deletion. Many proteins in the endocytic machinery have redundant function, where a deletion of one gene shows no effect as other proteins are there to compensate for its role. In contrast, the GFP library screening is

based on localization only, eliminating false positives caused by trafficking errors in knockout strains, and does not rely on a strong endocytic phenotype with knockout.

The GFP library screening is also sensitive enough to detect low abundance proteins. Creators of the TAP-tag yeast library, which was built similarly to the GFP library as C-terminal fusions at the endogenous loci, found 80% of the proteome expressed at normal growth conditions with the count of each protein ranging from less than 50 to more than 10^6 per cell [14]. Data on the abundance of proteins analyzed in the TAP library are available for those wishing to confirm expression or fluorescence levels (yeastgfp.yeastgenome.org). GFP fluorescence can be detected at very low levels, allowing visualization of almost any protein recruited to endocytic sites.

Use of the GFP library also provided the opportunity to narrow down the genome to potential endocytic localizations. This greatly reduced processing time for the study, while other screens use the entire genome. The creators of the GFP library performed high-throughput colocalization studies to identify subcellular localizations of most of their GFP collection [12]. This information allowed selection of only 319 strains for our screening, by selecting the categories containing known endocytic proteins, therefore most likely to contain additional endocytic proteins. These categories included proteins localized to actin, the plasma membrane, or punctae. The screen therefore contained positive controls of known endocytic proteins, as well as negative controls of proteins of known function in other processes. Finally, the screen was performed in a blind manner to prevent bias. Cells were imaged without knowledge of the identity of the GFP protein, ensuring a random selection of cells to be imaged and quantified with the Pearson correlation coefficient.

Despite the many advantages of the GFP library screening, there are still weaknesses associated with this method. First, this screening method does not encompass the whole genome. Creators of the GFP library only saw GFP fluorescence levels above background in ~75% of the ORFs tagged [12]. However, creators of the TAP-tag library only saw 80% of the proteome expressed [14], suggesting this is not a defect of the GFP library, but normal cell protein levels. Alternatively, C-terminal tags may disrupt protein folding and cause degradation. Second, though narrowing down of the strains to 319 created a much more efficient screening process, there is the possibility that unknown proteins involved in clathrin mediated endocytosis were eliminated. For example, clathrin heavy chain, despite its involvement in endocytosis, was not included in the screen as its localization in the GFP library is recorded as the Golgi. However, this screening method does allow visualization of essential proteins, while the knockout library cannot include these.

Another weakness of the GFP screening is there are many false positives. Almost 2/3 of the proteins analyzed colocalized with Sla1, yet most of these have unrelated functions. We were able to focus on the highest scoring uncharacterized colocalizing proteins, but other positive results may be buried in the long list of colocalizing proteins. A lower Pearson correlation coefficient score for an endocytic protein could be due to its localization not only at endocytic sites but also at other cellular locations, as seen with clathrin. Lastly, there is always a question of whether the GFP tag is disrupting normal protein function. As always, controls need to be performed to ensure normal protein function and verify initial colocalization results. Overall, the GFP library screening provided a unique approach for identification of previously unknown CME machinery.

4.2.3 Potential for GFP library screens in other cell processes

The successful use of the yeast GFP library in a screen for clathrin-mediated endocytosis, with which we confirmed two previously uncharacterized proteins as components of the endocytic machinery, raises the question of whether this method can be used for additional cell processes. The success of the CME screen was dependent on a distinct fluorescent localization pattern. Processes with diffuse, changing, or indistinct fluorescent patterns would likely not be successful in a screen. Additionally, an established protein or molecule involved in the process that can be used as a fluorescent marker is required. Results depend on a colocalization measure, which can only be as accurate as that which is being compared. Use of a marker protein involved in multiple cell processes, with low fluorescence, or varying localization patterns will return unreliable results.

In our screening, we narrowed down candidates based on initial GFP library localization. This is an added benefit for processes that may have a predictable localization pattern. Again, distinct cellular compartments are ideal for this aspect of a GFP library screening. Though endocytosis does not occur in an organelle, its distinct punctate pattern at the cell membrane allowed this filtering of possible GFP strains. Enough must be known about the potential process to be screened in order for a knowledgeable and accurate narrowing down of GFP strains as well as selection of fluorescent marker for comparison.

In conclusion, the GFP library can be successfully screened to identify previously uncharacterized components of a cellular process as demonstrated in CME. The cellular process must have distinct cellular localization and established fluorescent marker for the screen to be effective. Our screen of the yeast GFP library for components of the clathrin-mediated endocytic

machinery successfully identified at least two previously uncharacterized proteins, Ubx3 and Tda2.

4.3 Ubx3 is the first UBX domain-containing protein identified in endocytosis

4.3.1 UBX domain-containing proteins

The UBX domain is an 80 amino acid sequence typically located at the C-terminus of a protein. UBX domains are found in all eukaryotic species and are thought to have evolved from ubiquitin based on structural similarities. The structure of the UBX domain of human FAF1 can be superimposed on the ubiquitin structure with a r.m.s.d of 1.9 Å, however variances in the structure and sequence make it unlikely that the UBX domain is conjugated or part of a ubiquitin chain [15]. The UBX domain contains a conserved R…FPR surface patch which is not present in ubiquitin [15], and this region was found to be the major binding site for the UBX domain to Cdc48, which may explain why Cdc48 binds UBX domains but not ubiquitin [16]. A subset of UBX domain-containing proteins also contain a ubiquitin-binding UBA domain with which ubiquitinated proteins are recruited to Cdc48 [17].

There are seven UBX domain-containing proteins in yeast, all of which have been demonstrated to bind Cdc48 [17]. The yeast UBX domain-containing proteins represent four major UBX protein subfamilies, while there are 7-8 subfamilies represented across all eukaryotes [16]. UBX domain-containing proteins regulate Cdc48 (p97/VCP in mammalian cells) as cofactors that direct the many functions of Cdc48 discussed in the following section. Examples include Shp1 and Ubx2 which act as adaptors for Cdc48 for its role in ubiquitin-dependent proteasomal degradation [17, 18]. Another cofactor is Ufd1, which binds poly-ubiquitinated proteins as part of the Cdc48-Npl4-Ufd1 complex, recruits Cdc48 to proteins destined for

degradation by the 26S proteasome [19]. These proteins form a sort of core complex, which can further associate with accessory cofactors to further refine function. Hierarchy and exclusivity of cofactor binding is predicted to provide discrimination for Cdc48 functions [20]. Additionally, it has been demonstrated that after UBX proteins act as substrate-recruitment cofactors for Cdc48, substrate-processing cofactors may then associate, further expanding the roles and regulation of Cdc48. One such substrate-processing cofactor is the de-ubiquitinase VCIP135 [21].

There have been studies demonstrating the involvement of a UBX domain-containing protein in a specific cellular process, without yet clarifying an associated role for Cdc48. However, there are no well-established roles for UBX domain-containing proteins besides cofactors for Cdc48, indicating Cdc48 may still be implicated in these processes. Overall, UBX domains are well-conserved eukaryotic domains, which regulate a well-conserved eukaryotic protein Cdc48, which has many diverse functions.

4.3.2. Functions of Cdc48

Cdc48 (p97/VCP in mammalian cells) is an extremely abundant, essential, and highly conserved protein. Cdc48 forms a ring-shaped complex of 6 identical subunits each containing two ATPase domains. The N-terminal domain is responsible for most cofactor and substrate binding, while a few bind the C-terminal domain [22]. Cdc48/p97 has demonstrated roles in vastly different cellular processes as mediated by its cofactors. Roles for this ATPase include: homotypic membrane fusion of the ER and Golgi, protein transport in the endo-lysosomal pathway, protein degradation, nuclear envelope reassembly, cell cycle progression, endoplasmic reticulum associated protein degradation, structurally remodeling ubiquitinated proteins, editing ubiquitin modifications, and chromatin associated functions [16, 22]. Of note, Cdc48 has several

roles in proteasomal degradation and ubiquitin regulation. Cdc48 has the ability to bind several E3 ubiquitin ligases directly or through adaptors, the ability to transport proteins to the proteasome, as well as modify ubiquitinated proteins [16, 22].

An underlying theme of Cdc48 roles is the ATP-dependent disassembly of oligomeric substrate proteins [23]. Cdc48 has the ability to extract proteins from their host complexes, as well as from membranes. This has been termed "segregase" activity [16]. Several of the seemingly unrelated roles of this protein upon further investigation are all segregase-type functions. An example of this is homotypic membrane fusion; Cdc48 remodels SNARE complexes [16], an important aspect of membrane maintenance regulated by protein complex disassembly.

The roles of Cdc48 are diverse and permeate eukaryotic cell function, and a knockout of this protein is lethal. With six identical subunits and abundant cofactors, the possibilities for cofactor combinations, and therefore different functions of this protein, are vast. We propose a function for Cdc48 in clathrin-mediated endocytosis in yeast, mediated by cofactor Ubx3.

4.3.3. Potential roles of Cdc48 and Ubx3 in clathrin-mediated endocytosis

In our studies detailed in Chapter 2, we identified Ubx3 as a protein of the clathrin-mediated endocytic machinery by screening the yeast GFP library. We found Ubx3 binds clathrin directly as well as Cdc48 in cellular extracts. Heat inactivation of Cdc48 reduced clathrin-mediated endocytosis to minimal levels, and produced large aggregates of endocytic protein Ede1.

Potential connections between UBX domain-containing proteins, Cdc48, and endo-lysosomal transport have been previously identified in mammalian cells. p97 was shown to bind

clathrin [24], and could be regulating the oligomeric state of clathrin assembly. Mammalian UBX domain-containing protein TUG (a Ubx4 homolog) has been demonstrated to bind the GLUT4 receptor and regulate its transport to the membrane [25]. p97 inhibition also affects the endosomal cargo proteins transferrin receptor and mannose receptor [26], as well as others, suggesting a general role in endo-lysosomal trafficking [27].

Ubx3 may be related to the FAF1 subfamily of UBX domain-containing proteins [16]. This family is characterized by an N-terminal UBA ubiquitin binding domain, an uncharacterized UAS domain consisting of a thioredoxin-like fold, and the C-terminal UBX domain. Ubx3 however, is not predicted to contain a ubiquitin binding domain. The mammalian FAF1 protein has implications in apoptosis and the endo-lysosomal pathway [28] and the NFκB pathway [29] but has not been reported to localize at endocytic sites.

Upon deletion of Ubx3, early endocytic protein Ede1 had delayed recruitment to the endocytic site. High levels of Ub-Ede1 delay its recruitment to the endocytic patch [30], similar to the reduced recruitment rate we saw in the *ubx3Δ* strain. Deletion of Ubp2 and Ubp7, which are the major de-ubiquitinators (DUBs) of Ede1, cause high levels of Ub-Ede1[30]. These results raise the possibility that Ubp2 and Ubp7 could be cofactors of Cdc48, as DUBs have been established as cofactors previously [21]. When Ubx3 is deleted and Cdc48 is theoretically not recruited to the endocytic site, then Ubp2 and Ubp7 would also be absent, thus causing the delay in Ede1 recruitment. The binding of E3 ligases and other ubiquitin regulatory enzymes to Cdc48 has already been demonstrated. Another group found that Ubx3 co-purified with ubiquitin-ligase DSC complex [31], again suggesting a role in ubiquitin regulation. However, the presence of Ede1 aggregates suggests Cdc48 may be acting in its segregase activity regarding Ede1. Ede1 self-association into oligomers is necessary for its endocytic localization and function as a

scaffold for the early endocytic site [32]. Cdc48 may be acting as a regulator of the oligomerization state of Ede1, segregating complexes that are too large in order to prevent aggregation. Moreover, Cdc48 could be acting in both these roles, not only regulating the ubiquitination state of Ede1 but also its oligomerization state. The clathrin-binding ability of Ubx3 could mediate the localization of Cdc48 to sites of CME, where it then regulates Ede1 and potentially more endocytic proteins.

We imaged Cdc48-GFP using confocal and TIRF microscopy, but were unable to determine endocytic localization in wild type cells. This protein has high abundance and diffuse cellular localization, causing difficulty in distinguishing localization to specific cellular locales or compartments. Cdc48 may be present at endocytic sites but at levels similar to cytosol and other cellular compartments, as only a few molecules may be needed for catalytic activity. Despite this, our findings suggest Cdc48 cofactor Ubx3 is an important protein of the clathrin-mediated endocytic machinery. Cdc48 has diverse cellular roles, including disassembly of protein complexes. This "segregase" activity of Cdc48 may play an important role in clathrin-mediated endocytosis through regulation of Ede1 and be responsible for the endocytic defects we see in the *ubx3Δ* strain. To our knowledge, this is the first example of a UBX domain-containing protein in CME and the first implication of Cdc48 function in CME.

4.4 Tda2 is a dynein light chain with a dynein motor independent role

4.4.1 The dynein motor protein complex in mammals and yeast

In mammalian cells, the cytoplasmic dynein complex consists of dimers of each of the following: heavy chain, intermediate chain, light intermediate chain, roadblock light chain, LC8 light chain, and TcTex light chain. The heavy chain is a distant member of the AAA ATPase

family, and consists of a motor domain and microtubule binding domain at the C-terminus and dimerization region that doubles as intermediate chain binding region at the N-terminus. Motor activity is directed towards the minus end of microtubules and driven by hydrolysis of ATP. Functions of the cytoplasmic dynein complex in mammalian cells include spindle organization and nuclear migration in mitosis, positioning and function of the ER, Golgi apparatus, and nucleus, and the transport of vesicles as well as endosomes and lysosomes. Cell specific functions such as retrograde axonal transport in neurons also utilize this complex. There are two cytoplasmic dynein complexes; the second is only involved in intraflagellar transport and is comprised of fewer components. Additionally, axonemal dynein is responsible for movement of cilia and flagella. Cytoplasmic dynein associates with seven-protein complex dynactin, which acts as an adaptor to connect a range of cargoes and increases motor processivity [33].

In yeast, the dynein complex consists of dimers of the heavy chain, intermediate chain, light intermediate chain, and LC8 light chain. The yeast dynein heavy chain has 50% sequence identity with mammalian cells with the C-terminus containing the most conservation [33]. Dynactin plays a vital role in yeast dynein as well. The only established function of the cytoplasmic dynein motor protein complex in yeast is partitioning the mitotic spindle between mother and daughter cells. Dynein is anchored to the cell cortex via Num1 and walks along microtubules to pull the nucleus into the neck and allow even distribution of chromosomes. Deletion of dynein heavy chain or other components of the dynein complex including the LC8 light chain is not lethal in yeast, but causes errors in nuclear segregation during mitosis [34].

4.4.2 The dynein light chain families

Three families of dynein light chains have been identified in mammalian cells. All three dynein light chains purify with the dynein motor protein complex and bind near the N-termini of the intermediate chains [35]. Some light chains also have cellular functions independent of their role in the cytoplasmic dynein complex.

The roadblock family of dynein light chains consists of genes *DYNLRB1* and *DYNLRB2*. This family was first identified in *Drosophila* and mutations result in the accumulation of axonal cargoes, mitotic defects, reproductive deficits, and early lethality [33]. Roadblock sequences have a remarkably high conservation rate among species. Additionally, other proteins have incorporated roadblock sequences into their sequences, referred to as roadblock domains, but these proteins do not seem to be associated with dynein [33].

The LC8 light chain family consists of genes *DYNLL1* and *DYNLL2*. LC8 is a ubiquitously conserved eukaryotic protein and is the best studied of the dynein light chains. Many roles for LC8 have been uncovered outside its namesake dynein complex. LC8 binding promotes homodimerization of the dynein intermediate chain, but is also considered a hub protein to promote dimerization of many interaction partners, creating scaffolds for additional cellular complexes [36]. LC8 interacts with a KXTQT or GVQVD sequence or variant in disordered protein regions, and most binding partners are predicted to be dimeric [36]. The LC8 light chain forms a stable dimer-dimer complex with actin motor Myosin Va [37] and is also a major component of dendritic spines and growth cones. Abundant LC8-interacting proteins have been identified using yeast two-hybrid screens and other approaches [33].

The t-complex associated (TcTex) family, consisting of genes *DYNLT1* and *DYNLT3*, are the largest proteins of the dynein light chain families with ~113 amino acids. The dimeric

structure with β-strand domain swapping is similar to that of the LC8 light chain, and TcTex-1 also binds and promotes homodimerization of the intermediate chain. TcTex-1 binds partners in a similar region as LC8 [38] and despite high structural similarity, TcTex-1 and LC8 have very little sequence identity and no apparent overlap in other binding partners [36] as TcTex-1 interacts with an R/K-R/K-X-X-R/K binding motif [39]. *DYNLT3* is differentially expressed in a cell and tissue-dependent manner, and few binding partners have been identified for this protein. *DYNLT1*, or TcTex-1, has been found to bind many different cellular proteins, initially suggesting a role in attaching cargo proteins to the dynein complex [33]. However, more recent studies into binding sites put into question the ability of both intermediate chain and "cargo" simultaneous binding, suggesting another function for its numerous binding partners [40]. A dynein complex-independent pool of TcTex-1 has been demonstrated to exist [41] and a mutant of TcTex-1 that does not bind the intermediate chain still has neuronal function [42]. TcTex-1 has been implicated in multiple steps of neuronal development, and modulates neuronal outgrowth through binding of the G protein βγ subunit which may affect regulation of actin and microtubule dynamics [39]. TcTex-1 has been found to interact with many G-protein coupled receptors directly [43]. Additionally, TcTex-1 is essential for accurate chromosome segregation, independent of dynein's activity at the kinetochore [44]. Many more binding partners suggest diverse roles for this protein, with and without dynein motor association.

4.4.3 The dynein motor independent role of Tda2 in the actin cytoskeleton

As detailed in Chapter 3, we have identified a TcTex type dynein light chain in yeast for the first time based on structure and sequence homology. Previously, the only established dynein light chain in yeast was the LC8 type light chain and previous genetic analysis found no homolog

for *DYNLT1/*Tctex-1 in yeast [45]. Tda2 has not previously been identified as part of the yeast cytoplasmic dynein complex and studies screening for mitotic defects have not identified a phenotype for the Tda2 deletion. Our studies have further confirmed Tda2 is not stably associated with the dynein complex but suggest a role for Tda2 in the actin cytoskeleton associated with clathrin-mediated endocytosis.

Fluorescent localization of Tda2 shows strong colocalization with clathrin adaptor protein Sla1 as well as actin associated proteins Abp1, Cap1, and Aim21. Fluorescent dynamics also strongly suggest a role in the actin associated stages of clathrin-mediated endocytosis. If Tda2 is present at other cellular localizations, it is at levels not detectable in our studies. The visible localization further distances Tda2 from dynein as yeast LC8 dynein light chain localizes with the dynein heavy chain to the plus ends of microtubules [34].

A TAP-tag purification and mass spectrometry analysis of Cap1 in a high-throughput screening has revealed a candidate complex containing Cap1, Cap2, Tda2, and Aim21 [13]. Later studies found Tda2 associated with proteins at the schmoo, the yeast mating projection, which displays a high concentration of endocytic sites [46]. These studies suggest Tda2 is functionally associated with the actin cytoskeleton in CME, which was further confirmed by our studies detailed in Chapter 3. We also demonstrated Tda2 is in a stable complex with Aim21. Aim21 has many potential, though not perfect, R/K-R/K-X-X-R/K sequences which are established binding partners of mammalian TcTex-1. Aim21 is predicted to be a disordered protein, suggesting any of these potential sequences could be used to bind Tda2. Aim21 also has many polyproline motifs, which are predicted to interact with the numerous SH3 domains of the endocytic machinery [10] and could recruit Aim21 and bound Tda2 to the endocytic site. Our studies did not indicate a stable physical interaction between Cap1 and Tda2 as previously

indicated by mass spectrometry, but did suggest a functional association and similar localization. The yeast actin capping proteins Cap1 and Cap2 exist as a heterodimer which is required for their function and binding of the barbed end of actin filaments. A hypothesis that Tda2 aids in dimerization of Cap1/2 seems unlikely as binding assays did not show any direct binding of Tda2 to Cap1/2, and in gel filtration Cap1 eluted in different cytosolic fractions than Tda2. Dimerization may play a role in the binding of Tda2 to Aim21, as our gel filtration assay predicts a complex size consistent with two Aim21 molecules per Tda2 dimer (Chapter 3).

In the previous section, dynein-independent roles for dynein light chains are described. Our data indicate a new dynein-independent role for a TcTex-1 type dynein light chain, identified in yeast for the first time. Interestingly, *Schizosaccharomyces pombe* contain a *DYNLT1*-like gene that does have roles in dynein dependent activities. It is involved in movement of nuclear material and is localized to astral microtubule anchoring sites at the plasma membrane [47], though this protein is less like Tda2 than many other fungal homologs by sequence comparison. Phylogeny also distances Tda2 from the yeast LC8 light chain (Figure 3.4.C), which has dynein function similar to its mammalian homolog. The TcTex-1 homolog for budding yeast, Tda2, has no apparent connection with the cytoplasmic dynein complex but has a dynein motor independent role in the actin cytoskeleton associated with CME. This is the first identification of this light chain family in yeast, and the first dynein light chain in endocytosis.

4.5 Potential for additional unidentified proteins in the endocytic cargo and machinery

4.5.1 Endocytic cargo proteins

The diffuse nature of most transmembrane proteins around the plasma membrane prevented identification of new endocytic cargoes in our screening of the GFP library (Figure

2.1.A). We were unable to distinguish gathering of fluorescent transmembrane proteins into clathrin coated pits from normal diffuse localization. Known CME-dependent cargo proteins Mup1 and Wsc1 were similarly diffuse, suggesting this is a widespread phenotype and our screening method is unlikely to identify novel endocytic cargo proteins.

I propose that a screening using the GFP library may still be possible for identification of endocytic cargoes. However, instead of looking at a variety of deletion strains with a single cargo expressed, this method would apply a single deletion or inhibitor to a variety of potential GFP-labeled cargoes. Upon disruption of CME, cells with excess membrane fluorescence could identify cargo proteins dependent on clathrin-mediated endocytosis for their internalization. The GFP library can again be narrowed down in this screening method to include only membrane-localized proteins. A knockout of an essential component of CME or use of a temperature sensitive clathrin allele would allow this accumulation of cargo at the membrane. However, it may be labor intensive to introduce this knockout into each GFP yeast strain, despite narrowing down of the library for potential candidates; the GFP library creators scored 149 ORFs as localized to the cell periphery [12]. Instead, a chemical inhibitor of CME could easily be applied to cells. Latrunculin A is an effective inhibitor of clathrin-mediated endocytosis in yeast due to its inhibition of actin polymerization. Fluorescent CME-dependent cargo has previously been imaged gathered into stalled endocytic sites with Latrunctulin A treatment [5] . Weaknesses of this approach include the fact that cargoes dependent on certain conditions, such as nutrient levels, for internalization may not portray a phenotype under screening conditions. Cells are also stressed by chemical inhibitors such as Latrunculin A, which may affect results. Latrunculin A can also inhibit non-clathrin dependent endocytic processes which depend on actin, indicating cargoes identified could be dependent on either process. However, additional testing of the

proposed cargo with a clathrin temperature sensitive allele would confirm its function in CME rather than clathrin-independent endocytosis.

Systematic identification of cargo proteins for clathrin-mediated endocytosis would contribute a great deal to the field of CME research, and may address remaining questions surrounding cargo adaptors and the presence of a possible cargo checkpoint, as well as contribute to other fields such as signaling processes and nutrient sensing and regulation. Another outstanding question regarding endocytic cargo is the identification of amino acid endocytic signals beyond the known NPFXD sequence. This topic is further addressed in Appendix 1.

4.5.2 Clathrin-mediated endocytic machinery

As detailed in Chapter 2, 28 uncharacterized proteins colocalized with Sla1 in our screen of the GFP library. We investigated and confirmed two of these, Ubx3 and Tda2, and confirmed them as bona fide components of the clathrin-mediated endocytic machinery. However, 26 potential proteins remain uncharacterized and uninvestigated. The second, fourth, fifth, and sixth highest PCC scoring uncharacterized proteins (as recorded in Table 2.3) are pictured in Figure 4.1. By appearance, these candidates all have similar localization to clathrin-mediated endocytic proteins with punctate structures localized near the plasma membrane. YBL029C-A has no predicted membrane association while YDL012C has a predicted tail anchor to the plasma membrane, YOR104W and YGR026W have predicted transmembrane domains, and YOR104W is also predicted to be palmitoylated. Association with the membrane could indicate these proteins are cargo instead of endocytic machinery. However, several established endocytic machinery contain membrane binding regions suggesting the potential for machinery should not

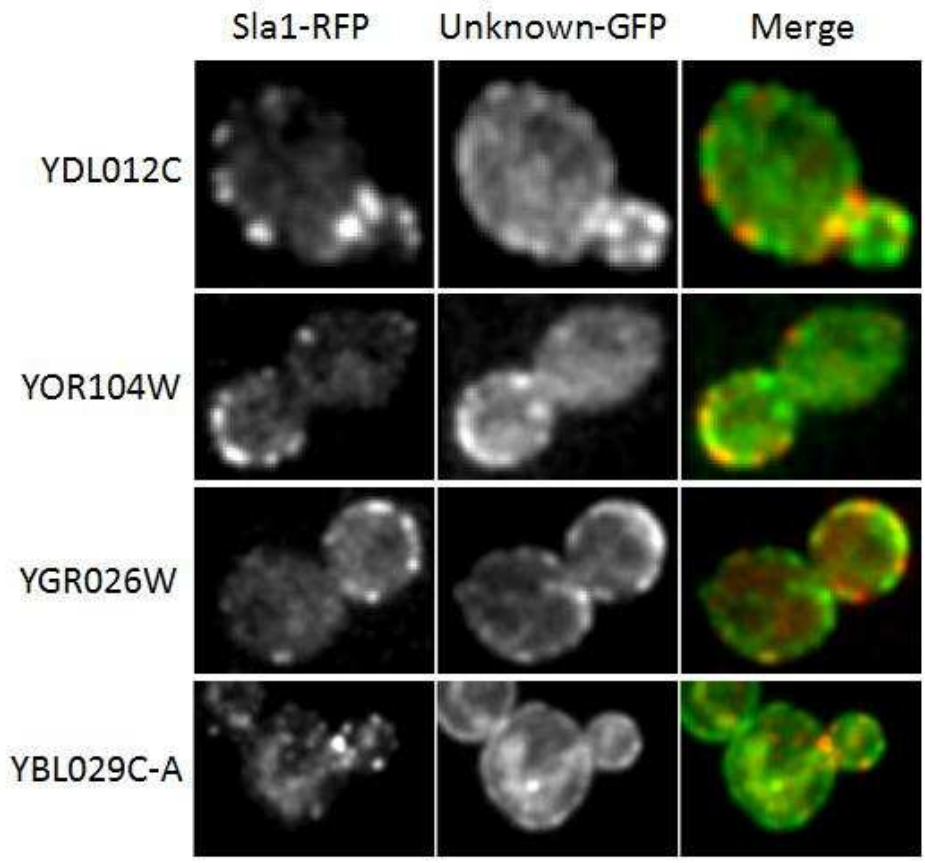

Figure 4.1: Other top scoring uncharacterized proteins in the GFP screening. Pearson correlation coefficients ± SD of GFP proteins with Sla1 are YDL012C 0.50 ± 0.14, YOR104W 0.45 ± 0.19, YGR026W 0.45 ± 0.03, and YBL029C-A 0.43 ± 0.12 and were ranked 2nd, 4th, 5th, and 6th respectively out of the uncharacterized proteins in the screen, and 23rd, 33rd, 36th and 42nd overall in the screen.

be eliminated. These proteins have no other predicted domains barring a prion-like domain in YOR104W, and will require further study to elucidate their function.

Twenty more uncharacterized colocalizing proteins still remain that are not pictured here, but listed in Table 2.3. The lower Pearson correlation coefficients of these strains suggest lower probability of uncharacterized endocytic machinery, but the possibility still exists. Weaknesses in the GFP screening detailed in Section 4.2.2 suggest that more uncharacterized proteins of the endocytic machinery could exist that were not identified in this study, and the colocalizing proteins identified here could prove to be unrelated to the endocytic process as false positive results. Confirmation of these uncharacterized proteins as CME machinery components must be performed as with Ubx3 and Tda2.

As questions in the clathrin-mediated endocytosis field remain unanswered, the potential for identification of additional CME machinery proteins remains high. Our screening of the GFP library successfully identified new proteins of the clathrin-mediated endocytic machinery despite decades of research, indicating a unique approach with distinct advantages over other screening methods. This screening method has the potential to identify many more previously uncharacterized components of this essential cell process.

REFERENCES

1. Raths, S., J. Rohrer, F. Crausaz, and H. Riezman, *end3 and end4: two mutants defective in receptor-mediated and fluid-phase endocytosis in Saccharomyces cerevisiae.* J Cell Biol, 1993. **120**(1): p. 55-65.
2. Wendland, B., J.M. McCaffery, Q. Xiao, and S.D. Emr, *A novel fluorescence-activated cell sorter-based screen for yeast endocytosis mutants identifies a yeast homologue of mammalian eps15.* J Cell Biol, 1996. **135**(6 Pt 1): p. 1485-500.
3. Riezman, H., *Endocytosis in yeast: several of the yeast secretory mutants are defective in endocytosis.* Cell, 1985. **40**(4): p. 1001-9.
4. Chvatchko, Y., I. Howald, and H. Riezman, *Two yeast mutants defective in endocytosis are defective in pheromone response.* Cell, 1986. **46**(3): p. 355-64.
5. Toshima, J.Y., J. Toshima, M. Kaksonen, A.C. Martin, D.S. King, and D.G. Drubin, *Spatial dynamics of receptor-mediated endocytic trafficking in budding yeast revealed by using fluorescent alpha-factor derivatives.* Proc Natl Acad Sci U S A, 2006. **103**(15): p. 5793-8.
6. Burston, H.E., L. Maldonado-Baez, M. Davey, B. Montpetit, C. Schluter, B. Wendland, and E. Conibear, *Regulators of yeast endocytosis identified by systematic quantitative analysis.* J Cell Biol, 2009. **185**(6): p. 1097-110.
7. Carroll, S.Y., P.C. Stirling, H.E. Stimpson, E. Giesselmann, M.J. Schmitt, and D.G. Drubin, *A yeast killer toxin screen provides insights into a/b toxin entry, trafficking, and killing mechanisms.* Dev Cell, 2009. **17**(4): p. 552-60.
8. Lin, C.H., J.A. MacGurn, T. Chu, C.J. Stefan, and S.D. Emr, *Arrestin-related ubiquitin-ligase adaptors regulate endocytosis and protein turnover at the cell surface.* Cell, 2008. **135**(4): p. 714-25.
9. Cornet, M., C. Gaillardin, and M.L. Richard, *Deletions of the endocytic components VPS28 and VPS32 in Candida albicans lead to echinocandin and azole hypersensitivity.* Antimicrob Agents Chemother, 2006. **50**(10): p. 3492-5.
10. Tonikian, R., X. Xin, C.P. Toret, D. Gfeller, C. Landgraf, S. Panni, S. Paoluzi, L. Castagnoli, B. Currell, S. Seshagiri, et al., *Bayesian modeling of the yeast SH3 domain interactome predicts spatiotemporal dynamics of endocytosis proteins.* PLoS Biol, 2009. **7**(10): p. e1000218.
11. Fromont-Racine, M., J.C. Rain, and P. Legrain, *Building protein-protein networks by two-hybrid mating strategy.* Methods Enzymol, 2002. **350**: p. 513-24.
12. Huh, W.K., J.V. Falvo, L.C. Gerke, A.S. Carroll, R.W. Howson, J.S. Weissman, and E.K. O'Shea, *Global analysis of protein localization in budding yeast.* Nature, 2003. **425**(6959): p. 686-91.
13. Gavin, A.C., M. Bosche, R. Krause, P. Grandi, M. Marzioch, A. Bauer, J. Schultz, J.M. Rick, A.M. Michon, C.M. Cruciat, et al., *Functional organization of the yeast proteome by systematic analysis of protein complexes.* Nature, 2002. **415**(6868): p. 141-7.
14. Ghaemmaghami, S., W.K. Huh, K. Bower, R.W. Howson, A. Belle, N. Dephoure, E.K. O'Shea, and J.S. Weissman, *Global analysis of protein expression in yeast.* Nature, 2003. **425**(6959): p. 737-41.

15. Buchberger, A., M.J. Howard, M. Proctor, and M. Bycroft, *The UBX domain: a widespread ubiquitin-like module.* J Mol Biol, 2001. **307**(1): p. 17-24.
16. Schuberth, C. and A. Buchberger, *UBX domain proteins: major regulators of the AAA ATPase Cdc48/p97.* Cell Mol Life Sci, 2008. **65**(15): p. 2360-71.
17. Schuberth, C., H. Richly, S. Rumpf, and A. Buchberger, *Shp1 and Ubx2 are adaptors of Cdc48 involved in ubiquitin-dependent protein degradation.* EMBO Rep, 2004. **5**(8): p. 818-24.
18. Hartmann-Petersen, R., M. Wallace, K. Hofmann, G. Koch, A.H. Johnsen, K.B. Hendil, and C. Gordon, *The Ubx2 and Ubx3 cofactors direct Cdc48 activity to proteolytic and nonproteolytic ubiquitin-dependent processes.* Curr Biol, 2004. **14**(9): p. 824-8.
19. Johnson, E.S., P.C. Ma, I.M. Ota, and A. Varshavsky, *A proteolytic pathway that recognizes ubiquitin as a degradation signal.* J Biol Chem, 1995. **270**(29): p. 17442-56.
20. Meyer, H.H., J.G. Shorter, J. Seemann, D. Pappin, and G. Warren, *A complex of mammalian ufd1 and npl4 links the AAA-ATPase, p97, to ubiquitin and nuclear transport pathways.* EMBO J, 2000. **19**(10): p. 2181-92.
21. Uchiyama, K., E. Jokitalo, F. Kano, M. Murata, X. Zhang, B. Canas, R. Newman, C. Rabouille, D. Pappin, P. Freemont, and H. Kondo, *VCIP135, a novel essential factor for p97/p47-mediated membrane fusion, is required for Golgi and ER assembly in vivo.* J Cell Biol, 2002. **159**(5): p. 855-66.
22. Buchberger, A., H. Schindelin, and P. Hanzelmann, *Control of p97 function by cofactor binding.* FEBS Lett, 2015. **589**(19 Pt A): p. 2578-89.
23. Zhang, X., F. Beuron, and P.S. Freemont, *Machinery of protein folding and unfolding.* Curr Opin Struct Biol, 2002. **12**(2): p. 231-8.
24. Pleasure, I.T., M.M. Black, and J.H. Keen, *Valosin-containing protein, VCP, is a ubiquitous clathrin-binding protein.* Nature, 1993. **365**(6445): p. 459-62.
25. Tettamanzi, M.C., C. Yu, J.S. Bogan, and M.E. Hodsdon, *Solution structure and backbone dynamics of an N-terminal ubiquitin-like domain in the GLUT4-regulating protein, TUG.* Protein Sci, 2006. **15**(3): p. 498-508.
26. Zehner, M., A.I. Chasan, V. Schuette, M. Embgenbroich, T. Quast, W. Kolanus, and S. Burgdorf, *Mannose receptor polyubiquitination regulates endosomal recruitment of p97 and cytosolic antigen translocation for cross-presentation.* Proc Natl Acad Sci U S A, 2011. **108**(24): p. 9933-8.
27. Bug, M. and H. Meyer, *Expanding into new markets--VCP/p97 in endocytosis and autophagy.* J Struct Biol, 2012. **179**(2): p. 78-82.
28. Ryu, S.W. and E. Kim, *Apoptosis induced by human Fas-associated factor 1, hFAF1, requires its ubiquitin homologous domain, but not the Fas-binding domain.* Biochem Biophys Res Commun, 2001. **286**(5): p. 1027-32.
29. Park, M.Y., J.H. Moon, K.S. Lee, H.I. Choi, J. Chung, H.J. Hong, and E. Kim, *FAF1 suppresses IkappaB kinase (IKK) activation by disrupting the IKK complex assembly.* J Biol Chem, 2007. **282**(38): p. 27572-7.
30. Weinberg, J.S. and D.G. Drubin, *Regulation of clathrin-mediated endocytosis by dynamic ubiquitination and deubiquitination.* Curr Biol, 2014. **24**(9): p. 951-9.
31. Ryan, C.J., A. Roguev, K. Patrick, J. Xu, H. Jahari, Z. Tong, P. Beltrao, M. Shales, H. Qu, S.R. Collins, et al., *Hierarchical modularity and the evolution of genetic interactomes across species.* Mol Cell, 2012. **46**(5): p. 691-704.

32. Boeke, D., S. Trautmann, M. Meurer, M. Wachsmuth, C. Godlee, M. Knop, and M. Kaksonen, *Quantification of cytosolic interactions identifies Ede1 oligomers as key organizers of endocytosis.* Mol Syst Biol, 2014. **10**: p. 756.
33. Pfister, K.K., P.R. Shah, H. Hummerich, A. Russ, J. Cotton, A.A. Annuar, S.M. King, and E.M. Fisher, *Genetic analysis of the cytoplasmic dynein subunit families.* PLoS Genet, 2006. **2**(1): p. e1.
34. Moore, J.K., M.D. Stuchell-Brereton, and J.A. Cooper, *Function of dynein in budding yeast: mitotic spindle positioning in a polarized cell.* Cell Motil Cytoskeleton, 2009. **66**(8): p. 546-55.
35. Williams, J.C., P.L. Roulhac, A.G. Roy, R.B. Vallee, M.C. Fitzgerald, and W.A. Hendrickson, *Structural and thermodynamic characterization of a cytoplasmic dynein light chain-intermediate chain complex.* Proc Natl Acad Sci U S A, 2007. **104**(24): p. 10028-33.
36. Rapali, P., A. Szenes, L. Radnai, A. Bakos, G. Pal, and L. Nyitray, *DYNLL/LC8: a light chain subunit of the dynein motor complex and beyond.* FEBS J, 2011. **278**(17): p. 2980-96.
37. Benashski, S.E., A. Harrison, R.S. Patel-King, and S.M. King, *Dimerization of the highly conserved light chain shared by dynein and myosin V.* Journal of Biological Chemistry, 1997. **272**(33): p. 20929-20935.
38. Williams, J.C., H. Xie, and W.A. Hendrickson, *Crystal structure of dynein light chain TcTex-1.* J Biol Chem, 2005. **280**(23): p. 21981-6.
39. Sachdev, P., S. Menon, D.B. Kastner, J.Z. Chuang, T.Y. Yeh, C. Conde, A. Caceres, C.H. Sung, and T.P. Sakmar, *G protein beta gamma subunit interaction with the dynein light-chain component Tctex-1 regulates neurite outgrowth.* EMBO J, 2007. **26**(11): p. 2621-32.
40. Wu, H., M.W. Maciejewski, S. Takebe, and S.M. King, *Solution structure of the Tctex1 dimer reveals a mechanism for dynein-cargo interactions.* Structure, 2005. **13**(2): p. 213-23.
41. Tai, A.W., J.Z. Chuang, and C.H. Sung, *Localization of Tctex-1, a cytoplasmic dynein light chain, to the Golgi apparatus and evidence for dynein complex heterogeneity.* J Biol Chem, 1998. **273**(31): p. 19639-49.
42. Chuang, J.Z., T.Y. Yeh, F. Bollati, C. Conde, F. Canavosio, A. Caceres, and C.H. Sung, *The dynein light chain Tctex-1 has a dynein-independent role in actin remodeling during neurite outgrowth.* Dev Cell, 2005. **9**(1): p. 75-86.
43. Nagler, M., L. Palkowitsch, S. Rading, B. Moepps, and M. Karsak, *Cannabinoid receptor 2 expression modulates Gbeta1gamma2 protein interaction with the activator of G protein signalling 2/dynein light chain protein Tctex-1.* Biochem Pharmacol, 2016. **99**: p. 60-72.
44. Liu, C., J.Z. Chuang, C.H. Sung, and Y. Mao, *A dynein independent role of Tctex-1 at the kinetochore.* Cell Cycle, 2015. **14**(9): p. 1379-88.
45. Wickstead, B. and K. Gull, *Dyneins across eukaryotes: a comparative genomic analysis.* Traffic, 2007. **8**(12): p. 1708-21.
46. Narayanaswamy, R., E.K. Moradi, W. Niu, G.T. Hart, M. Davis, K.L. McGary, A.D. Ellington, and E.M. Marcotte, *Systematic definition of protein constituents along the major polarization axis reveals an adaptive reuse of the polarization machinery in pheromone-treated budding yeast.* J Proteome Res, 2009. **8**(1): p. 6-19.

47. Miki, F., K. Okazaki, M. Shimanuki, A. Yamamoto, Y. Hiraoka, and O. Niwa, *The 14-kDa dynein light chain-family protein Dlc1 is required for regular oscillatory nuclear movement and efficient recombination during meiotic prophase in fission yeast.* Mol Biol Cell, 2002. **13**(3): p. 930-46.

APPENDIX 1

RECOGNITION OF MAMMALIAN ENDOCYTIC INTERNALIZATION AMINO ACID SEQUENCES IN *SACCHAROMYCES CEREVISIAE*

A.1.1 Summary

Amino acid sequences in the cytosolic portion of transmembrane proteins are recognized by clathrin adaptors for internalization of the protein by clathrin-mediated endocytosis (CME). The only established signals for recognition of cargo proteins in yeast include amino acid sequence NPFXD and ubiquitination. In mammalian cells, along with ubiquitination, many amino acid sequences are recognized by a number of different adaptors for CME and trafficking throughout the cell. In this study, we test whether the established mammalian sequence NPXY, dileucine motif, or tyrosine hydrophobic sequence are functional in yeast CME. We use native yeast CME cargo protein Wsc1 with modified endocytic signals via site-directed mutagenesis. We found the tyrosine hydrophobic sequence produced successful internalization of Wsc1-GFP in yeast. This was not dependent on putative adaptor proteins Syp1 or AP-2, leaving the responsible adaptor protein unknown.

A.1.2 Introduction

Despite the significant similarities between yeast and mammalian endocytosis [1, 2], little investigation has been performed into the function of mammalian amino acid endocytic signals in yeast. In most cases, transmembrane cargo proteins are signaled as endocytic cargo by ubiquitination or an amino acid sequence located in the cytosolic portion of the protein sequence

[3]. Adaptors serve to recognize the amino acid sequence or ubiquitin signal and recruit endocytic machinery to the site for endocytosis (Figure 1.2).

Along with ubiquitination, yeast utilize the amino acid sequence NPFXD in the cytosolic portion of an endocytic cargo protein to target it for endocytosis [4]. This sequence is recognized by the SHD1 domain of the yeast clathrin adaptor protein Sla1 [5, 6]. Mutation of the NPFXD amino acid sequence or of the SHD1 domain severely diminishes the ability of clathrin-mediated endocytosis to internalize proteins with this internalization signal. Wsc1, a cell wall stress response sensor [7], is one example of a yeast membrane protein which requires this amino acid sequence for internalization and recycling to the bud and is dependent on Sla1 for endocytic internalization [8].

In contrast to the single short sequence internalization signal known in yeast (NPFXD), many mammalian endocytic signals have been thoroughly studied. One such signal is NPXY, which is recognized by Dab2 and ARH adaptors for intake of LDLR family, as well as the μ subunit of AP-2 for general internalization from the membrane [9]. Other signals include the tyrosine hydrophobic signal (YXXΦ where Φ is a bulky hydrophobic residue F, I, L, M, or V), which is recognized by the μ subunit of AP-2 for membrane internalization as well as AP-1 and AP-3 for lysosomal sorting [10], and the dileucine signal [(D/E)XXXL(L/I)] which is recognized by hydrophobic pockets in the σ subunits of AP-1, AP-2, and AP-3 [10, 11].

The goal of this study is to determine if these sequences are found to produce a successful endocytic signal in yeast. If an amino acid signal does trigger cargo internalization in yeast, we will also determine if similar adaptors are responsible for recognition in yeast as in mammals. The yeast AP-2 adaptors are the logical choice, yet the AP-2 proteins have been generally described as having little general function in yeast endocytosis [12], barring few cargo-specific

studies including K28 toxin resistance [13], cell wall stress sensor Mid2 [14], and Snc1 [15]. Additional possible adaptors that have been identified include the Syp1/Ede1 complex and the Epsin/YAP180 proteins. Syp1 and Ede1 arrive at endocytic sites early in their formation, suggesting a possible role in placement selection of endocytic sites, and remain at sites with timing similar to clathrin, suggesting these proteins could be adaptors [16]. Additionally, Syp1 contains a domain homologous to the AP-2 μ subunit (Table 1.1). Ent1/2p and Yap1801/2p are putative adaptors based on their homology with known mammalian adaptors AP180/CALM [17], and loss of the Yap proteins had a demonstrated cargo-specific effect [15].

For this study, we have modified Wsc1, a known endocytic cargo, to remove its native endocytic signal of NPFXD and replace it with mammalian endocytic signals using site-directed mutagenesis. We then visualize using fluorescent microscopy whether the protein is internalized; suggesting the amino acid signal is recognized in yeast.

A.1.3 Results

To allow easy manipulation of cargo protein Wsc1-GFP, we first created a plasmid expressing wild type Wsc1-GFP from its endogenous promoter. Protein expressed from this construct had the same localization as Wsc1-GFP expressed from the genomic locus (Figure A.1.1). As Wsc1 functions in the signaling of cell wall production, it is localized to the plasma membrane of the bud during cell division, creating a bright fluorescent bud when tagged with GFP. As the protein diffuses away from the bud into the mother cell, it is recognized for clathrin-mediated endocytosis by Sla1 via its NPFXD signal and recycled back to the bud.

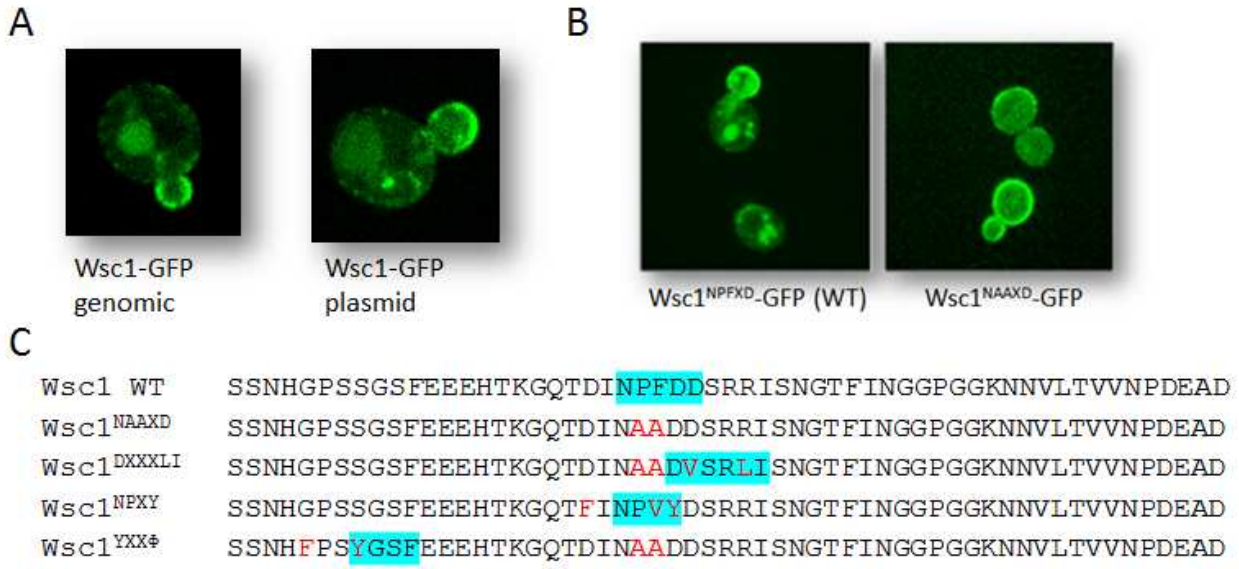

Figure A.1.1: Wsc1-GFP is dependent on its NPFXD signal for recycling to the bud. A) Wsc1-GFP has the same localization whether expressed at endogenous levels from the genomic locus or from a plasmid. B) Mutation of the NPFXD signal to NAAXD removes all polarization of Wsc1-GFP to the bud. C) Amino acid sequences from residues 322-378 of the cytosolic tail of Wsc1 in constructs used for this study. Mutated residues are in red, while endocytic signals are highlighted in cyan.

Mutation of the NPFXD sequence to NAAXD removes all evidence of polarization of Wsc1-GFP to the bud along with any evidence of internal fluorescent structures (Figure A.1.1.B).

The cytosolic portion of Wsc1 was then further mutated to exhibit three different mammalian endocytic signals (Figure A.1.1.C). The Wsc1-GFP constructs with the dileucine signal (DXXXLI) or the NPXY signal did not show any polarization or internal fluorescence (Figure A.1.2.A). However, the tyrosine hydrophobic signal (YXXΦ) did show fluorescent internal structures (Figure 1.2.A), suggesting this signal is recognized for internalization. Mutation of the tyrosine residue to an alanine (AXXΦ) in this construct removed any evidence of internal fluorescent structures (Figure 1.2.B). This suggests the tyrosine hydrophobic amino acid sequence is being recognized specifically as a single amino acid substitution ablates internal fluorescence.

To test which adaptor is responsible for recognition of the tyrosine hydrophobic signal, we expressed these Wsc1-GFP plasmid constructs in cells lacking the μ subunit of AP-2 (*Δapm4*). The μ subunit recognizes the tyrosine hydrophobic signal in mammalian cells, and deletion of one subunit destabilizes the entire AP-2 complex [14]. As expected, wild type Wsc1-GFP localization was unaffected, as its NPFXD signal is recognized by Sla1, not AP-2. Though this is the adaptor responsible for recognition of the tyrosine hydrophobic signal in mammalian cells, internalization of Wsc1-GFP^{YXXΦ} was not affected by the knockout of this adaptor (Figure 1.2.C). Similarly, deletion of Syp1, a putative adaptor protein which contains an AP-2 μ homology domain, had no effect on the internalization of Wsc1-GFP^{YXXΦ} (Figure 1.2.D). Lastly, as wild type Wsc1 is recognized by the SHD1 domain of Sla1, we expressed Wsc1-GFP^{YXXΦ} in cells with a mutated SHD1 domain to confirm there is no residual recognition causing internalization. Wild type Wsc1-GFP localization is dramatically affected by this mutation, but

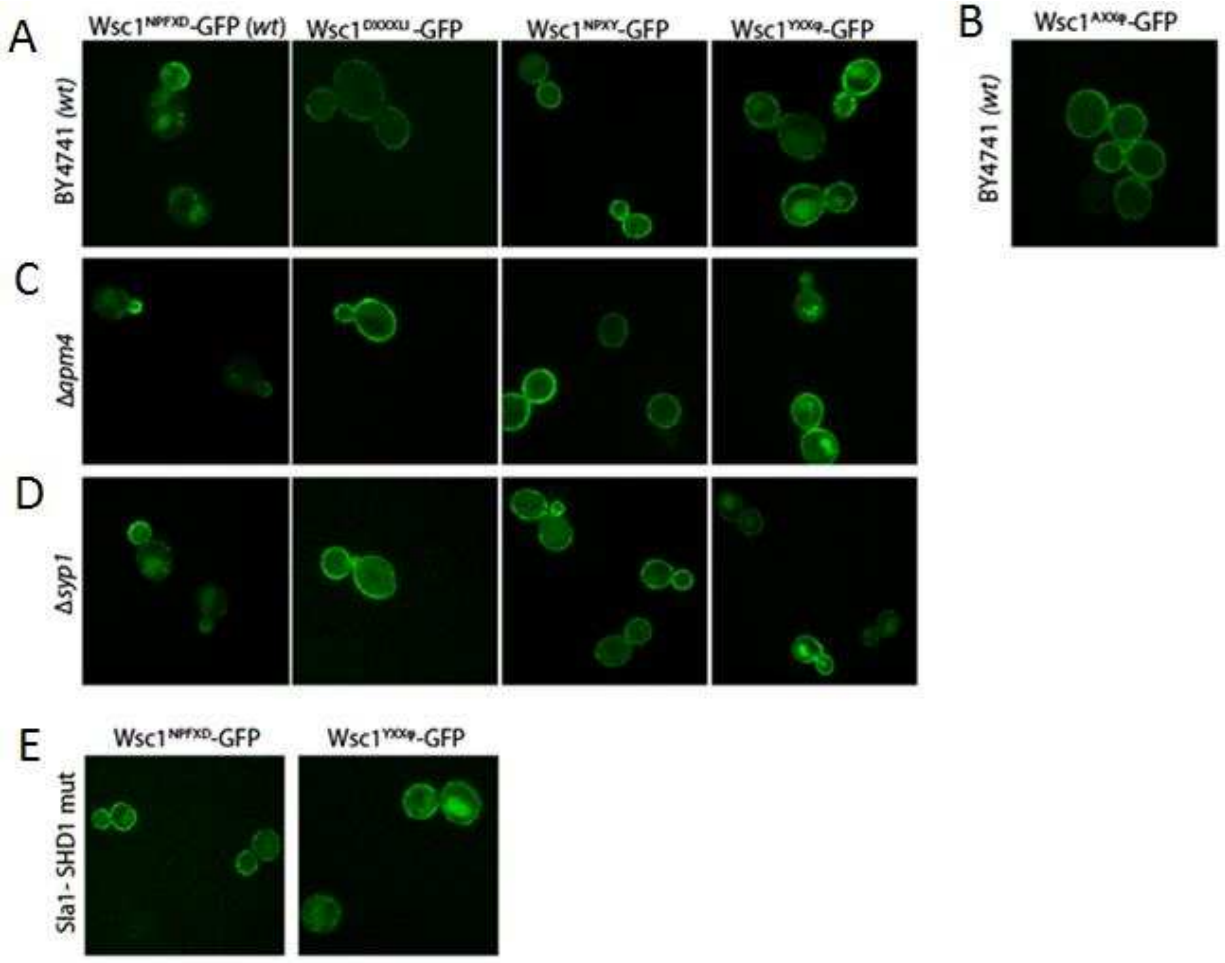

Figure A.1.2: The tyrosine hydrophobic signal is recognized for endocytosis in yeast. A) Wild type Wsc1-GFP and tyrosine hydrophobic signal displaying Wsc1-GFP show internal fluorescent structures, while the dileucine and NPXY signal displaying Wsc1-GFP constructs do not show internal fluorescence. B) Mutation of solely the tyrosine in the tyrosine hydrophobic signal ablates internal fluorescence. C) Deletion of the μ subunit of AP-2 does not eliminate internal fluorescence in the tyrosine hydrophobic signal expressing cells. D) Deletion of Syp1 does not eliminate internal fluorescence in the tyrosine hydrophobic signal expressing cells. E) Mutation of the SHD1 domain of Sla1 disrupts wild type Wsc1 internalization, but does not eliminate internal fluorescence in the tyrosine hydrophobic signal expressing cells.

Wsc1-GFP$^{YXX\Phi}$ still demonstrates the same internal fluorescent structures (Figure 1.2.E). Thus we have demonstrated a functional mammalian endocytic signal in yeast, but the adaptor responsible for internalization remains unknown.

A.1.4 Discussion

High levels of conservation exist between yeast and mammalian cells on many aspects of the clathrin-mediated endocytic process including protein involvement, dynamics, and function of the process. Thus it is probable that amino acid sequences recognized in one species are also recognized in another. We have demonstrated that the tyrosine hydrophobic signal that functions in mammalian clathrin-mediated endocytosis and protein trafficking can also drive internalization of plasma membrane cargo proteins in yeast. This signal is specific, as mutation of a single residue eliminates internalization. However, this signal does not seem to be recognized by the same adaptor in yeast cells as it is in mammalian cells. Neither deletion of the AP-2 μ subunit, deletion of Syp1, nor mutation of the Sla1 SHD1 domain had any effect on reducing internalization of Wsc1-GFP containing this sequence. The results of this study could be further confirmed by use of fluorescent labeled or radiolabeled alpha factor internalization assays. The alpha factor is internalized from the exterior of the cell and not produced in the cell. This would confirm recognition by clathrin-mediated endocytosis and oppose the possibility that Wsc1-GFP is being mistrafficked upon production, resulting in the internal fluorescent structures we see. Disruption of the AP-1 or AP-3 complexes may also reveal intricacies of the trafficking of Wsc1 with the tyrosine hydrophobic signal.

Examination of yeast proteins with transmembrane regions and cytosolic domains reveals potential tyrosine hydrophobic sequences existing throughout the yeast proteome. The presence

of this sequence in native yeast proteins further suggests it is a functional and recognized amino acid sequence for clathrin-mediated endocytosis. Future application of predictive algorithms for YXXΦ signals may identify proteins with this signal binding a functional adaptor in yeast [18]. This study also further confirmed that Wsc1-GFP is dependent on the NPFXD signal not only for internalization, but also for its polarization. Though Wsc1-GFP^{YXXΦ} is internalized, the wild type polarization of protein to the bud of the dividing cell is not present. Thus, the NPFXD signal is necessary for recycling to the plasma membrane in addition to clathrin-mediated endocytosis.

Further investigation into the adaptors recognizing this protein or its native function in yeast were suspended due to another group demonstrating this signal's function in yeast. The Lemmon lab demonstrated that cargo protein Atg27 is trafficked dependent on a tyrosine hydrophobic signal and adaptor protein AP-3 [19]. Additionally, though we saw no affect with AP-2 deletion in this study, AP-2 was recently identified as binding directly to cargo protein and cell wall stress sensor Mid2 [14]. This group also produced mutations to the μ subunit of AP-2 where interactions with YXXΦ occur in mammalian cells, and saw binding to Mid2 reduced by 50%. Similarly, this group mutated a potential YXXΦ signal in the Mid2 cytosolic tail and saw a 50% reduction in binding to AP-2. A double deletion of *Δamp4/Δsyp1* did not exacerbate any of the phenotypes they observed [14]. As the disruption of binding between cargo Mid2 and adaptor AP-2 by mutation of either protein was not complete, this may explain why our study still demonstrated internalization of the tyrosine hydrophobic signal upon disruption of AP-2. AP-2 may be acting in redundancy with another protein, allowing internalization in the absence of AP-2, or multiple binding sites or sequences may contribute to internalization.

We have confirmed the tyrosine hydrophobic amino acid sequence is recognized and is specific and functional in yeast. This has recently been confirmed by two other studies investigating proteins with an endogenous tyrosine hydrophobic signal. We were unable to determine the adaptor protein responsible for recognition of this sequence, but recent reports identify the μ subunit of AP-2 as binding specifically to this sequence, as it occurs in mammals.

A.1.5 Experimental Procedures

A.1.5.1 Plasmids and yeast strains

Wsc1-GFP plasmids were created using vector pRS313 digested with BamHI and SalI. Wsc1-GFP was amplified via PCR including 500bp of 5'UTR and 190bp of ADH1 terminator from endogenously expressed Wsc1-GFP in strain GPY3535 to create pSDP393, the wild type Wsc1-GFP construct. Site-directed mutagenesis was performed using a QuikChange XL Site-directed Mutagenesis Kit (Stratagene) to create constructs detailed in Figure A.1.1. pSDP417 contains the NAAXD sequence, pSDP419 contains the YXXΦ sequence, pSDP477 and pSDP478 contain the DXXXLI and NPXY constructs respectively. pSDP468 contains the mutated AXXΦ sequence. All constructs were subjected to sequencing before use.

Background yeast strain BY4741 was used in this study except for the Sla1-SHD1 mutation strain (GPY1805-I39E). Deletion strains (*Δapm4* and *Δsyp1*) were obtained from the yeast knockout library (GE). Plasmids were transformed into yeast using standard methods to create SDY397 (*MATa his3Δ1, leu2Δ0, met15-Δ0, ura3 Δ0 pRS313-Wsc1-GFP*), SDY398 (*MATa his3Δ1, leu2Δ0, met15-Δ0, ura3 Δ0 pRS313-Wsc1-GFP* ^{YXXΦ}), SDY400 (*MATa his3Δ1, leu2Δ0, met15-Δ0, ura3 Δ0 pRS313-Wsc1-GFP* ^{NPXY}), SDY401(*MATa his3Δ1, leu2Δ0, met15-Δ0, ura3 Δ0 pRS313-Wsc1-GFP* ^{DXXXLI}).

A.1.5.2 Fluorescent microscopy

Fluorescence microscopy was performed as described using an Olympus IX81 spinning disc confocal microscope [20]. Cells were grown to early log phase and imaged at room temperature. Slidebook 6 software (3I, Denver, CO) was used for analysis.

A.1.5.3 Acknowledgements

The yeast strain containing the Wsc1-GFP sequence used in this study originated from the laboratory of Gregory Payne. Knockout strains were a gift from the laboratory of Laurie Stargell.

REFERENCES

1. Taylor, M.J., D. Perrais, and C.J. Merrifield, *A high precision survey of the molecular dynamics of mammalian clathrin-mediated endocytosis.* PLoS Biol, 2011. **9**(3): p. e1000604.
2. Doyon, J.B., B. Zeitler, J. Cheng, A.T. Cheng, J.M. Cherone, Y. Santiago, A.H. Lee, T.D. Vo, Y. Doyon, J.C. Miller, et al., *Rapid and efficient clathrin-mediated endocytosis revealed in genome-edited mammalian cells.* Nat Cell Biol, 2011. **13**(3): p. 331-7.
3. Goode, B.L., J.A. Eskin, and B. Wendland, *Actin and endocytosis in budding yeast.* Genetics, 2015. **199**(2): p. 315-58.
4. Tan, P.K., J.P. Howard, and G.S. Payne, *The sequence NPFXD defines a new class of endocytosis signal in Saccharomyces cerevisiae.* J Cell Biol, 1996. **135**(6 Pt 2): p. 1789-800.
5. Mahadev, R.K., S.M. Di Pietro, J.M. Olson, H.L. Piao, G.S. Payne, and M. Overduin, *Structure of Sla1p homology domain 1 and interaction with the NPFxD endocytic internalization motif.* EMBO J, 2007. **26**(7): p. 1963-71.
6. Howard, J.P., J.L. Hutton, J.M. Olson, and G.S. Payne, *Sla1p serves as the targeting signal recognition factor for NPFX(1,2)D-mediated endocytosis.* J Cell Biol, 2002. **157**(2): p. 315-26.
7. Lodder, A.L., T.K. Lee, and R. Ballester, *Characterization of the Wsc1 protein, a putative receptor in the stress response of Saccharomyces cerevisiae.* Genetics, 1999. **152**(4): p. 1487-99.
8. Piao, H.L., I.M. Machado, and G.S. Payne, *NPFXD-mediated endocytosis is required for polarity and function of a yeast cell wall stress sensor.* Mol Biol Cell, 2007. **18**(1): p. 57-65.
9. Bonifacino, J.S. and L.M. Traub, *Signals for sorting of transmembrane proteins to endosomes and lysosomes.* Annu Rev Biochem, 2003. **72**: p. 395-447.
10. Mattera, R., M. Boehm, R. Chaudhuri, Y. Prabhu, and J.S. Bonifacino, *Conservation and diversification of dileucine signal recognition by adaptor protein (AP) complex variants.* J Biol Chem, 2011. **286**(3): p. 2022-30.
11. Kelly, B.T., A.J. McCoy, K. Spate, S.E. Miller, P.R. Evans, S. Honing, and D.J. Owen, *A structural explanation for the binding of endocytic dileucine motifs by the AP2 complex.* Nature, 2008. **456**(7224): p. 976-79.
12. Wendland, B. and S.D. Emr, *Pan1p, yeast eps15, functions as a multivalent adaptor that coordinates protein-protein interactions essential for endocytosis.* J Cell Biol, 1998. **141**(1): p. 71-84.
13. Carroll, S.Y., P.C. Stirling, H.E. Stimpson, E. Giesselmann, M.J. Schmitt, and D.G. Drubin, *A yeast killer toxin screen provides insights into a/b toxin entry, trafficking, and killing mechanisms.* Dev Cell, 2009. **17**(4): p. 552-60.
14. Chapa-y-Lazo, B., E.G. Allwood, R. Smaczynska-de, II, M.L. Snape, and K.R. Ayscough, *Yeast endocytic adaptor AP-2 binds the stress sensor Mid2 and functions in polarized cell responses.* Traffic, 2014. **15**(5): p. 546-57.

15. Burston, H.E., L. Maldonado-Baez, M. Davey, B. Montpetit, C. Schluter, B. Wendland, and E. Conibear, *Regulators of yeast endocytosis identified by systematic quantitative analysis.* J Cell Biol, 2009. **185**(6): p. 1097-110.
16. Stimpson, H.E., C.P. Toret, A.T. Cheng, B.S. Pauly, and D.G. Drubin, *Early-arriving Syp1p and Ede1p function in endocytic site placement and formation in budding yeast.* Mol Biol Cell, 2009. **20**(22): p. 4640-51.
17. Maldonado-Baez, L., M.R. Dores, E.M. Perkins, T.G. Drivas, L. Hicke, and B. Wendland, *Interaction between Epsin/Yap180 adaptors and the scaffolds Ede1/Pan1 is required for endocytosis.* Mol Biol Cell, 2008. **19**(7): p. 2936-48.
18. Mukherjee, D., C.B. Hanna, and R.C. Aguilar, *Artificial neural network for the prediction of tyrosine-based sorting signal recognition by adaptor complexes.* J Biomed Biotechnol, 2012. **2012**: p. 498031.
19. Segarra, V.A., D.R. Boettner, and S.K. Lemmon, *Atg27 tyrosine sorting motif is important for its trafficking and Atg9 localization.* Traffic, 2015. **16**(4): p. 365-78.
20. Feliciano, D. and S.M. Di Pietro, *SLAC, a complex between Sla1 and Las17, regulates actin polymerization during clathrin-mediated endocytosis.* Mol Biol Cell, 2012. **23**(21): p. 4256-72.

LIST OF ABBREVIATIONS

AAA: ATPases associated with diverse cellular activities

ABP: Actin binding protein

ADFH: Actin-depolymerizing factor homology domain

ADP: Adenosine diphosphate

AIM: Altered inheritance of mitochondria

ANTH: AP180 N-terminal homology domain

ARP: Actin related protein

ART: Arrestin-related trafficking adaptor

AP: Adaptor protein

ATP: Adenosine triphosphate

ATPase: Adenosine triphosphatase

BAR: Bin/Amphiphysin/Rvsp

CAP: Actin capping protein

CBM: Clathrin box motif

CC: Coiled coil

CDC: Cell division cycle

CH: Calponin homology domain

CHC: Clathrin heavy chain

CIE: Clathrin-independent endocytosis

CME: Clathrin-mediated endocytosis

COP: Coat protein complex

CP: Actin capping protein

DHC: Dynein heavy chain

DMSO: Dimethyl sulfoxide

DUB: De-ubiquitinase

EH: Eps15 homology domain

EM: Electron microscopy

ENTH: Epsin N-terminal homology domain

F-actin: Filamentous actin

F-BAR: Fes/CIP4 homology-Bin/Amphiphysin/Rvsp

FACS: Fluorescence activated cell sorting

G-actin: Globular actin

GFP: Green fluorescent protein

GGA: Golgi-localized, gamma adaptin ear-containing, ARF-binding

GST: Glutathione S-transferase

LatA: Latrunculin A

LDLR: Low density lipoprotein receptor

LGM: Las17 G-actin binding motif

MAT: Mating type

NPF: Nucleation promoting factor

ORF: Open reading frame

PCC: Pearson correlation coefficient

PCR: Polymerase chain reaction

Pi: Inorganic phosphate

PIP2: PtdIns(4,5)P_2

PR: Proline-rich domain

PXXP: Polyproline motif

r.m.s.d: Root-mean-square deviation

RFP: Red fluorescent protein

SCD: Suppressor of clathrin deficiency

SH3: Src homology 3

SHD1: Sla1 homology domain 1

SHD2: Sla1 homology domain 2

SLA: Synthetic lethal with actin binding protein 1

SNARE: Soluble NSF Attachment Protein Receptor

TAP: Tandem affinity purification

TDA: Topoisomerase damage affected

THATCH: Talin Hip1/R/Sla2 actin-tethering C-terminal homology domain

TIRF: Total internal reflection fluorescence

TUB: Tubulin

Ub: Ubiquitin

UBA: Ubiquitin-associated domain

UBX: Ubiquitin regulatory X

UIM: Ubiquitin-interacting motif

WASp: Wiskott-Aldrich syndrome protein

WH1: WASp homology 1 domain

WH2: WASp homology 2 domain

YXXΦ: Tyrosine hydrophobic signal where Φ is a bulky hydrophobic residue F, I, L, M, or V